False Vacuum Decay with Quantum Back-reaction

Dissertation

zur Erlangung des Grades eines
Doktors der Naturwissenschaften
dem Fachbereich Physik
der Universität Dortmund

vorgelegt von
Nina Kevlishvili

May 2007

Dedicated to all my teachers

Gewidmet allen meinen Lehrern

Посвящается всем моим учителям

ეძღვნება ყველა ჩემს მასწავლებელს

Abstract

This thesis addresses the topic of quantum backreaction in false vacuum decay, i.e., the transition from a local minimum to the global minimum of the potential. Two possible mechanisms of false vacuum decay will be discussed: the local tunneling via bounce solution and the global tunneling on compact spaces.

We compute the bounce solution in a Φ^4 model with an asymmetric double-well potential in 4 and 2 dimensions. The quantum backreaction of fluctuations is computed in two approximations: the one-loop approximation and Hartree approximation. The results of numerical simulations are compared with the semiclassical approach. The deviations are found to be sizeable.

The question of global tunneling is addressed within a simple $1 + 1$ dimensional model with the asymmetric double-well potential in compact space (S_1). The process is studied by real-time simulations. The wave function of the system is factorized into various modes. The zero mode which tunnels between two wells is treated exactly, while the nonhomogeneous modes are considered to be Gaussian. The simulations show a variety of tunneling phenomena depending on the parameters: there is resonant tunneling, we observe a sliding of the wave function if the potential is strongly modified the quantum fluctuations, and of course we find suppression if the size of the space becomes large.

Zusammenfassung

Diese Arbeit beschäftigt sich mit der Quantenrückwirkung beim Zerfall eines "falschen Vakuums", d.h., mit den Übergang von einem lokalen Minimums in das globale Minimum des Potentials. Zwei mögliche Mechanismen für diesen Zerfall werden diskutiert: das lokale Tunneln durch die sogenannte "Bounce-Konfiguration" und das globale Tunneln in kompakten Räumen.

Wir berechnen die Bounce-Lösung in einem Φ^4 Modell mit einem Doppelmuldenpotential in 4 und 2 Dimensionen. Die Quanten rückwirkung der Fluktuationen wird in zwei Näherungen berechnet: in der Ein-Schleifen-Näherung und dre Hartree-Näherung. Die Resultate der numerischen Simulationen werden mit der semiklassischen Näherung verglichen. Die Abweichungen sind beträchtlich.

Mit der Frage des globalen Tunnelns beschäftigen wir uns im Rahmen eines einfachen $1 + 1$-dimensionalen Modells mit asymmetrischem Doppelmuldenpotential in einem kompakten Raumes. Der Prozess wird in Realzeit-Simulationen untersucht. Die Wellenfunktion des Systems wird in verschiedene Moden faktorisiert. Der Nullmod, der zwischen den beiden Mulden tunnelt wird exakt behandelt, während für die inhomogenen Moden eine Gauß'sche Wellenfunktion angenommen wird. Die Simulationen zeigen in Abhängigkeit von den Parametern eine Reihe verschiedener Tunnelphänomene: es tritt resonantes Tunneln auf, wir beobachten ein Gleiten der Wellenfunktion, wenn das Potential durch die Quantenfluktuationen stark modifiziert wird, und wir finden wie erwartet, dass das Tunneln unterdrückt wird, wenn die Ausdehnung des Raumes groß wird.

Contents

"I don't know what I seem to the world, but as to myself, I seem to have been only like a boy playing on the sea-shore and diverting myself in now and then finding a smoother pebble or a prettier shell than ordinary, whilst the great ocean of truth lay all undiscovered before me."

<div align="right">Sir Isaac Newton</div>

Introduction

1. False Vacuum Decay

False vacuum decay is an old problem which can be addressed in the context of quantum mechanics, or quantum field theory. The decay process is described by a potential which displays a local minimum, separated from the absolute minimum by a potential barrier, i.e. one considers an asymmetric double-well potential. A system prepared in the local minimum, the metastable phase, may decay and find itself on the other side of barrier. Theoretically the decay process may happen *locally* in some part of space, via bounce or bubble solution, or *globally*, where the mean field tunnels through the barrier. The latter type of transition is impossible in an infinite space, as the process will have an infinite action. Therefore it can be considered only in compact spaces.

False vacuum decay finds its most important application in cosmological models. It may initiate inflation, or happen after inflation, if the universe gets trapped in one of the local minima of the Higgs potential in Grand Unified Theories. The false vacuum may decay by spinodal decomposition [1, 2, 3, 4], if for example, by decreasing of temperature or by cosmological expansion the minimum of the potential becomes a maximum. Other decay mechanisms are a thermal over-the-barrier transition, bubble nucleation, or the tunneling to the true vacuum. All these processes occur by spontaneous formation of regions of true vacuum inside the metastable state. If the transition occurs by tunneling in a space of infinite spatial extension, the classical solution which describes the local tunneling is called "the bounce" [5, 6, 7, 8]. For a N-dimensional space-time this is a $SO(N)$ symmetric solution in N-dimensional Euclidean space.

In realistic cosmological models one needs to include gravity. The tunneling may proceed in de Sitter space-time. Such a solution has first been considered by Coleman and De Luccia [9]. The renewed interest to the subject has been recently sparked by developments in string theory, the cosmic "landscapes" (see for example [10, 11]).

The most common approach to compute the transition rate (the decay probability per unit time per unit volume) is the semiclassical one, which was used by several groups for various models [12, 13, 14, 15, 16, 17]. A computation for bounces in 4 dimensions to one-loop accuracy has been presented in Ref.[18]. A similar computation recently was performed using ζ function regularization [19].

One may ask whether the transition rate computed by the semiclassical approximation receives strong corrections when the quantum back-reaction of the fluctuations is taken into account. Two ways of including the quantum back-reaction have been proposed in the literature: the one-loop backreaction, where the classical field is determined to be an extremum of the effective action [20] and the Hartree backreaction based on the $2PPI$ formalism [21, 22, 23].

Everything said above applies of infinite space, as one is used to in cosmology. However, the tunneling with compact spaces can be of interest in cosmology as well. Such transitions in some different context were used to describe the quantum creation of a universe [24, 25, 26, 27], or one can imagine the transition in a finite volume of the universe [28]. The question of quantum creation of universe is widely discussed using the WKB approximation [29, 30, 31, 32, 33, 34]. However, it may not be appropriate to use a continuation to the imaginary time, as one does in the WKB approximation, as the tunneling proceeds in real time. On another side the application of the WKB technique in the quantum field theory becomes very complicated. As to describe the evolution of the system during and after the tunneling requires matching of an infinite number of modes. A solution to the problem is to consider the system in the real time. Such approach was considered in case of quantum mechanics [35]. For the quantum field theory the tunneling process was discussed in Ref. [28], where the time-dependent Hartree-Fock approximation was applied.

In this thesis we will consider the both possibilities of false vacuum decay: the local tunneling via bounce and the global tunneling on a compact space. We restrict ourselves to models without gravity. For local tunneling we discuss false vacuum decay in 3+1 and 1+1 dimensional space-times and consider both the one-loop and Hartree approximations in order to include the quantum backreaction into the computation of transition rate. For the case of global tunneling we consider only $1 + 1$ dimensional space-time.

2. Publications

The most part of this thesis on local tunneling(bounce solution) have already been published and presented at conferences:

1. J. Baacke, N. Kevlishvili, 'False vacuum decay by self-consistent bounces in four dimensions', Phys. Rev. D75: 045001, hep-th/0611004

2. J. Baacke, N. Kevlishvili, 'Self-consistent bounces in two dimensions', Phys.Rev. D71:025008, 2005, hep-th/0411162

3. J. Baacke, N. Kevlishvili, 'False vacuum decay: the role of quantum backreaction', DPG conference, Heidelberg, March 05-09, 2007 (talk is unpublished)

Some aspects on global tunneling have been published and presented at conferences:

1. J. Baacke, N. Kevlishvili, 'Tunneling in quantum field theory on a compact one-dimesional space', Nucl.Phys. B 745:142-164, 2006, hep-th/0505118

2. J. Baacke, N. Kevlishvili, 'Quantum tunneling on a compact space and decay of the false vacuum', Kosmologie Tag, Bielefeld, May 11-12, 2006 (talk is unpublished)

3. Plan of this Thesis

The plan of this thesis is as follows. Part I covers the subject of local tunneling. In the first chapter of this part we give an overview on the theory of bounce solutions and present the basic relations of model and for the main quantity of interest, the tunneling rate. Then we introduce the formalisms used to include the quantum backreaction in different approximations, in the Hartree approximation, using the $2PPI$ expansion of effective action and in the one-loop approximation, as the lowest order of the $1PI$ formalism. In the next two sections (Sec. 1.5,1.6) we give detailed discussions of the mathematical formalism for the numerical computation of the Green's function and of the fluctuation determinant. In the last section 1.7 of this chapter we discuss some peculiarities of the unstable and translation modes. Chapter 2 contains the renormalization in great detail. In Chap. 3 we apply the methods discussed for 3+1 dimensions to the 1+1 dimensional model. The numerical results for the 3+1 and 1+1 dimensions, and their comparison are extensively worked out in chapter 4. Part I is finalized by a summary of the main results.

Part II of this thesis is given up to the subject of global tunneling in compact spaces. The first chapter of this part, chapter 5, contains the discussion of the model (Sec.5.1), the approximations we are working with, and their application to our model (Sec.5.2). In the last section 5.3 we consider the divergences in the fluctuation integral and in the energy, and renormalize our model. The corresponding numerical results are presented in chapter 6.

The thesis is completed by several appendices containing some definitions, some detailed calculations of technical points and some other additional aspects.

Part 1.
The Bounce

"Innocent light-minded men, who think that astronomy can be learnt by looking at the stars without knowledge of mathematics will, in the next life, be birds."

Plato, Timaeos

Chapter 1
The Bounce in 3+1 Dimensions

In this chapter we present the model and the main relations necessary for our computations. We start with the basic relations of the classical bounce solution and recall the formula for computing the transition rate in the semiclassical approximation. Then we discuss two different approaches of including the quantum backreaction, giving some details of $2PPI$ and $1PI$ formalisms. In the next two sections we present the general discussion as well as the technical tools used for the numerical computation of the Green's function and the fluctuation determinant. At the end of this chapter we discuss some special aspects concerning the the unstable and translation modes.

1.1 The model and basic relations

We will consider a scalar field theory in 3+1 dimensions, which is given by Lagrangian density

$$\mathcal{L} = \frac{1}{2}\partial_\mu \Phi \partial^\mu \Phi - U(\Phi) . \tag{1.1}$$

As it was already mentioned in the introduction we consider the asymmetric double-well potential with the following parameterization

$$U(\Phi) = \frac{1}{2}m^2\Phi^2 - \eta\Phi^3 + \frac{1}{8}\lambda\Phi^4 , \tag{1.2}$$

shown in Fig.1.1. It has two minima, one at $\Phi = 0$ corresponding to the unstable (false) vacuum, and the second one at some positive value of field $\Phi = \Phi_{tv} > 0$ the stable vacuum called presenting true vacuum.

The bounce is an $O(4)$ symmetric nontrivial classical solution of the Euclidean field equations ($t \rightarrow -i\tau$). If we denote the classical field as ϕ, then the classical
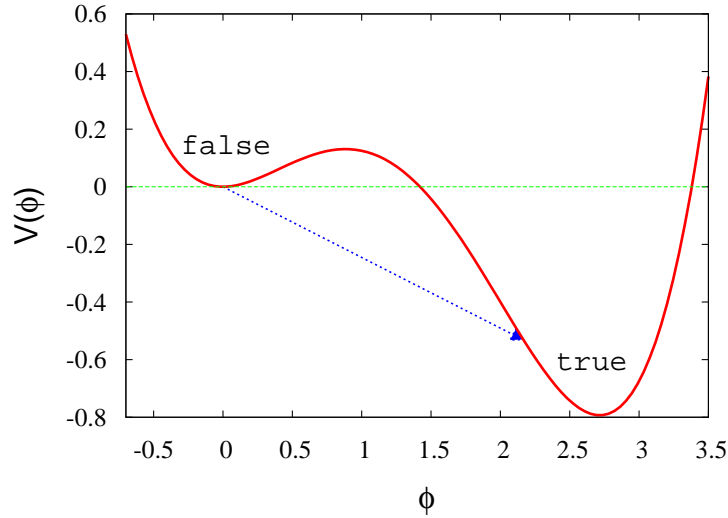
Figure 1.1: The tree level potential

Euclidean action is given by

$$S_{\text{cl}}[\phi] = \int d^4x \left[\frac{1}{2} \left(\nabla \phi \right)^2 + U(\phi) \right] , \tag{1.3}$$

and the bounce which minimizes this action satisfies

$$\left[-\left(\frac{\partial}{\partial t} \right)^2 - \Delta \right] \phi + U'(\phi) = 0 , \tag{1.4}$$

the Euler-Lagrange equation (Here we have denoted the Euclidean variables by $x_i = (x_1, x_2, x_3)$ and $x_0 = \tau$. The radius is $r = (x_0^2 + x_i^2)^{1/2}$). Using the spherical symmetry of this solution one can write the equation of motion as

$$-\frac{d^2\phi}{dr^2} - \frac{3}{r}\frac{d\phi}{dr} + U'(\phi) = 0 , \tag{1.5}$$

with the boundary conditions

$$\frac{d\phi}{dr}\Big|_{r=0} = 0, \qquad \phi_{r \to \infty} = \phi_{\text{fv}} . \tag{1.6}$$

They correspond to the end and the beginning of the tunneling, respectively.

As it was already mentioned in the Introduction the main quantity relevant for description of tunneling processes is the transition rate, the decay probability per unit time per unit volume γ [6]. The most common approach to compute the tunneling rate is the semiclassical one, where one starts with the tree level tunneling rate and then includes corrections of first order in $\hbar$. In this order, as discussed, e.g., in the work of C.G. Callan and S.R. Coleman [7], the fluctuations around the bounce profile contribute a pre-exponential factor to the decay rate. Then that the transition rate per unit volume and time takes the form

$$\Gamma^{1-\text{loop}} = \left(\frac{S_{\text{cl}}}{2\pi}\right)^2 \mathcal{D}^{-1/2} \exp(-S_{\text{cl}}) \, , \tag{1.7}$$

where

$$\mathcal{D}[\phi] = \text{det}' \frac{-\Delta_4 + \mathcal{M}^2}{-\Delta_4 + m^2} \tag{1.8}$$

determines the one-loop correction to the classical action

$$S_{1-\text{loop}} = \frac{1}{2} \ln \text{det}' \frac{-\Delta_4 + U''(\phi(x))}{-\Delta_4 + m^2} = \frac{1}{2} \ln \mathcal{D}[\phi] \, . \tag{1.9}$$

The detailed consideration and computation of the fluctuation determinant will be presented in Sec.1.6. Here Δ_4 is the Laplace operator in four dimensions. m is the mass in the false vacuum

$$m^2 = U''(0) \, . \tag{1.10}$$

The prime in the determinant implies that the translation zero mode is removed and that one replaces the imaginary frequency of the unstable mode by its absolute value. The prefactor in Eq.(1.7) arises from the quantization of the collective coordinate associated with translation mode. This subject will be discussed in more detail in Sec.1.7.

Once the quantum corrections become important one can ask whether these quantum fluctuations react back on the bounce profile and how significant is this influence. Two ways of including the quantum backreaction have been discussed in the literature: the one-loop backreaction and the Hartree backreaction. In next two sections we discuss these two approximations in general and in particular, for our model.

1.2 Non-perturbative approximations

There are phenomena in quantum field theory for which perturbation theory is inadequate. One of them is the process we are considering. For our computations

we will use approximations which are based on a non-perturbative resummation of Feynman diagrams involving one or more loops, i.e. containing arbitrary high orders of the coupling constants and propagators.

The first approximation which we present here is the simplest one, the one-loop approximation of the $1PI$ resummation scheme, summing all connected *one-particle-irreducible graphs*. The definitions of reducible and irreducible Feynman diagrams are briefly presented in Appendix A. At the one-loop level the summation corresponds to the graph displayed in Fig.1.2, where the line denotes the Green's function with all possible vertex insertions. Summing over all possible insertions results in
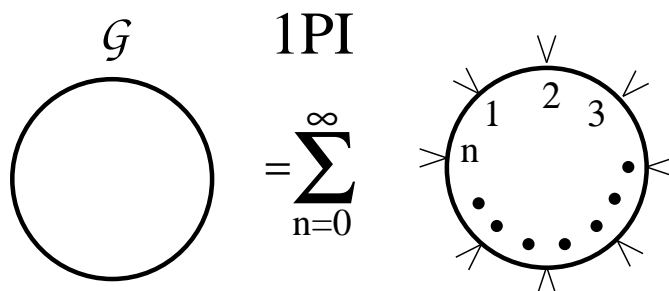
Figure 1.2: One-loop bubble diagram representing leading order of $1PI$. The line denotes a propagator $\mathcal{G}$.

the logarithm of the functional determinant

$$\Gamma_{1-loop}^{1PI} = \frac{1}{2} \ln \mathcal{D} , \qquad (1.11)$$

where $\mathcal{D}$ has been defined previously, see Eq. (1.8). All relevant equations are now derived by functional variation of the effective action, given by the sum of the classical and 1-loop actions

$$S_{eff} = S_{cl} + \Gamma_{1-loop}^{1PI}[\phi] . \qquad (1.12)$$

A detailed discussion of higher order $1PI$ graphs, including daisy, sunset (inclusive higher-loop), basketball graphs and chains of pearls can be found in Appendix C of [36].

The second approximation on which we focus our attention is the so called Hartree approximation, which is the one-loop level of the $2PPI$ resummation scheme. The $2PPI$ scheme sums all connected two-particle-point irreducible diagrams (in Appendix A one can find more detailed discussion of $2PPI$ expansion, which follows

the derivation given in [22]). At the one-loop level the summation corresponds to the simple loop diagram presented in Fig.1.3, where the resummation proceeds over
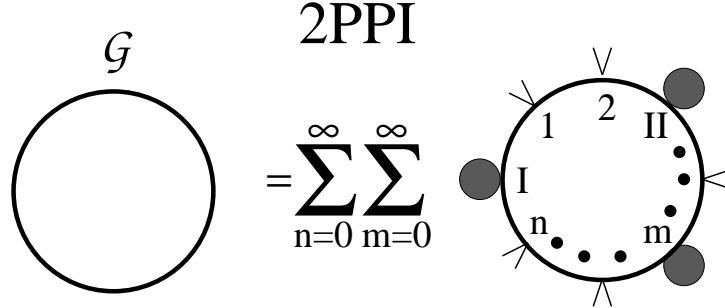
Figure 1.3: One-loop bubble diagram representing leading order of $2PPI$. The line denotes a propagator $\mathcal{G}$.

all possible vertex and self-energy insertions, i.e. all daisy and superdaisy graphs. Then the sum Γ^{2PPI} is truncated at

$$\Gamma^{2PPI}_{1-loop}[\phi, \mathcal{M}^2] = \frac{1}{2} \ln \mathcal{G}^{-1} \ , \tag{1.13}$$

where $\mathcal{G}$ represents the internal propagator with an effective mass $\mathcal{M}^2$. The effective mass fulfills the so-called gap equation, which is a simplified form of the Schwinger-Dyson equation. This equation indicates the connection of the effective mass to the self-energy. The self-energy is derived as a derivative of the quantum part of the effective action with respect to the effective mass

$$\frac{1}{2}\Delta(x) = \frac{\delta \Gamma^{2PPI}_{1-loop}[\phi, \mathcal{M}^2]}{\delta \mathcal{M}^2(x)} \ . \tag{1.14}$$

This is equivalent to cutting each internal line of the diagram and then connecting the two ends to the common point x.

1.3 The bounce in one-loop approximation

The backreaction to one-loop order consists in determining the classical field in such a way that it is an extremum of the one-loop effective action, the sum of classical and one-loop action. This approximation was introduced by Surig and applied for the bubble nucleation in a SU(2) gauge theory [20]. We will call this approximation

the one-loop backreaction. Sometimes quantum corrections are taken into account by means of the effective potential. In this case one determines the classical solution by solving the equations of motion using the effective potential instead of the tree level one. But we should notice that the effective potential is only the part of the effective action, as it does not take into account the space-time dependence of the background fields, i.e., it does not contain terms depending on the derivatives of the fields.

One can ask how good is the approximation where the terms including the derivatives of the background fields are neglected. This question was addressed for the electroweak phase transition, where using a derivative expansion obtained by the heat kernel method [37] and by an exact one-loop calculation [14] it was found that the corrections due to the nonlocal terms were of the same order as the classical action. That means that the nonlocal terms of the effective action are in general not negligible and should be taken into account already when computing the classical solution. The approximation we consider is exact to one loop, and thereby equivalent to a complete summation of the derivative expansion.

Based on the arguments given above the equations of motion (equations of bounce profile) will be derived not from the variation of the classical action, but of the effective action

$$\delta S_{eff} = \delta \left(S_{cl} + \Gamma^{1PI}_{1-loop} \right) = 0 \tag{1.15}$$

up to renormalization counterterms, which we will discuss in detail in chapter 3.

Recall that Γ^{1PI}_{1-loop} is the sum of all one-particle irreducible graphs defined in the previous section with the propagators

$$\mathcal{G}^{-1}(x) = -\Delta_4 + \mathcal{M}^2(x) \ , \tag{1.16}$$

where effective mass $\mathcal{M}^2$ is given by

$$\mathcal{M}^2 = U''(\phi) = m^2 - 6\eta\phi + \frac{3}{2}\lambda\phi^2 \ . \tag{1.17}$$

In this case it is just function of the field ϕ. The one-loop action is (as already discussed)

$$\Gamma^{1PI}_{1-loop}[\phi] = \frac{1}{2} \ln \det' \frac{-\Delta_4 + \mathcal{M}^2}{-\Delta_4 + m^2} \ . \tag{1.18}$$

Taking the partial derivative of the effective action with respect to the fields ϕ one gets the equation for the bounce profile

$$-\Delta_4\phi + U'(\phi(x)) + \frac{3}{2} \left[\lambda\phi(x) - 2\eta\right] \mathcal{F}(x) = 0 \ , \tag{1.19}$$

or using rotational symmetry,

$$-\frac{d^2\phi(r)}{dr^2} - \frac{3}{r}\frac{d\phi(r)}{dr} + m^2\phi(r) - 3\eta\phi^2(r) + \frac{\lambda}{2}\phi^3(r)$$
$$+\frac{3}{2}\left[\lambda\phi(r) - 2\eta\right]\mathcal{F}(x)\bigg|_{|x|=r} = 0 \ . \tag{1.20}$$

The first five terms are those of the classical equation of motion, the last one arises from the one-loop part using

$$\frac{\delta\Gamma^{1PI}}{\delta\phi(x)} = \frac{\delta\Gamma^{1PI}}{\delta\mathcal{M}^2(x)}\frac{d\mathcal{M}^2(x)}{d\phi(x)} = \frac{1}{2}\mathcal{F}(x)(3\lambda\phi(x) - 6\eta) \ . \tag{1.21}$$

Here we have introduced the fluctuation integral

$$\mathcal{F}(x) \equiv \mathcal{G}(x,x) = <x|\frac{1}{-\Delta_4 + \mathcal{M}^2}|x> = 2\frac{\delta\Gamma^{2PPI}}{\delta\mathcal{M}^2(x)} \ , \tag{1.22}$$

which is just the limit $x' \to x$ of the Green's function $\mathcal{G}(x,x')$.

1.4 The bounce in Hartree approximation

In the Hartree approximation one takes takes into account the backreaction not only onto the classical field, but also onto the quantum fluctuations. However, as discussed in Sec.1.2, one assumes that each fluctuation feels only the mean field of all others.

As in the one-loop approximation we should start our computation from the effective action of $2PPI$ formalism (the sum of all two-particle-point-irreducible diagrams, where all internal propagators have the effective mass $\mathcal{M}^2$[22]). We recall

$$S_{eff}[\mathcal{M}^2,\phi] = S_{cl}[\phi] + \Gamma^{2PPI}_{1-loop}[\mathcal{M}^2,\phi] - \frac{3\lambda}{8}\int d^4x\Delta^2(x) \ , \tag{1.23}$$

again up to renormalization counterterms. Here Δ is the self-energy discussed above

$$\frac{1}{2}\Delta(x) = \frac{\delta}{\delta\mathcal{M}^2(x)}\Gamma^{2PPI}[\phi,\mathcal{M}^2] \ . \tag{1.24}$$

It represents a local insertion into the propagator

$$\mathcal{G}^{-1}(x) = -\Delta_4 + \mathcal{M}^2(x) \ , \tag{1.25}$$

with effective mass defined as

$$\mathcal{M}^2 = m^2 - 6\eta\phi + \frac{3}{2}\lambda\phi^2 + \frac{3}{2}\lambda\Delta = U''(\phi) + \frac{3}{2}\lambda\Delta \ . \tag{1.26}$$

This is a self-consistent equation, called gap equation (the simplified form of the Schwinger-Dyson equation). To the lowest order in a loop expansion we consider (Hartree approximation)

$$\Gamma^{2PPI} = \frac{1}{2}\ln\det'\frac{-\Delta_4 + \mathcal{M}^2}{-\Delta_4 + m^2} \ . \tag{1.27}$$

So the self-energy Δ is given by

$$\Delta(x) = 2\frac{\delta\Gamma^{2PPI}}{\delta\mathcal{M}^2(x)} = <x|\frac{1}{-\Delta_4 + \mathcal{M}^2}|x> = \mathcal{G}(x,x) \ . \tag{1.28}$$

The Green's function is defined by equation

$$(-\Delta_4 + \mathcal{M}^2)\mathcal{G}(x,y) = \delta^4(x-y) \ . \tag{1.29}$$

We define the fluctuation integral as in the one-loop case

$$\mathcal{F}(x) \equiv \mathcal{G}(x,x) \ . \tag{1.30}$$

Taking the variational derivative of the effective action with respect to $\mathcal{M}^2$ we get again Eq. (1.26). In this procedure one considers Δ as a function of both the effective mass $\mathcal{M}^2$ and of the field ϕ. Therefore in the last term of the effective action (see Eq. (1.23)) we have to replace Δ by

$$\Delta = \frac{2}{3\lambda}\left(\mathcal{M}^2 - U''(\phi)\right) = -\phi^2 + \frac{2}{3\lambda}\left(\mathcal{M}^2 - m^2 + 6\eta\phi\right) \ . \tag{1.31}$$

The partial derivative of the effective action with respect to the field ϕ leads to the equation for the bounce profile in Hartree approximation

$$-\Delta_4\phi + U'(\phi(x)) + \frac{3}{2}\left[\lambda\phi(x) - 2\eta\right]\mathcal{F}(x) = 0 \ . \tag{1.32}$$

It is a complicated equation. As the fluctuation integral $\mathcal{F}$ is a nonlinear *functional* of the field ϕ this equation is not simply a differential or integro-differential equation. The backreaction of the quantum fluctuations onto themselves is contained in fluctuation integral $\mathcal{F}(x)$, or, equivalently, in effective mass $\mathcal{M}^2$.

Using the spherical symmetry one can write last equation in the radial form

$$-\frac{d^2\phi(r)}{dr^2} - \frac{3}{r}\frac{d\phi(r)}{dr} + m^2\phi(r) - 3\eta\phi^2(r) + \frac{\lambda}{2}\phi^3(r)$$

$$+\frac{3}{2}\left[\lambda\phi(r) - 2\eta\right]\mathcal{F}(x)\Big|_{|x|=r} = 0 . \qquad (1.33)$$

For a rotationally symmetric background field the fluctuation integral and correspondingly the effective mass are spherically symmetric as well.

1.5 The Green's Function

1.5.1 The formal discussion of Green's function

We have seen in last two sections that there is a universal quantity for both approximations necessary to compute the bounce profile, the Green's function $\mathcal{G}(x, x')$. It is very similar in both cases and needs the analogous technique of computation. The main difference comes from the effective mass, which as already discussed, in the one-loop formalism is simply a function of field ϕ, whereas in the Hartree approximation should be determined self-consistently.

The Green's function is usually discussed as a function of energy. We will need this generalization in order to be able to discuss the translation mode and to use the determinant theorem in the next section. For the basis see Sec. 1.6. To be consistent with future discussions we introduce the Euclidean energy ν^2 already here and determine the Green's function in more general form. However, at the end of our computations we will let $\nu = 0$, except for the treatment of the translation mode.

Within our generalization the field ϕ stays independent of ν, i.e. it still lives in four Euclidean dimensions. That means we have translation invariance in the direction of 'new time' (we have chosen fifth dimension to be spacelike). The Green's function $\mathcal{G}(x, x')$ now becomes $\mathcal{G}(x, x', \nu^2)$ and it satisfies equation

$$[-\Delta_4 + m^2 + V(r) + \nu^2]\mathcal{G}(x, x', \nu^2) = \delta^4(x - x') , \qquad (1.34)$$

with

$$V(r) = \mathcal{M}^2(\phi) - m^2 . \qquad (1.35)$$

where the effective mass $\mathcal{M}^2(\phi)$ is given by Eq. (1.17) or by Eq. (1.26) for the one-loop and Hartree approximations, respectively.

In the one-loop formalism $\mathcal{M}^2(0) = m^2$. So in the false vacuum when $r \to \infty$ the potential $V(r) \to 0$. In the Hartree formalism the effective mass contains the Green's function, i.e. it is a functional of field ϕ. Here the effective mass should be equal to bare mass $\mathcal{M}^2(0) = m^2$ for a constant field $\phi(x) \equiv 0$. This is one of requirements we impose on the effective potential as renormalization condition; otherwise, in the definition of $V(r)$ one would replace the bare mass m^2 with a different, renormalized mass in the false vacuum, and this would affect the boundary conditions of the fluctuations.

The Green's function can be expressed in terms of eigenfunctions of the fluctuation operator

$$\mathcal{G}(x, x', \nu^2) = \sum_{\alpha} \frac{\psi_\alpha(x)\psi_\alpha(x')}{\omega_\alpha^2 + \nu^2} \, , \tag{1.36}$$

which satisfy the equation

$$[-\Delta_4 + m^2 + V(r)]\psi_\alpha(x) = \omega_\alpha^2 \psi_\alpha(x) \, . \tag{1.37}$$

We decompose the Hilbert space into angular momentum subspaces, introducing the eigenfunctions $Y_{nlm}(\Omega_3)R_k^\alpha(r)$, where $Y_{nlm}(\Omega_3)$ are spherical functions on the 3-sphere (see Appendix of Ref.[38]). The radial wave functions are eigenfunctions of the partial wave fluctuation operator

$$\left[-\frac{d^2}{dr^2} - \frac{3}{r}\frac{d}{dr} + \frac{n(n+2)}{r^2} + m^2 + V(r) \right] R_{n\alpha}(r) = \omega_{n\alpha}^2 R_{n\alpha}(r) \, . \tag{1.38}$$

Here the index α labels the radial excitations, the spectrum is continuous, but may include some discrete states like unstable and translation modes. Using these eigenfunctions the Green's function can be written as

$$\mathcal{G}(x, x', \nu^2) = \sum_{nlm} \sum_{\alpha} Y_{nlm}(\Omega_3)Y_{nlm}(\Omega_3') \frac{R_{n\alpha}(r)R_{n\alpha}^*(r')}{\omega_{n\alpha}^2 + \nu^2} \, . \tag{1.39}$$

These expressions are formal. They are not suitable for numerical computations as they include summation over discrete states (unstable and translation modes) and integration over continuum states. In particular, if one uses this expressions for numerical computations, it is necessary to discretize the continuous spectrum by introduction a finite spatial boundary. But there is a well-known alternative possibility to express the Green's function.

1.5.2 Computation of the Green's function

Let us first consider free Green's function which one obtains if $V(r) = 0$. It can be written

$$G_0(x, x', \nu^2) = \int \frac{d^4k}{(2\pi)^4} \frac{e^{ik \cdot (x-x')}}{k^2 + m^2 + \nu^2} .$$ (1.40)

This quantity can be expanded as [39]

$$\int \frac{d^4k}{(2\pi)^4} \frac{e^{i\vec{k}(\vec{x}-\vec{x}')}}{\vec{k}^2 + m^2 + \nu^2} = \frac{\kappa^2}{4\pi^2} \frac{K_1(\kappa R)}{\kappa R}$$

$$= \frac{1}{2\pi^2} \sum_{n=0}^{\infty} (n+1) C_n^1(\cos\chi) \frac{I_{n+1}(\kappa r_<)}{r_<} \frac{K_{n+1}(\kappa r_>)}{r_>}$$

$$= \frac{1}{2\pi^2} \sum_{n=0}^{\infty} (n+1) C_n^1(\cos\chi) \mathcal{I}_n(r_<, \kappa) \mathcal{K}_n(r_>, \kappa) ,$$

where $r = |x|$ and $r' = |x'|$ and $r_< = \min\{r, r'\}$, $r_> = \max\{r, r'\}$. κ is defined as $\kappa = \sqrt{m^2 + \nu^2}$. R is given by

$$R^2 = |x - x'|^2 = r^2 + r'^2 - 2rr' \cos\chi ,$$ (1.41)

with χ as the angle between the directions Ω_3 and Ω'_3 of x and x', correspondingly. So the free Green's function can be expanded as

$$G_0(\vec{x}, \vec{x}', \nu^2) = \frac{1}{2\pi^2} \sum_{n=0}^{\infty} (n+1) C_n^1(\cos\chi) \mathcal{I}_n(r_<, \kappa) \mathcal{K}_n(r_>, \kappa) .$$ (1.42)

The functions C_n^1 are Gegenbauer polynomials, see corresponding section in Ref.[39]. The expansion of $K_1(\kappa R)$ in terms of products of $I_n(\kappa r_<)$ and $K_n(\kappa r_>)$ is the Gegenbauer expansion, given in section 7.61, Eq. (3) of Ref.[39]. For the case $x = x'$ one has $C_n^1(\cos\chi) = C_n^1(1) = n+1$. For convenience we have introduced functions $\mathcal{I}_n(r, \kappa)$ and $\mathcal{K}_n(r, \kappa)$ expressed by the modified Bessel functions in the following way

$$\mathcal{I}_n(r, \kappa) = I_{n+1}(\kappa r)/r , \qquad \mathcal{K}_n(r, \kappa) = K_{n+1}(\kappa r)/r .$$ (1.43)

They satisfy equation for the radial wave functions with $\omega = 0$

$$\left[-\frac{d^2}{dr^2} - \frac{3}{r} \frac{d}{dr} + \frac{n(n+2)}{r^2} + \kappa^2 \right] \mathcal{B}_n(r, \kappa) = 0 ,$$ (1.44)

where $\mathcal{B}_n$ stands for $\mathcal{I}_n$ or $\mathcal{K}_n$. $\mathcal{I}_n(r, \kappa)$ is regular at $r = 0$ and diverges exponentially as $r \to \infty$. $\mathcal{K}(r, \kappa)$ decreases exponentially as $r \to \infty$ and is singular as $r \to 0$. The Wronskian of these functions is given by

$$\mathcal{K}_n(r, \kappa) d\mathcal{I}_n(r, \kappa)/dr - \mathcal{I}_n(\kappa, r) d\mathcal{K}_n(r, \kappa)/dr = 1/r^3 . \tag{1.45}$$

Now we extend the expansion described above to the *exact* Green's function. We make the ansatz

$$\mathcal{G}(x, x', \nu^2) = \frac{1}{2\pi^2} \sum_{n=0}^{\infty} (n+1) C_n^1(\cos \chi) f_n^-(r_<, \kappa) f_n^+(r_>, \kappa) . \tag{1.46}$$

The functions $f_n^\pm(r, \kappa)$ satisfy the mode equations

$$\left[-\frac{d^2}{dr^2} - \frac{3}{r}\frac{d}{dr} + \frac{n(n+2)}{r^2} + \kappa^2 + V(r) \right] f_n^\pm(r, \kappa) = 0 , \tag{1.47}$$

and in addition the following boundary conditions:

$$\begin{aligned} f_n^-(r, \kappa) &\propto r^n & r \to 0 , \\ f_n^+(r, \kappa) &\propto \exp(-\kappa r)/\sqrt{\kappa r^3} & r \to \infty . \end{aligned} \tag{1.48}$$

So f_n^- is regular at $r = 0$ and f_n^+ is exponentially decreasing, i.e. bounded, as $r \to \infty$. For $V(r) = 0$ these boundary conditions are those satisfied by $\mathcal{I}_n(r, \kappa)$ and $\mathcal{K}_n(r, \kappa)$, respectively. As the behavior at $r = 0$ is determined by the centrifugal barrier, and the behavior for $r \to \infty$ by the mass term, these boundary conditions are independent of the potential. We can express these functions by means of $\mathcal{I}_n(r, \kappa)$ and $\mathcal{K}_n(r, \kappa)$ introducing the new functions $h_n^\pm(r, \kappa)$

$$\begin{aligned} f_n^-(r, \kappa) &= \mathcal{I}_n(r, \kappa)[1 + h_n^-(r, \kappa)] , \tag{1.49} \\ f_n^+(r, \kappa) &= \mathcal{K}_n(r, \kappa)[1 + h_n^+(r, \kappa)] . \tag{1.50} \end{aligned}$$

The functions $h_n^\pm(r, \kappa)$ become constant as $r \to 0$ and as $r \to \infty$, and for finite r they interpolate smoothly between these asymptotic constants. If we impose, for $r \to \infty$ the boundary conditions $h^\pm(r, \kappa) \to 0$ the Wronskian of f_n^+ and f_n^- becomes identical to the one between $\mathcal{K}_n(r, \kappa)$ and $\mathcal{I}_n(r, \kappa)$, i.e., equal to $1/r^3$.

Now applying the fluctuation operator Eq.(1.34) to our ansatz, Eq.(1.46), we find

$$\left[-\Delta_4 + \kappa^2 + V(r) \right] G(x, x', \nu^2) = \frac{1}{2\pi^2} \frac{1}{r^3} \delta(r - r') \sum_{n=0}^{\infty} (n+1) C_n^1(\cos \chi)$$

$$= \frac{1}{r^3} \delta(r - r') \frac{1}{\sin^2 \chi} \delta(\chi - \chi') \frac{1}{\sin \theta} \delta(\theta - \theta') \delta(\varphi - \varphi') , \tag{1.51}$$

where we have used the addition theorem

$$\sum_{l=0}^{n} \sum_{m=-l}^{l} Y_{nlm}(\Omega_3) Y_{nlm}^*(\Omega_3') = \frac{n+1}{2\pi^2} C_n^1(\cos \chi) \tag{1.52}$$

and the completeness relation for the $O(4)$ spherical harmonics.

Using the definitions of functions $h_n^\pm$, Eqs.(1.49) and (1.50), the Eq.(1.47) gives mode equations

$$\left\{ \frac{d^2}{dr^2} + \left[2\kappa \frac{I_{n+1}'(\kappa r)}{I_{n+1}(\kappa r)} + \frac{1}{r} \right] \frac{d}{dr} \right\} h_n^-(r, \kappa) = V(r) \left[1 + h_n^-(r, \kappa) \right] , \tag{1.53}$$

$$\left\{ \frac{d^2}{dr^2} + \left[2\kappa \frac{K_{n+1}'(\kappa r)}{K_{n+1}(\kappa r)} + \frac{1}{r} \right] \frac{d}{dr} \right\} h_n^+(r, \kappa) = V(r) \left[1 + h_n^+(r, \kappa) \right] , \tag{1.54}$$

which can be solved numerically. This point we will discuss in the next subsection. But before let us turn to the subtraction necessary in the process of renormalization.

To perform the subtractions we will need not only the functions $h_n^\pm$ exact to all orders in the potential $V(r)$, but also the functions of the first and second order. Let us denote them $h_n^{(1)\pm}$ and $h_n^{(2)\pm}$ (see Fig.1.4). In addition we have to define the

Figure 1.4: The structure of the first and second order $h_n^{(i)\pm}$ functions. The solid line represents the Green's function. Dots denote $V(r)$.

inclusive sums

$$h_n^{\overline{(m)}\pm} = \sum_{j=m}^{\infty} h_n^{(j)\pm} . \tag{1.55}$$

Here we follow the prescription developed in Ref. [40, 41, 12]. Obviously $h_n^\pm = h_n^{\overline{(1)}}$ as it includes all orders of $V(r)$ except the zero order part, which we have already separated by the definition of the functions $h_n^\pm$.

Eqs. (1.53) and (1.53) can be written in the following form

$$\mathcal{D}h = V(1 + h) \,, \tag{1.56}$$

where we introduce the notation $\mathcal{D}$ for the differential operator on the left hand side of equations and where for the moment we drop all indices. Using all definitions above it is easy to write down the equations for the first and second order as well as for the sum $h^{\overline{(2)}}$

$$
\begin{aligned}
\mathcal{D}h^{(1)} &= V \,, \\
\mathcal{D}h^{(2)} &= V h^{(1)} \,, \\
\mathcal{D}h^{\overline{(2)}} &= V h^{\overline{(1)}} \,.
\end{aligned}
\tag{1.57}
$$

The equations will have an analogous form for the functions of higher order in $V(r)$.

For the Green's function we likewise may define parts of a precise order in $V(r)$; and express them by means of functions $h_n^{(i)\pm}$ and sums $h^{\overline{(i)}\pm}$. For $x = x'$ we have

$$
\begin{aligned}
\mathcal{F}(x) \;=\; \mathcal{G}(x, x) &= \frac{1}{2\pi^2} \sum_{n=0}^{\infty} (n+1)^2 \mathcal{I}_n(r, \kappa) \mathcal{K}_n(r, \kappa) \\
&\times \left[1 + h_+^{\overline{(1)}}(r, \kappa) + h_-^{\overline{(1)}}(r, \kappa) + h_+^{\overline{(1)}}(r, \kappa) h_-^{\overline{(1)}}(r, \kappa) \right] \,,
\end{aligned}
\tag{1.58}
$$

$$
\begin{aligned}
\mathcal{F}^{\overline{(1)}}(x) \;=\; \mathcal{G}^{\overline{(1)}}(x, x) &= \frac{1}{2\pi^2} \sum_{n=0}^{\infty} (n+1)^2 \mathcal{I}_n(r, \kappa) \mathcal{K}_n(r, \kappa) \\
&\times \left[h_+^{\overline{(1)}}(r, \kappa) + h_-^{\overline{(1)}}(r, \kappa) + h_+^{\overline{(1)}}(r, \kappa) h_-^{\overline{(1)}}(r, \kappa) \right] \,,
\end{aligned}
\tag{1.59}
$$

$$
\begin{aligned}
\mathcal{F}^{\overline{(2)}}(x) \;=\; \mathcal{G}^{\overline{(2)}}(x, x) &= \frac{1}{2\pi^2} \sum_{n=0}^{\infty} (n+1)^2 \mathcal{I}_n(r, \kappa) \mathcal{K}_n(r, \kappa) \\
&\times \left[h_+^{\overline{(2)}}(r, \kappa) + h_-^{\overline{(2)}}(r, \kappa) + h_+^{\overline{(1)}}(r, \kappa) h_-^{\overline{(1)}}(r, \kappa) \right] \,.
\end{aligned}
\tag{1.60}
$$

While $\mathcal{G}^{\overline{(2)}}(x, x)$ is finite, $\mathcal{G}^{(0)}(x, x)$ and $\mathcal{G}^{(1)}(x, x)$ are divergent. This point will be discussed in the chapter 3.

1.5.3 Numerical procedure to compute Green's function

For the numerical computations we use the equations (1.53) and (1.54) for $h_n^{\pm}$ and equations for the functions of specified order in $V(r)$.

As it was already discussed in previous subsection the boundary conditions are chosen in such a way that at $r \to \infty$ $h_n^+ \to 0$. Therefore the differential equation for h_n^+, (1.54), is solved starting at large $r = \bar{r}$ with $h_n^+(\bar{r}, \kappa) = h_n^{+'}(\bar{r}, \kappa) = 0$, and running backward. In principle we should take $\bar{r} = \infty$. However, if $\bar{r}$ is chosen far outside the range of the potential the functions $h_n^{\pm}(r, \kappa)$ are already constant with high accuracy. In the numerical computation $r = \infty$ always means $r = \bar{r}$ with a suitable value of $\bar{r}$.

For the second differential equation (1.53) for h_n^- we first obtain a solution $\tilde{h}_n(r, \kappa)$ starting at $r = 0$, with $\tilde{h}_n(0, \kappa) = \tilde{h}_n'(0, \kappa) = 0$. This function does not satisfy the boundary condition required for the Green's function. The $h_n^-(r, \kappa)$ function we obtain in the following way: from the definition of the functions h_n we know

$$
\begin{aligned}
f_n^- &= \mathcal{I}_n(1 + h_n^-) \,, \\
\tilde{f}_n^- &= \mathcal{I}_n(1 + \tilde{h}_n^-) \,.
\end{aligned}
\tag{1.61}
$$

f_n^- and $\tilde{f}_n^-$ are both solutions of the same linear homogeneous differential equation and regular at $r = 0$, so they are proportional to each other, $f_n^- = C\tilde{f}_n^-$. The constant C can be fixed by means of the boundary condition at $r \to \infty$. It is given by

$$
C = \frac{1}{1 + \tilde{h}_n^-(\infty)} \,,
\tag{1.62}
$$

and as a result we obtain the solution of the differential equation with the appropriate boundary conditions in the following form:

$$
h_n^-(r, \kappa) = \frac{\tilde{h}_n(r, \kappa) - \tilde{h}_n(\infty, \kappa)}{1 + \tilde{h}_n(\infty, \kappa)} \,.
\tag{1.63}
$$

Of course, here as in the case of $h_n^+(\bar{r}, \kappa)$ $r = \infty$ is taken equal some finite value $r = \bar{r}$ in the numerical implementation.

The rescaling needed in order to get from preliminary result $\tilde{h}_n^-$ the function obeying the boundary conditions h_n^- is complicated by the mixing of orders. After some transformations one can obtain

$$
h^{(1)-} = \tilde{h}^{(1)-} - \tilde{h}_\infty^{(1)-}
\tag{1.64}
$$

and

$$
h^{\overline{(2)}-} = \frac{\tilde{h}^{(\bar{2})-} - \tilde{h}_\infty^{\overline{(2)}-} + \tilde{h}_\infty^{\overline{(1)}-}\tilde{h}_\infty^{(1)-} - \tilde{h}^{(1)-}\tilde{h}_\infty^{\overline{(1)}-}}{1 + \tilde{h}_\infty^{\overline{(1)}-}} \,.
\tag{1.65}
$$

So now we know enough about the Green's function and the functions entering the expression for it in order to implement them in the numerical simulations; of course, renormalization has still to be considered.

1.6 Computation of the Fluctuation Determinant

1.6.1 Application of the determinant theorem

We have seen that the quantum part of the effective action in both approximations is expressed by fluctuation determinant

$$\mathcal{D} = \det{}' \frac{-\Delta_4 + \mathcal{M}^2}{-\Delta_4 + m^2} \,, \tag{1.66}$$

which is formally an infinite product of eigenvalues of the fluctuation operator. The prime denotes taking the absolute value and removing the translation mode. This will be discussed in Sec. 1.7.

We will use the so called determinant theorem [42], or Gelfand-Yaglom theorem [43]. We introduce the generalization of the fluctuation determinant

$$\tilde{\mathcal{D}}(\nu^2) = \det \frac{-\Delta_4 + \mathcal{M}^2 + \nu^2}{-\Delta_4 + m^2 + \nu^2} \,, \tag{1.67}$$

where ν can be understood as an Euclidean energy in a fifth dimension. We should stress that this modification is purely technical and the computation itself refers to the four space-time dimensions, i.e. to $\nu = 0$. The only place there it will be used is a discussion of translation mode, as it gives a possibility to manipulate the pole in the Green's function in $l = 1$ partial wave (for more details see Sec. 1.7). Note that we have dropped prime here.

Using the decomposition of the Hilbert space into angular momentum subspaces we can rewrite

$$\tilde{\mathcal{D}}(\nu^2) = \prod_{l,n} \left[\frac{\omega_{ln}^2 + \nu^2}{\omega_{ln(0)}^2 + \nu^2} \right] = \prod_{n=0}^{\infty} \left[\frac{\det \mathbf{M}_n(\nu^2)}{\det \mathbf{M}_n^{(0)}(\nu^2)} \right]^{d_n} \,, \tag{1.68}$$

where

$$\mathbf{M}_n(\nu^2) = -\frac{d^2}{dr^2} - \frac{3}{r}\frac{d}{dr} + \frac{n(n+2)}{r^2} + m^2 + V(r) + \nu^2 \tag{1.69}$$

is radial fluctuation operator and d_n denotes the degeneracy. In four dimensions it is just $(n+1)^2$. $\mathbf{M}_n^{(0)}(\nu^2)$ corresponds to $V(r) = 0$.

According to a theorem on functional determinants of ordinary differential operators the ratio of the partial wave functional determinants can be expressed as

$$\frac{\det \mathbf{M}_n(\nu^2)}{\det \mathbf{M}_n^{(0)}(\nu^2)} = \lim_{r \to \infty} \frac{\psi_n(\nu^2, r)}{\psi_n^{(0)}(\nu^2, r)} \,, \tag{1.70}$$

Here the functions $\psi_n(\nu^2, r)$ and $\psi_n^{(0)}(\nu^2, r)$ are solutions of equations

$$\mathbf{M}_n(\nu^2)\psi_n(\nu^2, r) = 0 \;, \qquad \mathbf{M}_n^{(0)}(\nu^2)\psi_n^{(0)}(\nu^2, r) = 0 \;, \tag{1.71}$$

respectively, with identical regular boundary conditions at $r = 0$. A simple proof, given in Ref. [42], uses the fact that both sides have identical poles and zeros in the complex ν^2 plane.

It is obvious that the free partial wave function is given in terms of modified Bessel function, or in our notation by

$$\psi_n^{(0)}(\nu^2, r) = \mathcal{I}_n(r, \kappa) \;. \tag{1.72}$$

Furthermore, it is convenient to factorize the function $\psi_n(\nu^2, r)$ into the free solution $\psi_n^{(0)}(\nu^2, r)$ and a factor $1 + \tilde{h}_n(r, \kappa)$, which takes into account the modification due to potential $V(r)$:

$$\psi_n(\nu^2, r) = \left[1 + \tilde{h}_n(r, \kappa)\right] \mathcal{I}_n(r, \kappa) \;. \tag{1.73}$$

The function $\tilde{h}_n(r, \kappa)$, which satisfies $\tilde{h}_n(0, \kappa) = 0$ and $\tilde{h}'(0, \kappa) = 0$, has already been introduced previously (for details see Sec. 1.5).

So for the functional determinant we finally obtain

$$\frac{\det \mathbf{M}_n(\nu^2)}{\det \mathbf{M}_n^{(0)}(\nu^2)} = 1 + \tilde{h}_n(\infty, \kappa) \;, \tag{1.74}$$

and therefore

$$\ln \tilde{\mathcal{D}}(\nu^2) = \sum_{n=0}^{\infty} d_n \ln \left[1 + \tilde{h}_n(\infty, \kappa)\right] \;. \tag{1.75}$$

As already mentioned we need the fluctuation determinant only at $\nu^2 = 0$, except for the handling of the translation mode.

1.6.2 Expansion in terms of Feynman graphs and calculation of finite part

In order to have the possibility of renormalizing the fluctuation determinant we have to separate divergences. For this purpose we expand the full fluctuation determinant

in terms of external vertices

$$
\begin{aligned}
\ln \mathcal{D} &= \ln \det \frac{-\Delta_4 + U''(\phi)}{-\Delta_4 + U''(0)} = \ln \det \frac{-\Delta_4 + m^2 + V(x)}{-\Delta_4 + m^2} \\
&= \operatorname{tr} \ln \left[1 + (-\Delta_4 + m^2)^{-1} V(x)\right] = \sum_{N=1}^{\infty} \frac{(-1)^{N+1}}{N} \operatorname{tr} \left[(-\Delta_4 + m^2)^{-1} V(x)\right]^N \\
&= \sum_{N=1}^{\infty} \frac{(-1)^{N+1}}{N} A^{(N)} .
\end{aligned}
\tag{1.76}
$$

Actually

$$
A^{(N)} = \operatorname{tr} \left[(-\Delta_4 + m^2)^{-1} V(x)\right]^N
\tag{1.77}
$$

is identical to the one-loop Feynman graph of order N in the external potential $V(r)$. The first two terms in the expansion contain the logarithmic and quadratic ultraviolet divergences. They will be considered analytically in context of renormalization. However, the sum of all subsequent orders, resulting in $\ln \mathcal{D}^{\overline{(3)}}$, or explicitly

$$
\ln \mathcal{D}^{\overline{(3)}} = \sum_{n=0}^{\infty} d_n \ln \left[1 + h_n(\infty, \kappa)\right]^{\overline{(3)}} ,
\tag{1.78}
$$

will be computed numerically. The 'ln' term in the last expression is given by definition as

$$
\begin{aligned}
\ln \left[1 + h_n(\infty, \kappa)\right]^{\overline{(3)}} &= \ln \left(1 + h_n(\infty, \kappa)\right) - h_n^{(1)}(\infty, \kappa) \\
&\quad - \left[h_n^{(2)}(\infty, \kappa) - \frac{1}{2}(h_n^{(1)}(\infty, \kappa))^2\right] .
\end{aligned}
\tag{1.79}
$$

All contributions to $\ln \mathcal{D}^{\overline{(3)}}$ are finite, i.e. it can be computed numerically. However, in order to avoid delicate numerical subtractions of terms of different order in $V(r)$ we first rewrite the last expression in the following form

$$
\begin{aligned}
\ln \left[1 + h_n(\infty, \kappa)\right]^{\overline{(3)}} &= \left[\ln \left(1 + h_n(\infty, \kappa)\right) - h_n(\infty, \kappa) + \frac{1}{2}\left(h_n(\infty, \kappa)\right)^2\right] \\
&\quad + h_n^{\overline{(3)}}(\infty, \kappa) - \frac{1}{2} h_n^{\overline{(2)}}(\infty, \kappa) \left(h_n(\infty, \kappa) + h_n^{(1)}(\infty, \kappa)\right) .
\end{aligned}
\tag{1.80}
$$

Now each term on the right-hand side of the last expression is of order $V^3(r)$. And it is almost ready to be implemented in numerical code. First we should consider the question of unstable and translation modes.

1.7 Unstable and Translation Modes

Let us recall that determinant of the fluctuation operator was defined with a prime denoting modifications with respect to the naive determinant. We have ignored these modifications in the previous section when considering the computation of the determinant and of its finite part. As mentioned in sections 1.1 and 1.6 these modification concern:

(i) the unstable mode – the negative eigenvalue mode $\omega_u^2 < 0$ appearing in the s-wave, $n = 0$. It manifests itself by the fact that $1 + \tilde{h}_0(\infty, m) < 0$. So the original fluctuation determinant for $n = 0$ is negative and its square root appearing as a prefactor in Γ would be imaginary. However, as discussed, e.g., in Ref. [42], the transition rate appears as the imaginary part $i\Gamma$ of the energy. This implies that the factor i has to be removed in order to get Γ itself. This means that we have to replace the the fluctuation determinant by its absolute value. So for our computation this corresponds to just taking the absolute value of the expression $1 + \tilde{h}_0(\infty, m)$ in the logarithm in Eq. (1.78), for the $n = 0$ term. Incidentally this discussion implies that there should be exactly one unstable mode, this is the case here.

(ii) the translation mode – zero mode with vanishing of $\omega_t^2 = 0$, the lowest radial excitation in the $n = 1$ channel with degeneracy $(n + 1)^2 = 4$, which are Goldstone modes associated with the breaking of translation invariance (because we have four infinitesimal translations, we have four eigenfunctions with eigenvalue zero, proportional to $\partial_\mu \phi$), and thereby by the vanishing of $1 + \tilde{h}_1(\infty, m)$ at $\nu = 0$.

The presence of zero mode in the semiclassical approximation can be shown by taking the gradient of the classical equation of motion (see for example Ref. [42]):

$$\nabla_i \left[-\Delta_4 \phi + U'(\phi) \right] = \left[-\Delta_4 + U''(\phi) \right] \nabla_i \phi = 0 . \tag{1.81}$$

Here the operator acting on $\nabla_i \phi$ is just the fluctuation operator. The wave function associated with this mode is not Gaussian, so the translation mode does not appear in the fluctuation determinant, which arises from Gaussian integrations. This is implied by the prime on the determinant.The coordinate associated to the zero mode is a collective coordinate which has to be handled separately.

In the semiclassical approximation the quantization of the collective coordinate results in a prefactor $(\mathcal{N}_0^{-2}/2\pi)^2$ where

$$\mathcal{N}_0^{-2} = \int d^4x \, (\nabla_i \phi)^2 \tag{1.82}$$

is the normalization of the zero mode. Using a virial theorem this is usually converted into $(S_{\rm cl}/2\pi)^2$. Furthermore the dimension of the determinant with the prime

is different by 8 energy dimensions because four modes have been removed. As it appears in the denominator with a square root, this gives Γ the correct dimension (per volume, per time).

In semiclassical approximation the transition mode can be removed numerically following the prescription in Ref. [12]: one computes $\tilde{h}_1(\infty, \pm\epsilon^2)$ for some sufficiently small ϵ and replaces it everywhere as follows

$$\left[1 + \tilde{h}_1(\infty, m)\right] \to \frac{\tilde{h}_1(\infty, \epsilon^2) - \tilde{h}_1(\infty, -\epsilon^2)}{2\epsilon^2} \ , \tag{1.83}$$

i.e., one takes the numerical derivative at $\omega^2 = 0$.

There is another method of computation of $n = 1$ contribution to the transition rate recently discussed in the literature [19]. The authors integrate the radial equation for modes for some arbitrary but small quantity, similar to ν^2 we use. letting this parameter to zero they find the expression for the determinant with removed zero mode. Recalling that the zero mode one can express by means of the classical bounce solution and performing some transformations they find a simple formula

$$\left(\frac{S_{cl}[\phi]}{2\pi}\right)^2 \left(\frac{\det' \mathcal{M}_{n=1}}{\det \mathcal{M}_{n=1}^{(0)}}\right)^{-1/2} = \left[\frac{\pi}{2}\phi_\infty \left(\phi_0 - \frac{3}{2}\phi_0^2 + \frac{\alpha}{2}\phi_0^3\right)\right]^2 \ , \tag{1.84}$$

for the $n = 1$ prefactor contribution to the transition rate. Here ϕ_∞ corresponds to the point there the tunneling ends and is simply $\phi_0 = \phi(0)$. Such a simple formula one can understand as a technical simplification.

The method just described cannot be used for the case when the backreaction is included as there is no exact zero mode. The classical equation of motion receives additional contributions from the fluctuation integral, and so does the fluctuation operator in the Hartree approximation. In neither case $\nabla_i\phi$ is an eigenmode of the fluctuation operator. Basically the problem is that now the fluctuations enter the dynamics and they have to be taken into account when discussing translation invariance. This is an involved matter, for a discussion beyond the semiclassical approximation see, e.g. [44], a similar treatment in the present context is beyond the scope of this thesis.

Of course the exact theory is still translation invariant, the problem which we encounter is an artefact of the approximations we are making. So we have to find a pragmatic way for taking into account the collective coordinates and we have to remove four modes, otherwise we will not obtain a proper transition rate.

In fact, when backreaction is taken account we still find, in the $n = 1$ partial wave, a zero of $1 + \tilde{h}_1(\infty, -\omega_t^2)$ with ω_t^2 close to zero. This has been found already

in [20] in calculations for bubble nucleation. We will remove this mode as being the approximate translation mode.

By numerical computations we first should determine the position of the eigenvalue. This we do by requiring $1 + \tilde{h}_1(-\omega_t^2, \infty)$ to vanish and then compute the numerical derivative as in the semiclassical approximation (1.83) not at $\nu^2 = 0$ but at $\nu^2 = -\omega_t^2$, i.e., we remove a factor $\omega_t^2 + \nu^2$.

As the Green's function appears as a functional derivative of effective action we have to remove the zero mode as well. Recalling the form of Green's function in terms of eigenfunctions (1.39) we can separate the zero modes in $n = 1$ channel at $r = r'$

$$\mathcal{G}_1(r, r, \nu^2) = \frac{R_t^2(r)}{\nu^2 + \omega_t^2} + \sum_{\alpha \neq 0} \frac{R_{1\alpha}^2(r)}{\nu^2 + \omega_{1\alpha}^2} \ . \tag{1.85}$$

As a next step we can use the fact that the pole term is antisymmetric with respect to $\nu^2 + \omega_t^2$. So we compute the Green's function at $\nu^2 = -\omega_t^2 \pm \epsilon^2$ and take the average of these two values. Then the pole term disappears and the averaged Green's function takes the form

$$\frac{1}{2} \left[\mathcal{G}_1(r, r, -\omega_t^2 + \epsilon^2) + \mathcal{G}_1(r, r, -\omega_t^2 - \epsilon^2) \right] = \sum_{\alpha \neq 0} R_{1\alpha}^2(r) \frac{\omega_{1\alpha}^2 - \omega_t^2}{(\omega_{1\alpha}^2 - \omega_t^2)^2 - \epsilon^4} \ . \tag{1.86}$$

As long as ω_t^2 and ϵ^2 are much smaller than the ω_{1n}^2 this is a good approximation to the desired reduced Green's function

$$[\mathcal{G}_1(r, r, 0)]_{\text{red}} = \sum_{n \neq 0} \frac{R_{1n}^2(r)}{\omega_{1n}^2} \ . \tag{1.87}$$

This was again very formal discussion. However, the averaging used here one can apply to the explicit computations.

In the real numerical computations of the Green's function we use of course expression (1.46). It is obvious that the pole arise from the rescaling of the mode function $\tilde{h}_1(\nu^2, r)$, i.e., from dividing by $1 + \tilde{h}_-(\nu^2, \infty)$ (see Eq.(1.63)).

By the averaging over the Green's functions at $\nu^2 = -\omega_t^2 \pm \epsilon^2$ we add two very large terms which almost cancel. This is a delicate point and it should be done in a somewhat smoother way: if ϵ^2 is sufficiently small we can assume that $1 + \tilde{h}_1(\nu^2, \infty)$ passes through zero linearly and we may replace

$$1 + \tilde{h}_1(\infty, -\omega_t^2 \pm \epsilon^2) \to \pm \frac{1}{2} \left[\tilde{h}_1(\infty, -\omega_t^2 + \epsilon^2) - \tilde{h}_1(\infty, -\omega_t^2 - \epsilon^2) \right] \ . \tag{1.88}$$

So that the average over the Green's functions takes a form

$$[\mathcal{G}_1(r,r,0)]_{\text{red}} \simeq \frac{f_1^+(-\omega_t^2 + \epsilon^2, r)\tilde{f}_1(-\omega_t^2 + \epsilon^2, r) - f_1^+(-\omega_t^2 - \epsilon^2, r)\tilde{f}_1(-\omega_t^2 - \epsilon^2, r)}{\tilde{h}_1(-\omega_t^2 + \epsilon^2, \infty) - \tilde{h}_1(-\omega_t^2 - \epsilon^2, \infty)} ,$$

(1.89)

where $\tilde{f}_1(\nu^2, r) = I_1(\kappa r)[1 + \tilde{h}_1(\nu^2, r)]$ is the mode function f_1^- before the renormalization.

As the translation mode is only approximate, the virial theorem used for the semiclassical case no longer holds and we have to go back to the original expression for the prefactor of the transition rate. This prefactor is then just the normalization of the zero mode. Therefore one can compute the false vacuum decay rates via

$$\Gamma = \left(\frac{1}{2\pi\mathcal{N}_0'^2}\right)^2 \exp(-S_{eff}) .$$

(1.90)

Of course the treatment of the approximate zero mode is an additional approximation, beyond the one-loop or Hartree approximations. The question of allowable regions, justifying such an approximation, will be discussed along with the numerical results.

Chapter 2
Renormalization

In this chapter we present the discussion of the divergences and of renormalization. As we have already seen in the previous chapter the Green's function and the fluctuation determinant have divergences of logarithmic, quadratic and quartic order. For regularization we will use dimensional regularization, the numerical approach would admit other regularizations, like Pauli-Villars.

Besides the regularization we have to discuss the renormalization conditions. One way of renormalization we consider is $\overline{MS}$ scheme. This renormalization is often used when presenting the parameters of a theory as determined from experiment, or when making predictions for experimental data. In the context of semiclassical corrections this prescription was used in [18, 19]. The $\overline{MS}$ prescription has to be complemented by specifying a renormalization scale μ.

On the other hand, one may wish to compare the results of the various approaches for situations were the two vacua between which the tunneling takes place have similar "physical" properties. This would be the case if the renormalized one-loop or Hartree effective potentials and their classical counterparts have, e.g., the same position of the local minima and the same energy differences between the two vacua. The effective potential decribes the quantum corrections if the classical field is homogeneous in space-time. It is therefore relevant for the properties of the vacua and for qualitative features, as the double-well structure. Of course, the bounce is not homogeneous in space-time. However, we will use the effective potential to impose the renormalization conditions and fix the parameters of two vacua between which the tunneling takes place.

Altogether we will consider two approximations, Hartree approximation and one-loop approximation, in two different renormalization schemes, the $\overline{MS}$ scheme and the 'physical' renormalization, where in the last one we pose renormalization conditions on the effective potential in such a way as to have the same parameters for the vacua as in the classical theory. Details of the calculations can be found in the

corresponding Appendices.

2.1 Divergences of the Green's function and their regularization

We have already seen in Sec.1.5 that one can decompose the Green' function into parts of a well-defined order in $V(r)$

$$
\begin{aligned}
\mathcal{F}(x) &= \mathcal{F}^{(0)}(x) + \mathcal{F}^{(1)}(x) + \mathcal{F}^{\overline{(2)}}(x) \\
&= \int \frac{d^4k}{(2\pi)^4} \frac{1}{k^2 + m^2} \\
&\quad - \int d^4y V(y) \int \frac{d^4k}{(2\pi)^4} \frac{e^{ik(x-y)}}{k^2 + m^2} \int \frac{d^4k'}{(2\pi)^4} \frac{e^{-ik'(x-y)}}{k'^2 + m^2} + \mathcal{F}^{(\bar{2})}(x) \ .
\end{aligned}
\tag{2.1}
$$

Here, as we have discussed, the first and second terms are divergent and the last one convergent. The convergent part will be computed numerically (see section 1.5). The divergent terms will be considered analytically, renormalized and then the finite terms we will compute numerically.

Let us start with leading order part:

$$
\mathcal{F}^{(0)}(x) = \int \frac{d^4k}{(2\pi)^4} \frac{1}{k^2 + m^2} = -\frac{m^2}{16\pi^2} \left(L_\epsilon - \ln \frac{m^2}{\mu^2} + 1 \right) \ ,
\tag{2.2}
$$

the second equality is taken from appendix A, in particular equation (A.11).

The next to leading order term is more complicated:

$$
\begin{aligned}
\mathcal{F}^{(1)}(x) &= -\int d^4y V(y) \int \frac{d^4k d^4q}{(2\pi)^8} \frac{e^{ik(x-y)-k(x-y)+q(x-y)}}{(k^2+m^2)((k+q)^2+m^2)} \\
&= -\int d^4y V(y) \int \frac{d^4k}{(2\pi)^4} \int \frac{d^4q}{(2\pi)^4} \frac{e^{iq(x-y)}}{(k^2+m^2)((k+q)^2+m^2)} \\
&= -\int \frac{d^4k}{(2\pi)^4} \int \frac{d^4q}{(2\pi)^4} \frac{e^{iqx}\tilde{V}(q)}{(k^2+m^2)((k+q)^2+m^2)} \ ,
\end{aligned}
$$

where we have introduced $q = k' - k$ and where we have defined the Fourier transformation

$$
\tilde{V}(q) = \int d^4y e^{-iq \cdot y} V(y) \ .
\tag{2.3}
$$

The integration over k can be done analytically:

$$
\begin{aligned}
\mathcal{F}^{(1)}(x) &= -\int \frac{d^4q}{(2\pi)^4}e^{iqx}\tilde{V}(q)\int \frac{d^4k}{(2\pi)^4}\frac{1}{(k^2+m^2)((k+q)^2+m^2)} \\
&= \int \frac{d^4q}{(2\pi)^4}e^{iqx}\tilde{V}(q)\Bigg\{ -\frac{L_\epsilon - \ln\frac{m^2}{\mu^2}}{16\pi^2} \\
&\qquad -\frac{1}{16\pi^2}\left[2 - \frac{\sqrt{|q|^2+4m^2}}{|q|}\ln\frac{\sqrt{|q|^2+4m^2}+|q|}{\sqrt{|q|^2+4m^2}-|q|}\right]\Bigg\} \, .(2.4)
\end{aligned}
$$

In the last expression we have used results obtained in appendix A, in particular equation (A.12).

So we can decompose the next to leading term in the divergent and the finite parts

$$
\mathcal{F}^{(1)}(x) = -\frac{1}{16\pi^2}V(x)\left(L_\epsilon - \ln\frac{m^2}{\mu^2}\right) + \mathcal{F}^{(1)}_{fin}(x) \, , \tag{2.5}
$$

with

$$
\mathcal{F}^{(1)}_{fin}(x) = -\frac{1}{16\pi^2}\int \frac{d^4q}{(2\pi)^4}e^{iqx}\tilde{V}(q)\left[2 - \frac{\sqrt{|q|^2+4m^2}}{|q|}\ln\frac{\sqrt{|q|^2+4m^2}+|q|}{\sqrt{|q|^2+4m^2}-|q|}\right] \, .(2.6)
$$

The Fourier transformed potential $\tilde{V}(q)$ can be computed using the Fourier-Bessel transformation:

$$
\tilde{V}(q) \to \tilde{V}(|q|) = \frac{4\pi^2}{|q|}\int_0^\infty dr\, r^2 J_1(|q|r)V(r) \tag{2.7}
$$

For the detailed intermediate steps of Fourier-Bessel transformation see equation (A.13). As one can see, the integrand on the right hand side of (2.6), except for the exponential, depends only on the absolute value of q. As a consequence the fluctuation integral itself is a function of only the absolute value of x,

$$
\mathcal{F}^{(1)}_{fin}(x) \to \mathcal{F}^{(1)}_{fin}(r) \tag{2.8}
$$

which likewise is obtained as a Fourier-Bessel transformation.

2.2 Divergences of the fluctuation determinant and their regularization

As we already have seen in the Sec.1.6 the fluctuation determinant has divergences in the first $\mathcal{D}^{(1)}$ and second $\mathcal{D}^{(2)}$ order of expansion in the external potential $V(r)$

$$
\mathcal{D} = \mathcal{D}^{(1)} + \mathcal{D}^{(2)} + \mathcal{D}^{\overline{(3)}} \, . \tag{2.9}
$$

We will need this quantity in the 1-loop part of the effective action

$$S_{1-\text{loop}} = \frac{1}{2} \ln \mathcal{D} \ . \tag{2.10}$$

As discussed previously, see Eq. 1.76, the logarithm of the fluctuation determinant can be expanded with respect to powers of $V(r)$

$$\ln \mathcal{D} = \sum_{N=1}^{\infty} \frac{(-1)^{N+1}}{N} A^{(N)} \ . \tag{2.11}$$

The first two terms in the expansion are divergent. One can write

$$\ln \mathcal{D} = A^{(1)} - \frac{1}{2} A^{(2)} + (\ln \mathcal{D})^{\overline{(3)}} \ . \tag{2.12}$$

Let us consider each term separately.

$$A^{(1)} = \text{tr} \left[(-\Delta_4 + m^2)^{-1} V(x) \right] = \int \frac{d^4 k}{(2\pi)^4} \frac{\tilde{V}(0)}{k^2 + m^2} \ . \tag{2.13}$$

The Fourier transform of the potential has been defined in the previous section, and in particular

$$\tilde{V}(0) = \int d^4 x V(x) \ .$$

Using equation (A.11) we get

$$
\begin{aligned}
A^{(1)} &= \int \frac{d^{4-\epsilon} k}{(2\pi)^{4-\epsilon}} \frac{1}{k^2 + m^2} \int d^4 x V(x) = 2\pi^2 \int dr r^3 V(r) \int \frac{d^{4-\epsilon} k}{(2\pi)^{4-\epsilon}} \frac{1}{k^2 + m^2} \\
&= -2\pi^2 \int dr r^3 V(r) \frac{m^2}{16\pi^2} \left[\frac{2}{\epsilon} - \gamma + \ln 4\pi - \ln \frac{m^2}{\mu^2} + 1 \right] \ . \tag{2.14}
\end{aligned}
$$

In the last expression one can separate the divergent and finite terms:

$$A^{(1)} = -\frac{m^2}{16\pi^2} \left(L_\epsilon - \ln \frac{m^2}{\mu^2} \right) \int d^4 x V(x) + A_{fin}^{(1)} \ , \tag{2.15}$$

where finite part is

$$A_{fin}^{(1)} = -\frac{m^2}{8} \int dr r^3 V(r) \ . \tag{2.16}$$

For the second order term we have

$$
\begin{aligned}
A^{(2)} &= \operatorname{tr}\left[(-\Delta_4 + m^2)^{-1}V\right]^2 \\
&= \int \frac{d^4k}{(2\pi)^4}\frac{d^4k'}{(2\pi)^4}\int d^4x d^4y \, \frac{e^{i\vec{k}(\vec{x}-\vec{y})}e^{-i\vec{k}'(\vec{x}-\vec{y})}V(x)V(y)}{(k^2+m^2)(k'^2+m^2)} \, .
\end{aligned}
\tag{2.17}
$$

In terms of the Fourier transforms of the potential this can be rewritten as

$$
\begin{aligned}
A^{(2)} &= \int \frac{d^4k}{(2\pi)^4}\frac{d^4k'}{(2\pi)^4}\frac{1}{(k^2+m^2)(k'^2+m^2)}\int \frac{d^4q d^4q'}{(2\pi)^8}\tilde{V}(q)\tilde{V}(q') \\
&\times \int d^4x d^4y e^{i(k-k'+q)x}e^{i(q'+k'-k)y} \\
&= \int \frac{d^4k}{(2\pi)^4}\int \frac{d^4q}{(2\pi)^4}\frac{\tilde{V}(q)\tilde{V}(-q)}{(k^2+m^2)((k+q)^2+m^2)} \\
&= \int \frac{d^4k}{(2\pi)^4}\int \frac{d^4q}{(2\pi)^4}\frac{|\tilde{V}(q)|^2}{(k^2+m^2)((k+q)^2+m^2)} \, .
\end{aligned}
$$

Using result of appendix A (Eq.(A.12)) we have

$$
A^{(2)} = \frac{1}{16\pi^2}\left(L_\epsilon - \ln\frac{m^2}{\mu^2}\right)\int d^4x (V(x))^2 + A^{(2)}_{fin} \, ,
\tag{2.18}
$$

with the finite term

$$
A^{(2)}_{fin} = \frac{1}{128\pi^4}\int q^3 dq |\tilde{V}(q)|^2 \left[2 - \frac{\sqrt{q^2+4m^2}}{q}\ln\frac{\sqrt{q^2+4m^2}+q}{\sqrt{q^2+4m^2}-q}\right] \, .
\tag{2.19}
$$

Here as well as in the case of Green's function the finite terms will be evaluated numerically. But before discussing the numerical evaluation we will have to consider the divergent parts, i.e., we have to consider the renormalization in the one-loop and Hartree approximations.

2.3 Renormalization conditions

As it was already mentioned in the introduction of this chapter we will consider two different re normalizations: the $\overline{MS}$ scheme and a 'physical' scheme where we try to keep the effective potential close to the tree level one. While the $\overline{MS}$ prescription

is more or less straightforward, the renormalization conditions for the 'physical' scheme have to be discussed in some detail.

Because the bounce is not homogeneous in space-time one should use for the computations the *effective action*, this is what we have done until now. However, as we want to put some "physical" conditions on the quantum corrections and get renormalization conditions, we use the *effective potential* in order to fix the parameters of the two vacua between which the tunneling takes place.

The bounce solution is defined by the false vacuum boundary condition $r \to \infty$, i.e. $\phi(r) \to 0$ and $\mathcal{M}(r) \to m^2$ as $r \to \infty$. It is essential to maintain this asymptotic behavior of the bounce in one-loop and Hartree approximations. In other words we require that the left minimum of the effective potential remains at $\phi = 0$:

$$U_{eff}(0) = U(0) = 0 , \tag{2.20}$$

$$U'_{eff}(0) = U'(0) = 0 . \tag{2.21}$$

Next, we require that the mass remains the bare mass, i.e. the curvature of effective potential at $\phi = 0$ is unchanged

$$U''_{eff}(0) = U''(0) = m^2 . \tag{2.22}$$

Furthermore, it is reasonable to fix the true vacuum of the effective potential at its tree level value:

$$U'_{eff}(\phi_+) = 0 . \tag{2.23}$$

The last condition we can require is the conservation of the energy difference between two vacua:

$$U_{eff}(\phi_+) = U(\phi_+) = -\epsilon . \tag{2.24}$$

Of course the exact shapes of the effective potential in the semiclassical, one-loop and Hartree approximations will be different, but the two vacua, specified by the behavior near the two minima, will be similar to the tree level ones.

2.4 Renormalization in the one-loop approximation

For the one-loop backreaction case we choose the counterterm potential to be a fourth order polynomial of field ϕ with the following parameterization

$$\delta U = -\delta \mathcal{L} = \delta \rho \phi + \frac{1}{2} \delta m^2 \phi^2 - \delta \eta \phi^3 + \frac{1}{8} \delta \lambda \phi^4 , \tag{2.25}$$

where we have already taken into account that there will be no ϕ-independent "cosmological constant" term.

The detailed computation of the counterterms for the 'physical' renormalization conditions is given in the Appendix B. Here we present only the results:

$$\delta\rho = -\frac{12\eta m^2}{64\pi^2}(L_\epsilon - \ln\frac{m^2}{\mu^2} + 1) , \qquad (2.26)$$

$$\delta m^2 = \frac{3}{32\pi^2}(12\eta^2 + \lambda m^2)\left(L_\epsilon - \ln\frac{m^2}{\mu^2}\right) + \frac{3\lambda m^2}{32\pi^2} , \qquad (2.27)$$

$$\delta\eta = \frac{9\eta\lambda}{32\pi^2}\left(L_\epsilon - \ln\frac{m^2}{\mu^2}\right) + \delta\eta_f , \qquad (2.28)$$

$$\delta\lambda = \frac{9\lambda^2}{32\pi^2}\left(L_\epsilon - \ln\frac{m^2}{\mu^2}\right) + \delta\lambda_f . \qquad (2.29)$$

The finite terms $\delta\eta_f$ and $\delta\lambda_f$ are the solutions of a system of linear equations given in Appendix B.

The corresponding counter terms in the $\overline{\text{MS}}$ scheme are, by definition, just the parts proportional to L_ϵ. However, we have to deviate slightly from this convention and have to choose the linear counter term $\delta\rho\phi$ to coincide with the one for the 'physical' scheme, so $\delta\rho$ has to be chosen as in Eq. (2.26)); otherwise the false vacuum is shifted away from its tree level position $\phi = 0$. All other finite parts are set zero. A more detailed discussion of this point is given in the corresponding part of Appendix B.

With these counterterms the equations of motion and the effective action of the bounce become finite. Let us discuss them in more details.

The equation for the bounce profile in one-loop approximation is given by

$$\phi'' + \frac{3}{r}\phi' - U'(\phi) + \delta U'(\phi) + \frac{1}{2}U'''(\phi)\mathcal{F} = 0 . \qquad (2.30)$$

Using everything we have discussed in the previous sections the fluctuation term and the derivative of counterterm potential in the equation of motion are given by

$$\begin{aligned}
\delta U'(\phi) + \frac{1}{2}U'''\mathcal{F} &= \delta\rho + \delta m^2\phi - 3\delta\eta\phi^2 + \frac{1}{2}\delta\lambda\phi^3 \\
&+ \frac{1}{2}(3\lambda\phi - 6\eta)\left[-\frac{m^2}{16\pi^2}\left(L_\epsilon - \ln\frac{m^2}{\mu^2} + 1\right)\right. \\
&\left. - \frac{1}{16\pi^2}\left(\frac{3}{2}\lambda\phi^2 - 6\eta\phi\right)\left(L_\epsilon - \ln\frac{m^2}{\mu^2}\right) + \mathcal{F}_{fin}^{(1)} + \mathcal{F}^{\overline{(2)}}\right] .
\end{aligned}$$

After inserting the explicit expressions for counterterms, we see that all divergent terms cancel and one gets a finite expression for the sum of the fluctuation term and the counterterm potential

$$\delta U'(\phi) + \frac{1}{2}U'''\mathcal{F} = -3\delta\eta_f\phi^2 + \frac{1}{2}\delta\lambda_f\phi^3 + \frac{3}{2}(\lambda\phi - 2\eta)(\mathcal{F}_{fin}^{(1)} + \mathcal{F}^{\overline{(2)}}) \ .$$

So the finite equation for the bounce profile in the 'physical' renormalization scheme is given by

$$\phi'' + \frac{3}{r}\phi' - U'(\phi) - 3\delta\eta_f\phi^2 + \frac{1}{2}\delta\lambda_f\phi^3 + \frac{3}{2}(\lambda\phi - 2\eta)(\mathcal{F}_{fin}^{(1)} + \mathcal{F}^{\overline{(2)}}) = 0 \ . \qquad (2.31)$$

In the $\overline{\text{MS}}$ scheme, after some simple transformations using the counterterms we have discussed above, the equation for the bounce profile will have the form

$$\phi'' + \frac{3}{r}\phi' - U'(\phi) - \frac{3m^2\lambda}{32\pi^2}\phi\left(1 - \frac{m^2}{\mu^2}\right)$$
$$+ \frac{3}{2}(\lambda\phi - 2\eta)(\mathcal{F}_{fin}^{(1)} + \mathcal{F}^{\overline{(2)}}) = 0 \ , \qquad (2.32)$$

which we get from the previous one if we put the $\delta\eta_f$ and $\delta\lambda_f$ counterterms zero and take into account the finite part of the leading order of the fluctuation integral, as it does not cancel in this scheme.

The next quantity we should discuss is the effective action

$$\begin{aligned}
S_{eff} &= S_{cl} + S_{1-loop} + \int d^4x\,\delta U \\
&= S_{cl} - \frac{m^2}{32\pi^2}\left(L_\epsilon - \ln\frac{m^2}{\mu^2}\right)\int d^4x\,V(x) + \frac{1}{2}A_{fin}^{(1)} - \frac{1}{4}A_{fin}^{(2)} \\
&\quad - \frac{1}{64\pi^2}\left(L_\epsilon - \ln\frac{m^2}{\mu^2}\right)\int d^4x\,(V(x))^2 + \frac{1}{2}(\ln\mathcal{D})^{\overline{(3)}} + \int d^4x\,\delta U \ .
\end{aligned}$$

After some simple transformations the full one-loop action for the physical renormalization becomes

$$S_{eff} = S_{cl} + \frac{1}{2}(\ln\mathcal{D})^{\overline{(3)}} - \frac{1}{4}A_{fin}^{(2)} + \int d^4x\left(-\delta\eta_f\phi^3 + \frac{1}{8}\delta\lambda_f\phi^4\right) \ . \qquad (2.33)$$

Note that the finite term $A_{fin}^{(1)}$ cancels against the finite parts of the ϕ independent, the linear and the mass counterterms.

In the $\overline{\text{MS}}$ scheme the one-loop effective action has a similar form. If we put the finite parts of the counterterms equal zero, except in $\delta\rho$, we get

$$
\begin{aligned}
S_{eff} &= S_{cl} + \frac{1}{2}\left(\ln\mathcal{D}\right)^{\overline{(3)}} + \frac{1}{2}A^{(1)}_{fin} - \frac{1}{4}A^{(2)}_{fin} \\
&\quad - \frac{3m^2\eta}{16\pi^2}(1 - \ln\frac{m^2}{\mu^2})\int d^4x\,\phi \ .
\end{aligned}
\tag{2.34}
$$

2.5 Renormalization in the Hartree approximation

For the Hartree backreaction case all divergent parts are related. As a consequence these divergences can be removed by one counter term

$$
\delta U_{div} = B(\mathcal{M}^4 - m^4) = \frac{1}{64\pi^2}\left(L_\epsilon - \ln\frac{m^2}{\mu^2} + 1\right)(\mathcal{M}^4 - m^4) \ .
\tag{2.35}
$$

Here we have used notations of Appendix C for the counterterm. The part proportional to m^2 is an infinite renormalization of the vacuum energy.

If we want to make the results of this approximation comparable with the ones in the one-loop approximation we have to do the finite renormalization. So we define the counterterm potential in Hartree approximation to be a sum of the divergent counterterm (2.35) and the finite fourth order polynomial in field ϕ

$$
\delta U = \delta U_{div} + \delta\Lambda_{fin} + \delta\rho_{fin}\phi + \frac{1}{2}\delta m^2_{fin} - \delta\eta_{fin}\phi^3 + \frac{1}{8}\delta\lambda_{fin}\phi^4 \ .
\tag{2.36}
$$

Using the detailed calculations of Appendix C we find the cosmological constant, the linear and the mass counterterms to be zero. Two other counterterms satisfy a system of linear equations which contain the effective mass, i.e., because of the gap equation we get a set of nonlinear equations. These can be solved numerically using an iterative procedure (see Appendix C).

Using this counterterms we find the finite gap equation of the following form:

$$
\mathcal{M}^2(x) = m^2 - 6(\eta + \delta\eta_f)\phi(x) + \frac{3}{2}(\lambda + \delta\lambda_f)\phi^2(x) + \frac{3}{2}\lambda\mathcal{F}_{fin}(x) \ ,
\tag{2.37}
$$

with

$$
\mathcal{F}_{fin}(x) = \frac{\mathcal{M}^2 - m^2}{16\pi^2} + \mathcal{F}^{(1)}_{fin}(x) + \mathcal{F}^{\overline{(2)}}(x) \ .
\tag{2.38}
$$

The finite equation for bounce profile becomes

$$
-\Delta_4\phi + U'(\phi) + \delta U'_{fin}(\phi) + \frac{1}{2}[-6(\eta + \delta\eta_f) + 3(\lambda + \delta\lambda_f\phi)]\mathcal{F}_{fin} = 0 \ ,
\tag{2.39}
$$

and the effective action is

$$
\begin{aligned}
S_{eff} &= S_{cl} + S_{1-loop} - \frac{3\lambda}{8} \int d^4 x \Delta^2(x) + \int d^4 x \delta U \\
&= S_{cl} + \frac{1}{2} \left(\ln \mathcal{D} \right)^{\overline{(3)}} + \frac{1}{2} A^{(1)} - \frac{1}{4} A^{(2)} - \frac{3\lambda}{8} \int d^4 x \mathcal{F}_{fin}^2 + \int d^4 x \delta U \ .
\end{aligned}
$$

After some simple transformations the effective action for the 'physical' renormalization scheme becomes

$$
\begin{aligned}
S_{eff} &= S_{cl} + \frac{1}{2} \left(\ln \mathcal{D} \right)^{\overline{(3)}} - \frac{1}{4} A_{fin}^{(2)} + \frac{1}{64\pi^2} \int d^4 x V^2(x) - \frac{3\lambda}{8} \int d^4 x \mathcal{F}_{fin}^2(x) \\
&\quad + \int d^4 x \left[-\delta \eta_f \phi^3(x) + \frac{1}{8} \delta \lambda_f \phi^4(x) \right] \ .
\end{aligned} \tag{2.40}
$$

Note that finite term $A_{fin}^{(1)}$ cancels as a whole against some combination of the counterterms.

Unlike the one-loop approximation in the Hartree $\overline{\mathrm{MS}}$ scheme $A_{fin}^{(1)}$ does not appear, it cancels with the finite part of the only counterterm we introduce in this case. So that the effective action reduces to

$$
S_{eff} = S_{cl} + \frac{1}{2} \left(\ln \mathcal{D} \right)^{\overline{(3)}} - \frac{1}{4} A_{fin}^{(2)} + \frac{1}{64\pi^2} \int d^4 x V^2(x) - \frac{3\lambda}{8} \int d^4 x \mathcal{F}_{fin}^2(x) \ . \tag{2.41}
$$

In this case gap equation and the equation of motion do not contain any finite counterterms

$$
\mathcal{M}^2(x) = m^2 - 6\eta \phi(x) + \frac{3}{2} \lambda \phi^2(x) + \frac{3}{2} \lambda \mathcal{F}_{fin}(x) \ , \tag{2.42}
$$

$$
-\Delta_4 \phi + U'(\phi) + \frac{3}{2} (-2\eta + \lambda \phi(x)) \mathcal{F}_{fin} = 0 \ . \tag{2.43}
$$

As it was already mentioned in Appendix C, none of equations in Hartree approximation depend on renormalization scale. Due to the special structure of divergences the μ dependence is removed automatically together with the divergent term.

Chapter 3
Self-consistent bounce in 1+1 dimensions

Along with numerical results for the 3+1 dimensional case we will present numerical results of the computations in 1+1 dimensions, and compare these results with the corresponding ones in 3+1 dimensions. Therefore in this chapter we discuss briefly the modifications, or more precisely the simplifications of the analytical background presented in the previous chapters.

The initial motivation for considering the 1+1 dimensional model was the work of Bergner and Bettencourt [45] who have computed the self-consistent corrections for two systems: the kink in one space dimension and the bounce solution in two Euclidean dimensions. In Ref. [46] we have reconsidered their approach, using different methods for computing the quantum corrections, the methods we have presented for 3+1 dimensional in the previous chapters.

3.1 Changes in Basic Relations

3.1.1 The model

We consider a scalar field theory in 2D, with Lagrange density

$$\mathcal{L} = \frac{1}{2}\partial_\mu \Phi \partial^\mu \Phi - U(\Phi) \, , \tag{3.1}$$

where the potential is given as before by

$$U(\Phi) = \frac{1}{2}m^2\Phi^2 - \eta\Phi^3 + \frac{1}{8}\lambda\Phi^4 \, . \tag{3.2}$$

The bounce is an SO(2) symmetric classical solution of the Euclidean field equations $(t \rightarrow -i\tau)$. Denoting the Euclidean variables by $x_1 = x$ and $x_2 = \tau$ the radius becomes $r = \sqrt{x_1^2 + x_2^2}$.

The classical Euclidean action is given by

$$S_{cl}[\phi] = \int d^2x \left[\frac{1}{2} (\nabla \phi)^2 + U(\phi) \right] \, , \tag{3.3}$$

and the bounce which minimizes this action satisfies

$$-\Delta_2 \phi + U'(\phi) = 0 \, , \tag{3.4}$$

or in the radial form

$$-\frac{d^2\phi}{dr^2} - \frac{1}{r}\frac{d\phi}{dr} + U'(\phi) = 0 \, , \tag{3.5}$$

with boundary conditions

$$\frac{d\phi}{dr}\Big|_{r=0} = 0, \qquad \phi_{r\to\infty} = \Phi_+ \, , \tag{3.6}$$

as in 4-dimensional case.

The form of the semiclassical transition rate remains the same, the only difference appears in the S_{1-loop} part, where Δ_4 should be replaced by the Laplace operator in two dimensions, Δ_2. So the one-loop correction to the classical action is now given by

$$S_{1-loop} = \frac{1}{2} \ln \det' \frac{-\Delta_2 + U''(\phi(\vec{x}))}{-\Delta_2 + m^2} = \frac{1}{2} \ln \mathcal{D}[\phi] \, , \tag{3.7}$$

where m is the mass in the false vacuum, as before,

$$m^2 = U''(0) \, . \tag{3.8}$$

and the prime again denotes that the translation zero mode has to be removed and that one replaces the imaginary frequency of the unstable mode by its absolute value.

3.1.2 The one-loop and Hartree approximations for the 2D bounce

There are no changes of principle in the formalism of the one-loop and Hartree backreactions. All changes should be done are connected to the replacement of the four dimensional partial derivatives with two dimensional ones.

In the both approximations corresponding propagators are defined as

$$\mathcal{G}^{-1}(x) = -\Delta_2 + \mathcal{M}^2(x) . \tag{3.9}$$

The Green's function is defined by the equation

$$(-\Delta_2 + \mathcal{M}^2)\mathcal{G}(\vec{x}, \vec{y}) = \delta^2(\vec{x} - \vec{y}) . \tag{3.10}$$

The equation for the bounce profile in both cases is

$$-\Delta_4 \phi + U'(\phi(x)) + \frac{3}{2} \left[\lambda\phi(x) - 2\eta\right] \mathcal{F}(x) = 0 , \tag{3.11}$$

or using rotational symmetry,

$$-\frac{d^2\phi(r)}{dr^2} - \frac{1}{r}\frac{d\phi(r)}{dr} + m^2\phi(r) - 3\eta\phi^2(r) + \frac{\lambda}{2}\phi^3(r)$$
$$+ \frac{3}{2}\left[\lambda\phi(r) - 2\eta\right]\mathcal{F}(x)\bigg|_{|x|=r} = 0 . \tag{3.12}$$

The structure of the effective masses remains as before.

3.1.3 Green's function

Here as well as in the 4 dimensional case we consider generalization of the Green's function, which in equivalent to the introduction of an additional dimension, needed for handling the translation mode. The translation mode we will not be discussed again for the 2 dimensional case, as this discussion is similar to the one for 4 dimensions.

The Green's function satisfies

$$[-\Delta_2 + m^2 + V(r) + \nu^2]\mathcal{G}(\vec{x}, \vec{x}') = \delta^2(\vec{x} - \vec{x}') , \tag{3.13}$$

with

$$V(r) = -6\eta\phi(r) + \frac{3}{2}\lambda\left(\phi^2(r) + \mathcal{G}(\vec{x}, \vec{x})\right) . \tag{3.14}$$

The Green's function can be expressed by the eigenfunctions of the fluctuation operator

$$\mathcal{G}(\vec{x}, \vec{x}', \nu^2) = \sum_\alpha \frac{\psi_\alpha(\vec{x})\psi_\alpha(\vec{x}')}{\omega_\alpha^2 + \nu^2} . \tag{3.15}$$

which satisfy

$$[-\Delta_2 + m^2 + V(r)]\psi_\alpha(\vec{x}) = \omega_\alpha^2 \psi_\alpha(\vec{x}) . \tag{3.16}$$

After the decomposition of the Hilbert space into angular momentum subspaces, the radial wave functions $R_{nl}(r)$ are eigenfunctions of the partial wave fluctuation operator:

$$\left[-\frac{d^2}{dr^2} - \frac{1}{r}\frac{d^2}{dr^2} + \frac{l^2}{r^2} + m^2 + V(r) \right] R_{nl}(r) = \omega_{nl}^2 R_{nl}(r) . \tag{3.17}$$

Then the Green's function takes the form

$$\mathcal{G}(\vec{x}, \vec{x}') = \sum_l \sum_n e^{il(\varphi-\varphi')} \frac{R_{nl}(r)R_{nl}(r')}{\omega_{nl}^2 + \nu^2} . \tag{3.18}$$

For the real computations again we will use the expansion of the Green's function in the modes. The free Green's function is now given by

$$G_0(\vec{x}, \vec{x}', \nu^2) = \int \frac{d^2k}{(2\pi)^2} \frac{e^{i\vec{k}(\vec{x}-\vec{x}')}}{k^2 + \nu^2 + m^2} \tag{3.19}$$

and for the expansion into partial waves one gets

$$G_0(\vec{x}, \vec{x}', \nu^2) = \frac{1}{2\pi} \sum_{l=-\infty}^{\infty} e^{il(\varphi-\varphi')} I_l(\kappa r_<) K_l(\kappa r_>) , \tag{3.20}$$

where $r_< = \min |\vec{x}|, |\vec{x}'|$, $r_> = \max |\vec{x}|, |\vec{x}'|$ and $\kappa^2 = m^2 + \nu^2$. The modified Bessel functions satisfy

$$\left[-\frac{d^2}{dr^2} - \frac{1}{r}\frac{d^2}{dr^2} + \frac{l^2}{r^2} + \kappa^2 \right] B_l(\kappa r) = 0 , \tag{3.21}$$

where B_l stands for I_l or K_l. Their Wronskian is given by

$$K_l(\kappa r)dI_l(\kappa r)/dr - I_l(\kappa r)dK_l(\kappa r)/dr = 1/r . \tag{3.22}$$

The expansion of the exact Green's function is based on the ansatz

$$\mathcal{G}(\vec{x}, \vec{x}', \nu^2) = \frac{1}{2\pi} \sum_{l=-\infty}^{\infty} e^{il(\varphi-\varphi')} f_l^-(r_<, \nu^2) f_l^+(r_>, \nu^2) . \tag{3.23}$$

The functions $f_l^\pm(r, \nu^2)$ satisfy the mode equations

$$\left[-\frac{d^2}{dr^2} - \frac{1}{r}\frac{d^2}{dr^2} + \frac{l^2}{r^2} + \kappa^2 + V(r) \right] f_l^\pm(r, \nu^2) = 0 , \tag{3.24}$$

and exactly the same boundary conditions as in the 4 dimensional theory.

From the technical point of view we introduce the functions $h^{\pm}(r, \nu^2)$ which interpolate smoothly between the boundaries at $r \to 0$ and $r \to \infty$ and satisfy the equations

$$\{\frac{d^2}{dr^2} + [2\kappa\frac{I_l'(\kappa r)}{I_l(\kappa r)} + \frac{1}{r}]\frac{d}{dr}\}h_l^-(r, \nu^2) = V(r)[1 + h_l^-(r, \nu^2)] , \tag{3.25}$$

$$\{\frac{d^2}{dr^2} + [2\kappa\frac{K_l'(\kappa r)}{K_l(\kappa r)} + \frac{1}{r}]\frac{d}{dr}\}h_l^+(r, \nu^2) = V(r)[1 + h_l^+(r, \nu^2)] , \tag{3.26}$$

which we have to solve numerically in a way it was described in the numerical part of Sec.1.5. Finally the Green's function is given by

$$\mathcal{G}(\vec{x}, \vec{x}', \nu^2) = \frac{1}{2\pi} \sum_{l=-\infty}^{\infty} e^{il(\varphi-\varphi')} I_l^-(\kappa r_<) K_l^+(\kappa r_>)(1 + h_l^-(r_<, \nu^2))(1 + h_l^+(r_>, \nu^2)) . \tag{3.27}$$

3.1.4 Fluctuation determinant

The formal discussion of the fluctuation determinant will be left out. There one should just make changes corresponding to the change of number of dimensions.

The fluctuation determinant can be expressed by means of $\tilde{h}_l(\infty, \nu^2)$ functions (which are solutions of equation for $h_l^-(r, \nu^2)$ starting a $r = 0$)

$$\frac{\det \mathbf{M}_l(\nu^2)}{\det \mathbf{M}_l^{(0)}(\nu^2)} = 1 + \tilde{h}_l(\infty, \nu^2) , \tag{3.28}$$

and

$$\ln \tilde{\mathcal{D}}(\nu^2) = \sum_{l=0}^{\infty} d_l \ln \left[1 + \tilde{h}_l(\infty, \nu^2)\right] , \tag{3.29}$$

where d_l denotes the degeneracy, $d_l = 2$ for $l > 0$ and $d_l = 1$ for $l = 0$. As before the fluctuation determinant in the transition rate formula refers to the fluctuation operator at $\nu^2 = 0$ and therefore in the numerical computations we will just need the functions $\tilde{h}_l(\infty, 0)$ as for the Green's function, except for the $l = 1$ mode.

3.2 Renormalization

3.2.1 Divergences and the renormalization of the non-perturbative part

It is well-known that renormalization in $1 + 1$ dimensions requires only normal ordering. This means that we have to redefine the Green's function by

$$\mathcal{G}(\vec{x}, \vec{x}) \rightarrow \mathcal{G}(\vec{x}, \vec{x}) - \mathcal{G}_0(\vec{x}, \vec{x}) \ , \tag{3.30}$$

which in the Hartree approximation will redefine the $\Delta(\vec{x})$ as well. The last expression can be written in terms of $h_l^{\pm}(r)$ functions

$$\Delta(\vec{x}) = \sum_{l=0}^{\infty} d_l I_l(mr) K_l(mr) \left[h_l^-(r) + h_l^+(r) + h_l^-(r) h_l^+(r) \right] \ . \tag{3.31}$$

In addition one has to subtract the tadpole diagram in the fluctuation determinant as well. The only divergent part of the perturbative expansion is

$$\left[\frac{1}{2} \ln \mathcal{D} \right]_{div} = \frac{1}{2} \int d^2 x V(r) \mathcal{G}_0(\vec{x}, \vec{x}) \ , \tag{3.32}$$

which has to be removed. It is less trivial to remove it from the non-perturbative part. It was computed using the partial waves. Now we notice that the part we want to remove is of order $V(r)$, so in the partial waves it should be given by the contributions of the first order in $V(r)$. This is easy to compute. One just calculates the first order contribution $\tilde{h}_l^{(1)}(r)$ solving numerically the mode equation

$$\{ \frac{d^2}{dr^2} + [2m \frac{I_l'(mr)}{I_l(mr)} + \frac{1}{r}] \frac{d}{dr} \} \tilde{h}_l^{(1)}(r) = V(r) \ , \tag{3.33}$$

and then subtracts it from contribution to the fluctuation determinant of a l partial wave

$$d_l \ln(1 + \tilde{h}_l(\infty)) \rightarrow d_l \left[\ln(1 + \tilde{h}_l(\infty)) - \tilde{h}_l^{(1)}(\infty) \right] \ . \tag{3.34}$$

The normal ordering is not unique. It depends on the mass used. In our calculations we use the mass of the false vacuum. It can be changed and this change will correspond to the redefinition of the couplings of our model η and λ.

Removing the divergent parts proceeds by adding counterterms corresponding to the 1-loop and Hartree approximations.

3.2.2 Counterterms for the 1-loop approximation

Here as well as in the 4 dimensional case we will compare two different renormalization schemes, $\overline{MS}$ and the one with "physical" renormalization conditions. These conditions we leave as before, they should keep the effective potential close to the tree-level one, i.e. they fix two vacua between which the tunneling takes place. The computational technique we use for this purpose is the same as in the 4D case, therefore we will not go into details and present only the results.

From the form of the divergent terms one can infer that for the renormalization for the one-loop backreaction one just needs a polynomial of the second order. However, in order to have the possibility to fix the position of both vacua we add to it finite terms of the third and fourth order, so that it has a form

$$\delta U = -\delta\mathcal{L} = \Lambda + \delta\rho\phi + \frac{1}{2}\delta m^2\phi^2 - \delta\eta_f\phi^3 + \frac{1}{8}\delta\lambda_f\phi^4 \ . \tag{3.35}$$

Using the conditions we have discussed in Sec. 2.3, we get the following counterterms

$$
\begin{aligned}
\Lambda &= 0 \ , \\
\delta\rho &= -\frac{3\eta}{4\pi}\left(L_\epsilon - \ln\frac{m^2}{\mu^2} - 1\right) \ , \\
\delta m^2 &= \frac{3\lambda}{8\pi}\left(L_\epsilon - \ln\frac{m^2}{\mu^2} - \frac{12\eta^2}{m^2\lambda} - 1\right) \ .
\end{aligned}
\tag{3.36}
$$

For the finite counterterms $\delta\eta_f$ and $\delta\lambda_f$ we get a system of two linear equations which have to be solved numerically

$$-\delta\eta_f\phi_+^3 + \frac{1}{8}\delta\lambda_f\phi_+^4 = -\frac{\mathcal{M}_+^2}{8\pi}\ln\frac{\mathcal{M}_+^2}{m^2} - \frac{3\eta}{4\pi}\phi_+ + \frac{3\lambda}{16\pi}\left(1 + \frac{12\eta^2}{m^2\lambda}\right)\phi_+^2 \tag{3.37}$$

$$-3\delta\eta_f\phi_+^2 + \frac{1}{2}\delta\lambda_f\phi_+^3 = \frac{36\eta^2}{8\pi m^2}\phi_+ - \frac{3\lambda\phi_+ - 6\eta}{8\pi}\ln\frac{\mathcal{M}_+^2}{m^2} \ . \tag{3.38}$$

In the $\overline{MS}$ scheme we do not add finite terms, but to keep the local minimum of effective potential at the tree-level minimum we again have to introduce a finite linear counterterm, exactly as we have done in the 4 dimensional case. The counterterms are

$$
\delta\rho_d = -\frac{3\eta}{4\pi}L_\epsilon \ , \tag{3.39}
$$

$$
\delta m_d^2 = \frac{3\lambda}{8\pi}L_\epsilon \tag{3.40}
$$

and

$$\delta\rho_f = \frac{3\eta}{4\pi}\left(\ln\frac{m}{\mu^2} + 1\right) . \tag{3.41}$$

The equation for the bounce profile in the scheme with 'physical' renormalization conditions will be

$$-\frac{d^2\phi}{dr^2} - \frac{1}{r}\frac{d\phi}{dr} + U(\phi) + \frac{1}{2}U'''(\phi)\overline{\mathcal{F}^{(1)}} + \frac{3\eta}{4\pi} - \frac{3\lambda}{8\pi}\left(1 + \frac{12\eta^2}{m^2\lambda}\right)\phi$$
$$-3\delta\eta_f\phi^2 + \frac{1}{2}\delta\lambda_f\phi^3 = 0 . \tag{3.42}$$

The same equation in the $\overline{MS}$ scheme is

$$-\frac{d^2\phi}{dr^2} - \frac{1}{r}\frac{d\phi}{dr} + U(\phi) + \frac{1}{2}U'''(\phi)\overline{\mathcal{F}^{(1)}} + \frac{3\eta}{4\pi} - \frac{3\lambda}{8\pi}\ln\frac{m^2}{\mu^2}\phi = 0 . \tag{3.43}$$

It depends on the renormalization scale μ as it was to expected.

And at last the quantity of our interest, the effective action, is given by

$$S_{eff} = S_{cl} + \frac{1}{2}\left(\ln\mathcal{D}\right)^{\overline{(2)}}$$
$$+ \int d^2x\left[\frac{3\eta}{4\pi}\phi - \frac{3\lambda}{16\pi}\left(1 + \frac{12\eta^2}{m^2\lambda}\right)\phi^2 - \delta\eta_f\phi^3 + \frac{1}{8}\delta\lambda_f\phi^4\right] \tag{3.44}$$

and

$$S_{eff} = S_{cl} + \frac{1}{2}\left(\ln\mathcal{D}\right)^{\overline{(2)}} + \int d^2x\left[\frac{3\eta}{4\pi}\phi + \frac{3\lambda}{16\pi}\ln\frac{m^2}{\mu^2}\phi^2\right] . \tag{3.45}$$

for the scheme with 'physical' renormalization conditions and for the $\overline{MS}$ scheme, respectively.

3.2.3 Counterterms for the Hartree approximation

For 2D case of Hartree backreaction is again true, as a consequence of the structure of this approximation, that the divergences can be removed by one counterterm

$$\delta U_{div} = B(\mathcal{M}^2 - m^2) = \frac{1}{8\pi}\left(L_\epsilon - \ln\frac{m^2}{\mu^2} - 1\right)(\mathcal{M}^2 - m^2) . \tag{3.46}$$

In addition we consider the finite counterterm potential

$$\delta U_{fin} = \delta\rho_f\phi + \frac{1}{2}\delta m_f^2 - \delta\eta_f\phi^3 + \frac{1}{8}\delta\lambda_f\phi^4 . \tag{3.47}$$

The renormalization conditions we require fix the linear and quadratic terms to be zero

$$\delta\rho_f = 0 \ , \tag{3.48}$$

$$\delta m_f^2 = 0 \tag{3.49}$$

and for the last two terms we get the linear system of two equations

$$\delta\eta_f \phi_+^3 - \frac{1}{8}\delta\lambda_f\phi_+^4 = \frac{\mathcal{M}_+^2}{8\pi}\left(\ln\frac{\mathcal{M}_+^2}{m^2} - 1\right) - \frac{3\lambda}{8}\Delta_+^2 + \frac{m^2}{8\pi} \ , \tag{3.50}$$

$$\frac{1}{2}\delta\lambda_f\phi_+^3 - 3\delta\eta_f\phi_+^2 = -\frac{3}{2}\Delta_+\left((\lambda + D_f)\phi_+ - 2(\eta + C_f)\right) \ . \tag{3.51}$$

In the $\overline{MS}$ scheme we get only one counterterm given by Eq. (3.46). So that the effective potential in this case is

$$U_{eff} = \frac{m^2}{2}\phi^2 - \eta\phi^3 + \frac{\lambda}{8}\phi^4 + \frac{\mathcal{M}^2}{8\pi}\left(\ln\frac{\mathcal{M}^2}{m^2} - 1\right) - \frac{m^2}{8\pi}\ln\frac{m^2}{\mu^2} - \frac{3\lambda}{8}\Delta^2 \ . \tag{3.52}$$

The equations for the bounce profile will coincide with ones in 4D case

$$-\Delta_4\phi + U'(\phi) + \delta U'_{fin}(\phi) + \frac{1}{2}[-6(\eta + \delta\eta_f) + 3(\lambda + \delta\lambda_f\phi)]\mathcal{F}_{fin} = 0 \tag{3.53}$$

and

$$-\Delta_4\phi + U'(\phi) + \frac{3}{2}(-2\eta + \lambda\phi(x))\mathcal{F}_{fin} = 0 \ , \tag{3.54}$$

for the 'physical' renormalization scheme and the $\overline{MS}$ scheme, respectively, where the finite part of fluctuation integral is $\mathcal{F}_{fin} = \mathcal{F}^{(1)} - \frac{1}{8\pi}$. Finally the expressions of the effective action are

$$\begin{aligned} S_{eff} &= S_{cl} + \frac{1}{2}\left(\ln\mathcal{D}\right)^{\overline{(2)}} - \frac{3\lambda}{8}\int d^2x\mathcal{F}_{fin}^2 \\ &+ \int d^2x\left[-\frac{1}{8\pi}V(x) - \delta\eta_f\phi^3 + \frac{1}{8}\delta\lambda_f\phi^4\right] \end{aligned} \tag{3.55}$$

and

$$S_{eff} = S_{cl} + \frac{1}{2}\left(\ln\mathcal{D}\right)^{\overline{(2)}} - \frac{1}{8\pi}\int d^2xV(x) - \frac{3\lambda}{8}\int d^2x\mathcal{F}_{fin}^2 \ , \tag{3.56}$$

again for the case with 'physical' renormalization conditions and for the $\overline{MS}$ scheme, respectively.

Chapter 4
Numerical Results

The subject of this Chapter are the numerical results obtained in the 4D and 2D model we have considered. Most of the computational technique was already discussed in the appropriate places during the description of the analytical part. Here we will briefly address the question of obtaining the bounce profile and some tricks we have used in order to cover as big a part of the parameter space as possible.

The theory we consider has a 2 dimensional parameter space (the third parameter, the mass m we have set to be equal unity). Instead of the couplings η and λ which we have used up to now we introduce a more convenient parameterization which makes transparent the relative importance of the quantum part of the action and of the classical one.

In the both cases, for 4D model as well as for the 2D, we first discuss the question of convergence of bounce profile. Then we present the relative changes of the effective action and transition rate in the two approximations we consider here, as compared to the semiclassical approximation. The last section of this chapter will dedicate to the question of dependence of our results on the renormalization scale we choose. One should notice that all results before (Sec. 4.2 and Sec. 4.3) are computed for $\mu = m = 1$.

4.1 General remarks

4.1.1 $\alpha - \beta$ parameterization

For a better understanding of our numerical results, we have decided to use so called '$\alpha - \beta$' parameterization (see for example [12, 47, 48]), which makes transparent the relative importance of the classical and quantum parts of effective action.

We introduce the parameters

$$\alpha = \lambda\beta \,, \tag{4.1}$$

$$\beta = \frac{m^4}{4\eta^2} \,, \tag{4.2}$$

and the rescaling of the coordinates $x^\mu = X^\mu/m$ for $\mu = 0, 1, 2, 3$ and of the field $\phi = \sqrt{\beta}\hat{\phi}$. In this new parameterization the classical action takes the form

$$S_{cl}(\phi) = \beta\hat{S}_{cl}(\hat{\phi}) \,, \tag{4.3}$$

where the rescaled classical action $\hat{S}_{cl}(\hat{\phi})$ is given by

$$\hat{S}_{cl}[\hat{\phi}, \alpha] = \int d^4X \left(\frac{1}{2}(\nabla\hat{\phi})^2 + U(\hat{\phi}) \right) \,. \tag{4.4}$$

Here the tree level potential with the rescaled field depends only on the parameter α

$$U(\hat{\phi}) = \frac{1}{2}\hat{\phi}^2 - \frac{1}{2}\hat{\phi}^3 + \frac{\alpha}{8}\hat{\phi}^4 \,. \tag{4.5}$$

From this expressions one can understand the meaning of the parameters α and *beta*. The parameter α parameterizes the shape of the potential: for small value of α potential is strongly asymmetric, for $\alpha = 0$ the second minimum disappears, for $\alpha \to 1$ two minima become degenerate and the potential is symmetric double-well potential. That is so called thin-wall approximation (for details see, for example, Appendix A in Ref.[18]). For values of α larger than 1 the rôles of false and true vacua are interchanged, so one can restrict the values of the parameter α to the interval from 0 to 1.

The parameter β controls the size of the quantum corrections. In the semiclassical approximation the one-loop action as well as the classical one depends on the parameter α only, i.e.

$$S_{eff} = \beta\hat{S}_{cl}[\hat{\phi}, \alpha] + S_{1-loop}(\alpha) \,, \tag{4.6}$$

so for large values of β the effective action is dominated by classical part and for small β by the quantum correction. Of course this is not really true after the backreaction is included. But one can still expect the effects of backreaction to be small for large β and relatively important for small values of the parameter β.

In our numerical computations we have set mass m equal unity. So all dimensionful parameters and results are given in the mass units.

For large values of β the tunneling rate gets strongly suppressed, so we will be mostly interested in small values of β.

4.1.2 The bounce profile

The self-consistent profiles $\phi(r)$ are obtained by iteration, each iteration consists of two steps: in the first step we solve the equation for the bounce profile $\phi(r)$ with a given $\mathcal{F}(r)$. In the second step the fluctuation integral $\mathcal{F}(r)$ is computed for the profile $\phi(r)$ obtained in the first step. The iteration proceeds until the largest difference along the profiles of two subsequent iterations $\max_r \Delta\phi(r)$ is smaller than 10^{-5}. Of course in the very first step for a new parameter set the function $\mathcal{F}(r)$
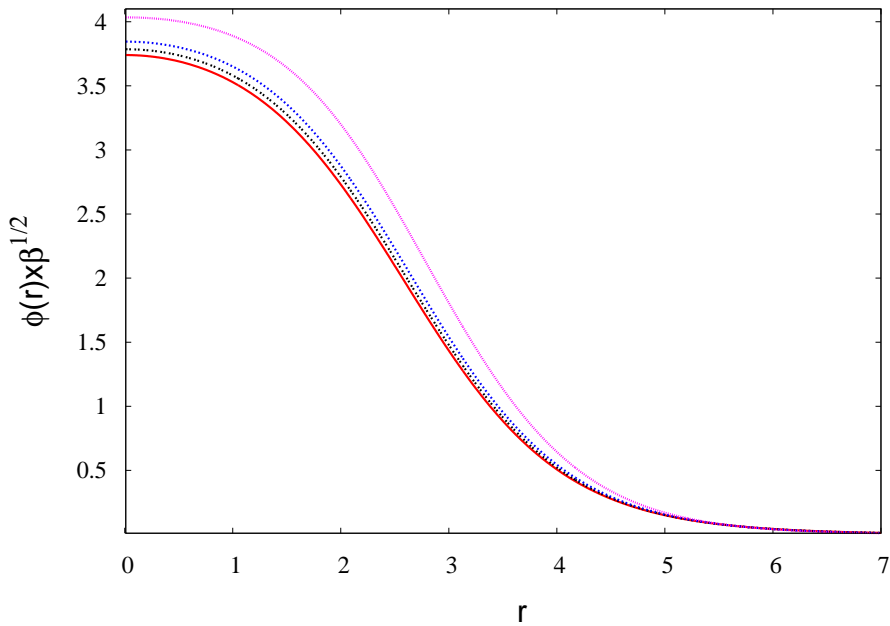
Figure 4.1: Behavior of $\hat{\phi}(r) = \phi(r)/\sqrt{\beta}$ for $\beta = 20, 0.5, 0.2$ and 0.05 at $\alpha = 0.6$, for Hartree with renormalization conditions. These profiles are seen to increase with decreasing β while they are independent of β in the semiclassical approximation.

is not yet known and we would start by solving the classical equation of motion. However, if the quantum corrections are large it is dangerous to start the iteration with $\mathcal{F}(r) \equiv 0$, we would start with a bad approximation for $\phi(r)$, and the procedure might diverge immediately. In order to avoid this problem we have organized our numerical code in such a way that we run a series of solutions for fixed α starting

with a large value of β. There the quantum corrections are small. We then stepwise decrease the values of β, using the self-consistent value of $\mathcal{F}(r)$ for a given β in the first iteration step of next lower value of β.

In the semiclassical approximation the profiles $\phi(r)$ are, at fixed parameter α and arbitrary values of β, determined by one universal profile

$$\hat{\phi}_\alpha(r) = \beta^{-1/2}\phi(r) \tag{4.7}$$

which is independent of β. Therefore, to make transparent the changes of the profile by the backreaction for fixed α but different values of β, i.e. different amount of quantum corrections we will can display the normalized profiles

$$\hat{\phi}(r) = \beta^{-1/2}\phi(r) \tag{4.8}$$
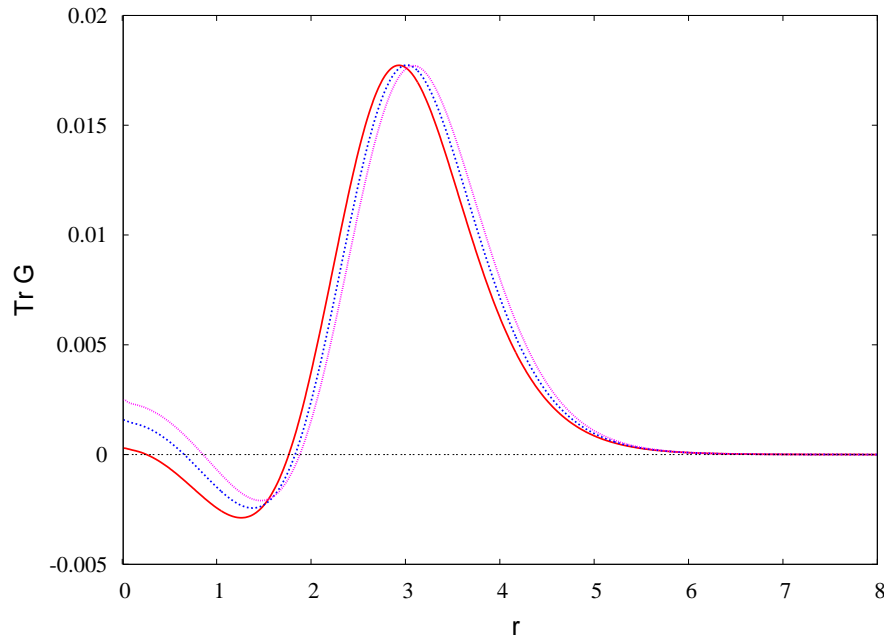
Figure 4.2: The fluctuation integral $\mathcal{F}(r)$ for the Hartree backreaction (case III) as a function of r for $\alpha = 0.6$. The curves display a change with β (the parameter β takes the values $10, 0.1, 0.05$.

For large β, when the backreaction is weak, these profiles are expected to be independent of β and close to $\hat{\phi}_\alpha(r)$. This was observed for the $\beta \gtrsim 10$. The β-dependence observed for smaller values of β depends on the type of backreaction

and on the renormalization conditions. In Fig. 4.1 we present the bounce profile in the Hartree approximation with the physical renormalization conditions for $\alpha = 0.6$ and different values of β. The corresponding fluctuation integral one can see in Fig. 4.2 (we have just taken different values of β to make the changes visible).

With decreasing β the normalized profiles get higher for the 4D model. The change in profile becomes substantial for the very small values of $\beta \simeq 0.05$. In 2D model gets lower with decrease of β. If β becomes smaller than 1, this decrease becomes substantial. For some lower limiting value of $\beta \simeq 0.8$ the iterative procedure ceases to converge, during the iteration the profile collapses to $\phi(r) \equiv 0$.
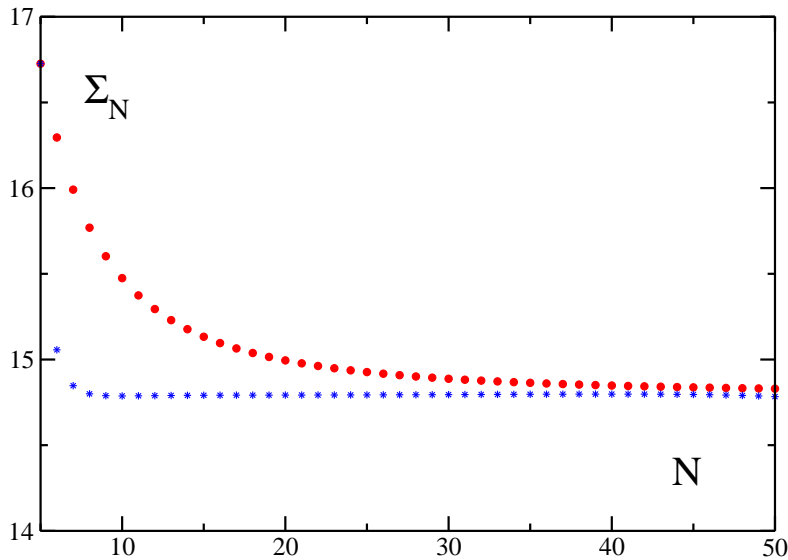
Figure 4.3: Convergence of the sum over the angular-momentum as a function of maximal value N. $\alpha = 0.5$, $\beta = 1$ for the 4D model; circles correspond to Σ_N; stars - Σ_N^{as}.

For the 3+1 dimensional case the required accuracy is obtained after 20-30 iterations in the whole parameter space, this takes about 3 min of CPU time. In the 1+1 dimensional case, for parameters near the collapse of procedure, one needs 80-100 iterations, this takes about 5 min with 1.7 GHz processor. In the regions of parameter space far away from the critical points we again need only $20 - 30$

iterations. .

4.1.3 The mode functions

The functions $h_l^{(i)}$ and $h_l^{\overline{(i)}}$ have to be determined by solving the Eqs. (1.5.3). Numerically this is done using the Runge-Kutta integration method [49]. The integration should be extended up to $r = \infty$. In fact we have integrated until the maximal value $R = r_{max}$ for which the profile $\phi(r)$, and correspondingly $V(r)$ are known. This value R has to be large enough so that the field $\phi(r)$ is sufficiently close to its value $\phi = 0$ in the false vacuum. Then we are also in the region where $V(r)$ has become sufficiently small and where the mode functions have become constant. As $\phi(r)$ decreases exponentially, this can be ensured with moderate values of R. In numerical computations we have taken $R = r_{max} = 20$.

The expressions for finite part of the Green's function and fluctuation determinant imply summation over the angular momentum n. The single terms in the sum (including the degeneracy factor) are proportional to the n^{-3}. This has been verified numerically for the 2D as well as for the 4D case and presents one of the cross-checks of the procedure and accuracy. The sum over n was separated in two parts. Until some value $N = n_{max}$ it was computed exactly. The rest of sum from N to ∞ was added in its asymptotic form. In order to parameterize the terms at large $n > N$ which represent the asymptotic tail we have used a fit $A/n^3 + B/n^4 + C/n^5$ for the five highest terms $(N-5, ..., N)$ in the sum. In the Fig. 4.3 we show the dependence of Σ_N, the exact sum up to $n = N$, and of the sum Σ_N^{as} which has the sum over the asymptotic tail appended. As to be expected the latter one converges much faster to the asymptotic value Σ_∞.

The convergence is seen to be excellent in both 4D and 2D cases. In the 3+1 dimensional model one has to extend up to $N = 40-50$, whereas in 1+1 dimensions it is sufficient to choose $N = 25 - 30$. So for the computations in the 4 dimensions we have set $N = 50$ and in 2 dimensions $N = 25$.

4.1.4 Some notations

To make the discussion of the results in different approximations and different renormalization schemes simpler we introduce the following short notations:

- Case I: one-loop back-reaction, with renormalization conditions.

- Case II: one-loop back-reaction, with $\overline{MS}$ renormalization.

- Case III: Hartree back-reaction, with renormalization conditions.

- Case IV: Hartree back-reaction, with $\overline{MS}$ renormalization.

4.1.5 The effective potential

Before we go on with the detailed presentation of results for the 3+1 and 1+1 dimensional models, we have to see the changes due to the to different renormalization schemes we implement in our computations. The best possibility to do this is to show the effective potential. In Fig. 4.4 five curves are plotted for $\alpha = 0.7$ and $\beta = 0.3$: the tree-level potential (solid line) and four effective potentials for two approximations and two renormalization schemes. As one can see the effective po-
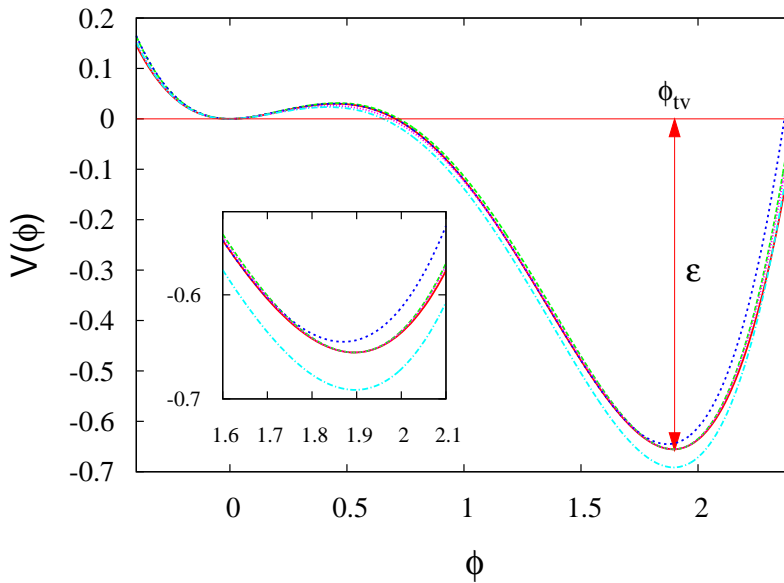
Figure 4.4: The effective potential for $\alpha = 0.7$ and $\beta = 0.3$. solid line: tree level potential; dotted line: case I; dash-dotted line: case II; short-dashed line: case III; long-dashed line: case IV; cases I and III are hardly visible.

tentials for case III and case III are very close to the tree-level one over the whole range and exactly coincide in the minima (are hardly visible). For two other cases, in $\overline{MS}$ scheme the position of true vacuum is shifted and the energy difference between two vacua differs from the tree-level one as well.

4.1.6 Dependence on the renormalization scale

We have studied dependence of our results on the renormalization scale. In some sense the change of μ scale corresponds to the change of couplings, the connection between these changes is given by the renormalization group.

Here in general we have chosen $\mu = m$ for convenience. Usually one considers $\mu^2 \simeq q^2$ as an appropriate scale, where q^2 is a momentum transfer squared of a scattering process. Here the "external momenta" can be related to the size of the classical solution. So a reasonable value for μ^2 can be obtained by computing the average of momentum q^2 in the classical solution:

$$\overline{q^2} = \frac{\int dq \; q^3 \; |\varphi(q)|^2 \; q^2}{\int dq \; q^3 \; |\varphi(q)|^2} \tag{4.9}$$

We find that the typical average momentum q has values between 0.5 and 1. This shows that our standard choice was reasonable. Nevertheless we have computed the effective action for a range of values between $\mu = 0.5$ and 2, for the one-loop backreaction with the $\overline{MS}$ scheme for different values of α and β parameters. The dependence on the renormalization scale within this range is very small, the absolute values of the differences are $10^{-4} - 10^{-3}$ while absolute value of action is of order $10^3 - 10^4$.

4.2 Results of 3+1 Dimensional Model

4.2.1 The translation mode

Discussion of numerical results we start with the translation mode and notice that the squared frequency of the mode in the one-loop and Hartree backreaction which we identify as translation zero mode ω_t^2 is generally of the order 10^{-3} in mass units. It is not much larger than in the semiclassical approximation, where as one expects, it is located closer to the zero. We find it at $10^{-5} - 10^{-4}$. As already mentioned above, it does not stay so small near the critical points. It becomes at most of order 10^{-1} there.

4.2.2 Effective actions

As mentioned in Sec. 4.1 the effective action in the semiclassical approximation can be written in the form

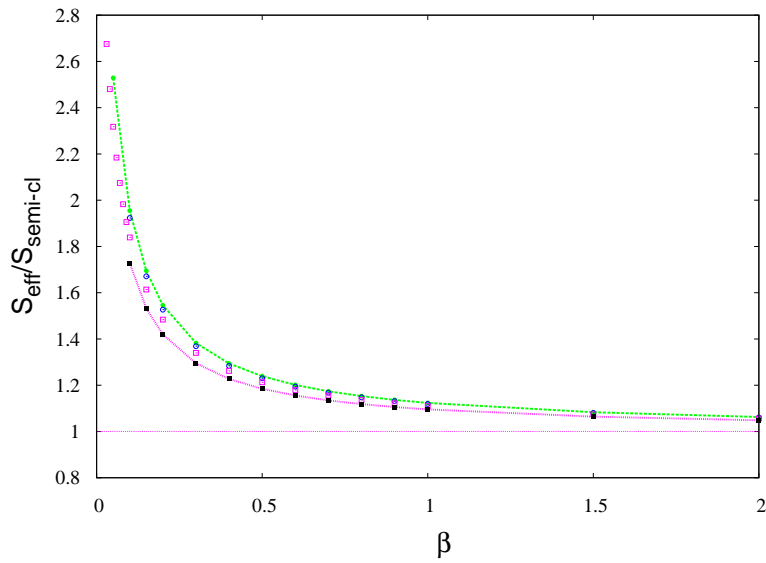$$S_{semi-cl} = \beta \hat{S}_{cl}[\hat{\phi}] + S_{1-loop} \;, \tag{4.10}$$

Figure 4.5: Ratio $S_{eff}/S_{semi-cl}$ as a function of β for $\alpha = 0.05$; for this and the next two figure: dotted line with full squares: case I; empty squares: case II; long-dashed line with full circles: case III; empty circles: case IV.
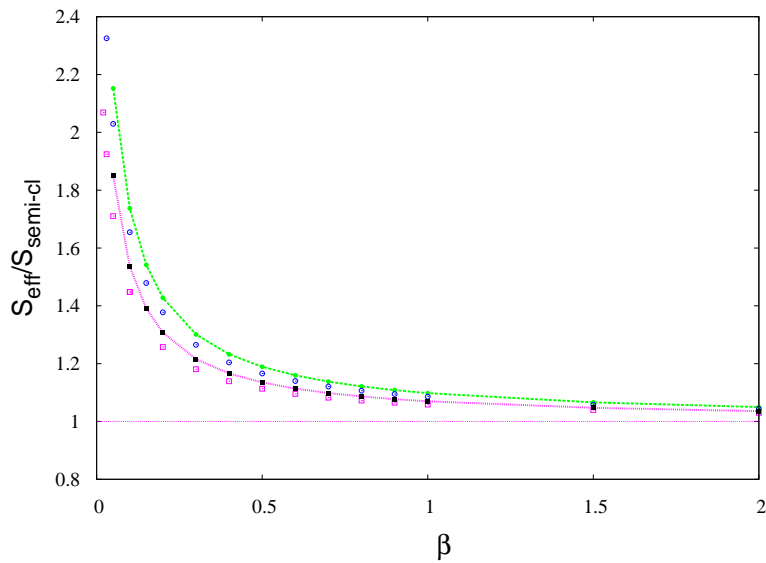

Figure 4.6: Ratio of S_{eff} and $S_{semi-cl}$ as a function of β for $\alpha = 0.2$; (for notation see figure 4.5).

where $\hat{S}_{cl}$ and S_{1-loop} are functions of α only. To make the deviations due to the backreaction more transparent we display the ratio of the effective action with backreaction in various approximations to the semiclassical one

$$\rho = \frac{S_{eff}}{\beta\hat{S}_{cl}[\hat{\phi}] + S_{1-loop}} = \frac{backreaction}{semiclassical} \ . \tag{4.11}$$

It is obvious that the ratio should go to unity for $\beta \to \infty$ as η becomes $\eta = 1/2\sqrt{\beta}$ and $\lambda = \alpha/\beta$ goes to zero. Actually already for $\beta \gtrsim 5$ ρ is very close to one.

We present the ratio (4.11) in n Figs. 4.5, 4.6 and 4.7 for $\alpha = 0.05$, $\alpha = 0.2$ and $\alpha = 0.6$ respectively. All figures display the deviation for four different cases. One can see that for all values of α the ratio goes to 1 for $\beta \gtrsim 5$. However, for $\alpha = 0.05$ and $\alpha = 0.2$ ρ is always larger than 1 for all four cases. But for $\alpha = 0.6$ $\rho > 1$ in the one-loop approximation and $\rho < 1$ in the Hartree approximation.
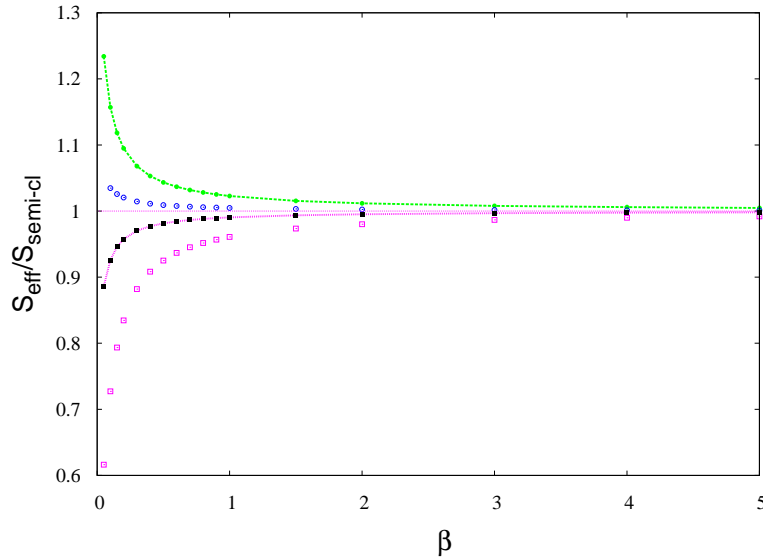
Figure 4.7: Ratio of S_{eff} and $S_{semi-cl}$ as a function of β for $\alpha = 0.6$; (for notation see figure 4.5).

One should notice that in the semiclassical approximation the effective action is mostly dominated by the classical part of action and one-loop part has a relatively small contribution. For example, for $\alpha = 0.6$ $S_{\text{semi-cl}} = 395.08\beta + 13.03$ where the first term is the classical action, and the second one the one-loop action, or for

$\alpha = 0.05$ $S_{\text{semi-cl}} = 97.87\beta + 3.562$. This dominance of the classical action is not always true then the quantum backreaction is included. For large values of β the dominance holds, but for the small β the quantum corrections become of the same order as the classical action. However, one should notice that the increase of the ration ρ is not due to the one-loop and double- bubble part. The contribution of the classical action is equally important. It strongly deviates from its semiclassical value, as a result of the strong change in the $\phi(r)$ profile (The separation of the effective action in the classical and quantum parts is very qualified after the quantum backreaction is included)

As one sees on the vertical axis the deviation from the semiclassical action is quite strong in the whole parameter space. And if we recall that we are considering the relative changes of the effective action and the effective actions are of the order of a few hundred this implies a very substantial changes (several magnitudes) in the transition rates. Therefore, as one expects the next quantity we will present is the transition rate.

We have not studied the region $\alpha > 0.8$ in detail, as here we approach the thin-wall limit and the classical action becomes so large that the semiclassical action is of order of few thousands (e.g. 1500β for $\alpha = 0.8$) and correspondingly the transition rates are incredibly small.

4.2.3 Transition rates

The transition rate we have for to discuss in the same way as the effective action, we consider the ratio of the transition rate to its semiclassical value. Of course, in principle it reflects the behavior of the effective action, but also includes the ratio of the prefactors. We present again three plots with logarithm of the ratio of transition rates as a function of parameter β for $\alpha = 0.05$, $\alpha = 0.2$ and $\alpha = 0.6$, in Figs. 4.8, 4.9 and 4.10 respectively.

As we see the ratios amount several orders of magnitude. For small and middle values of α all four cases with backreaction are suppressed with respect to the semiclassical rate. But for the large α the Hartree backreaction rates are suppressed with respect to the semiclassical one in both cases. For the one-loop backreaction the rates are enhanced (for all $\alpha \gtrsim 0.5$).
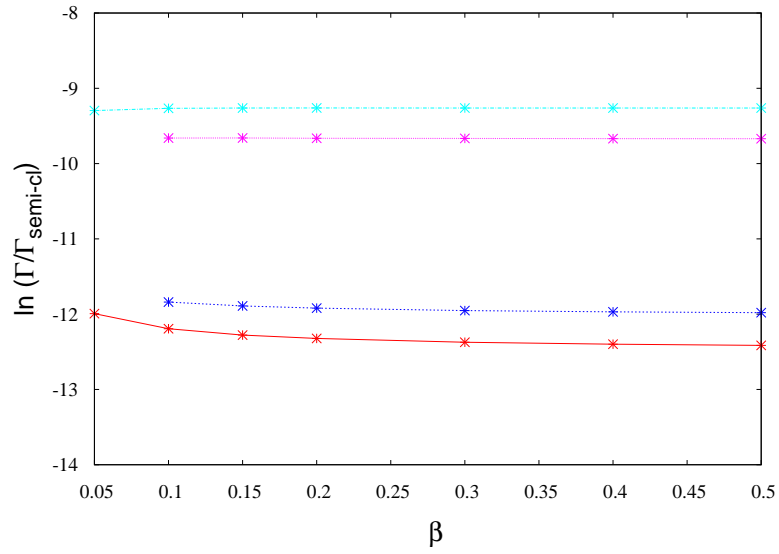
Figure 4.8: Logarithm of the ratio $\Gamma/\Gamma_{semi-cl}$ as a function of β for $\alpha = 0.05$; notation here and in two next figure: violet curve: case I; light blue: case II; red curve: case III; blue curve: case IV.

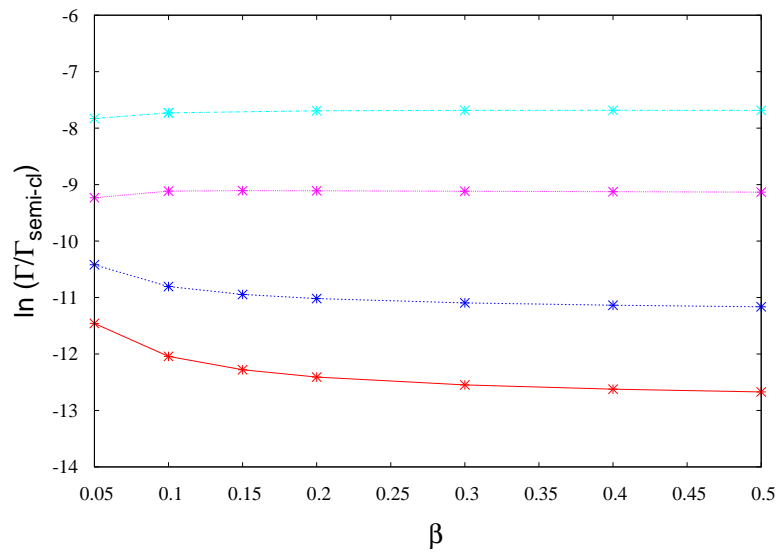Figure 4.9: Logarithm of the ratio $\Gamma/\Gamma_{semi-cl}$ as a function of β for $\alpha = 0.2$; (for notation see figure 4.8.
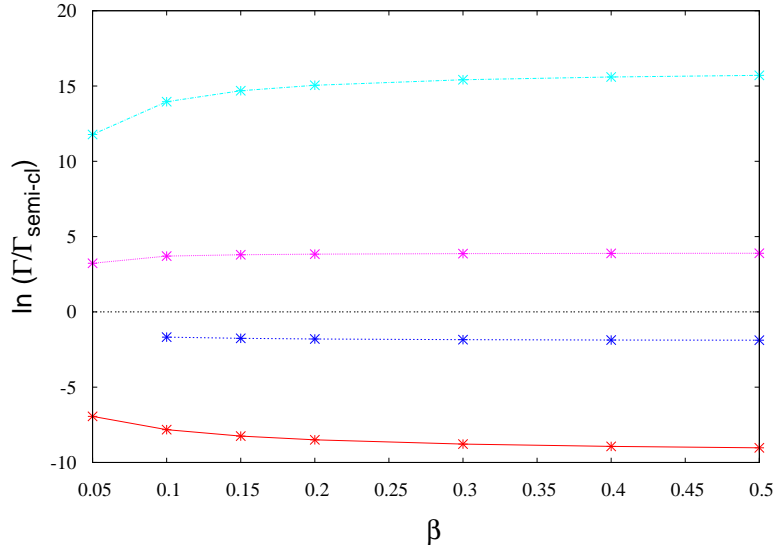
Figure 4.10: Logarithm of the ratio $\Gamma/\Gamma_{semi-cl}$ as a function of β for $\alpha = 0.6$; (for notation see figure 4.8).

4.3 Results of 1+1 Dimensional Model

The numerical results of the 2D model are in most points very similar to the ones for the 4D model. Therefore we will not discuss them in details and do only the short comments.

4.3.1 Convergence of iteration procedure and some remarks

We present the numerical results for the middle and large value of α parameter $\alpha = 0.3$ and $\alpha = 0.6$ and cover the range between $0.8 \lesssim \beta \leqslant 20$ in β parameter. In the order to avoid the convergence of iteration procedure over the not suitable choice of initial value for the fluctuation integral, we use the same technic as in the 4D model and let the numerical code run for a fix value of α, starting from the large values of β, slowly decreasing it and using the self-consistent value of the fluctuation integral $\mathcal{F}(r)$ for the next step.

On the Fig. 4.11 we present the normalized start value of field $\phi(0)/\sqrt{\beta}$. As one can see the plot ends around $\beta \simeq 0.8$ for all four schemes we consider. Below this value the iteration procedure converges. The expression of this phenomena one finds in the collapse of the bounce profile to $\phi(r) \equiv 0$, in the rapid increase of the

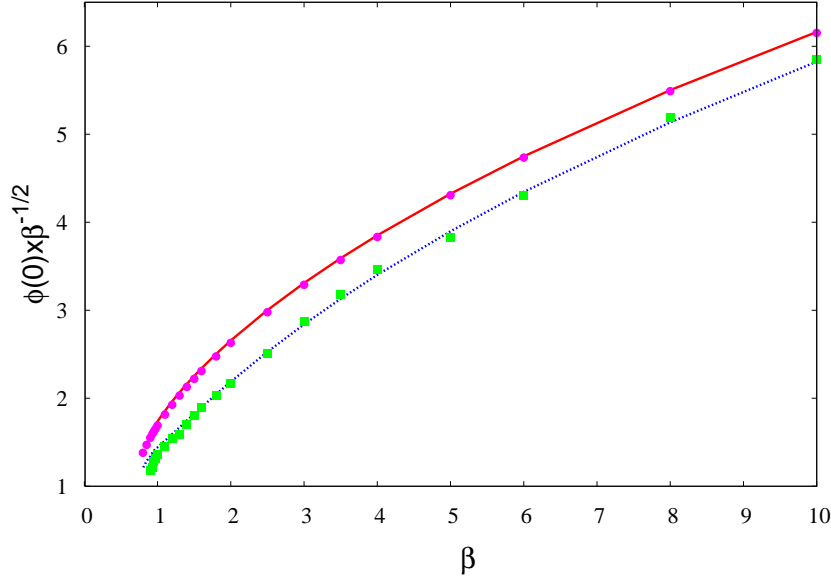effective action and in the large squared frequency of the zero mode ω_t^2 which near

Figure 4.11: Behavior of $\phi(0)/\sqrt{\beta}$ near the critical values for $\alpha = 0.6$. Short-dashed line: case I; full squares: case II; solid line: case III and full circles: case IV.

the critical point becomes of order 10^{-1}.

We have tried to modify the iteration procedure by implementing so called "over-relaxation" scheme, where one defines the portion of the result in each iteration step to be taken for the further computations:

$$f_{i+1}(r) = \sigma f_i(r) + (1 - \sigma)(\mathcal{O}f_i)(r) \, . \tag{4.12}$$

Here the function $f_i(r)$ denotes the i'th iteration of a function to be iterated, in our case $\phi(r)$ or $\mathcal{M}(r)$. $\mathcal{O}$ stays for the operator producing the new iteration result, profile or effective mass and the number σ defines the relative portion of the i'th step and the new iteration results. For the normal iteration $\sigma = 0$. Implementation of this scheme in the numerical code and running it for different values of σ has shown the common runaway behavior below the critical value of β.

We have investigated the behavior of another quantities important for the computation of bounce profiles, like fluctuation integral (it appears in the equation

of bounce profile multiplied by factor $\lambda\phi = \alpha\phi/\beta$, with small β this contribution becomes more and more important) and the sums over the partial waves in the fluctuation determinant and fluctuation integral. The fluctuation integral shows no anomaly in the critical region, that means that the instability of the bounce solution is not result of appearance of a additional unstable mode in the fluctuation operator (if squared frequency of such mode will cross zero the fluctuation integral will get very large contribution proportional to the square of its wave function).

So we have not been able to find the reason for the unusual behavior of iteration procedure. All included quantities shown no anomalies. Therefore we conclude that the disappearance of the bounce solution under the critical value of β is a genuine phenomenon and not a technical problem of iteration scheme. We suspect that bounce solution just does not exist below this critical value and that the decay of the false vacuum proceeds via some different mechanisms.

The translation zero mode is found at $\omega_t^2 = 10^{-3} - 10^{-2}$ for the most part of the parameter space. Near the critical value of β it receives the largest values, which are so about 0.1.
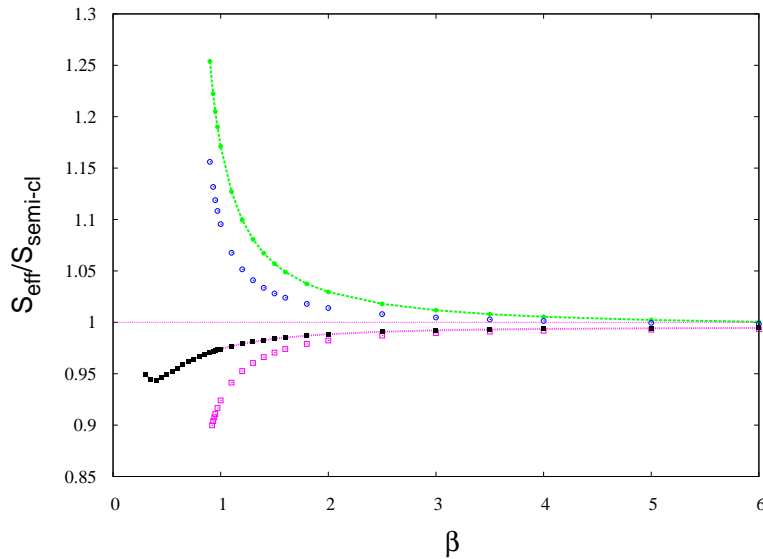

Figure 4.12: Ratio of S_{eff} to $S_{semi-cl}$ as a function of β for $\alpha = 0.3$; for this and the next figure: dotted line with full squares: case I; empty squares: case II; long-dashed line with full circles: case III; empty circles: case IV.
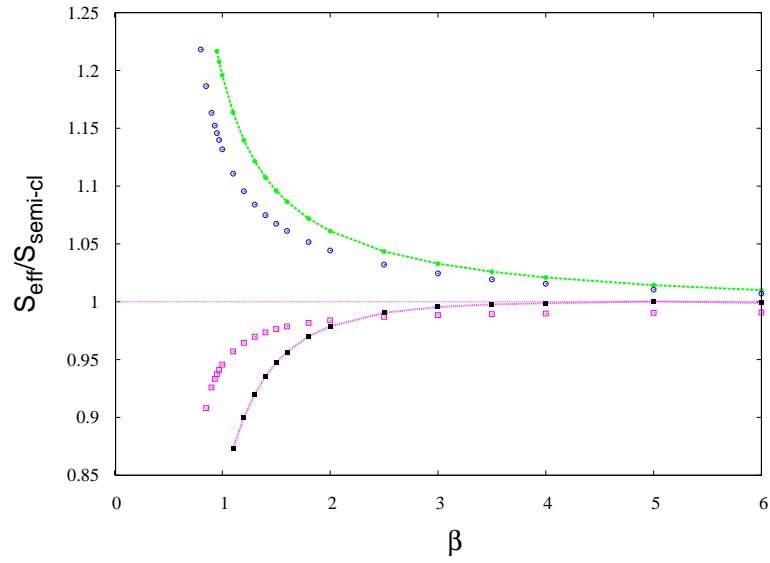
Figure 4.13: Ratio of S_{eff} and $S_{semi-cl}$ as a function of β for $\alpha = 0.6$; (For notation see previous figure).
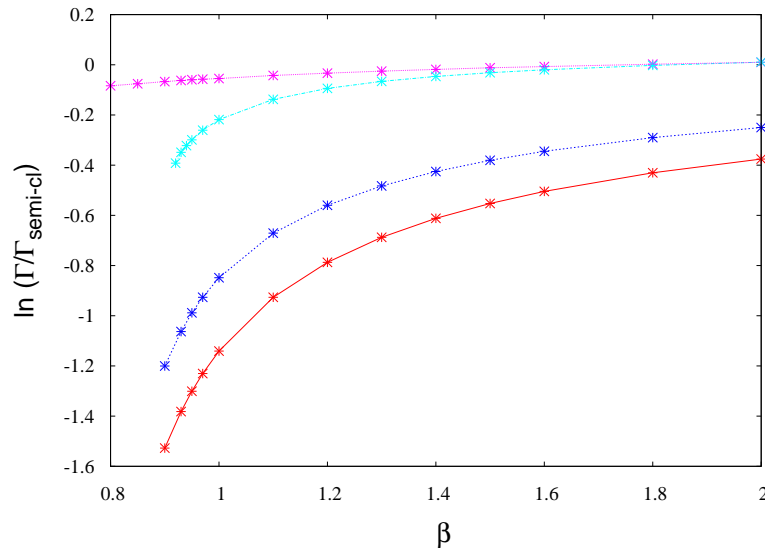

Figure 4.14: Logarithm of the ratio $\Gamma/\Gamma_{semi-cl}$ as a function of β for $\alpha = 0.3$; notation here and in two next figure: violet curve: case I; light blue: case II; red curve: case III; blue curve: case IV.

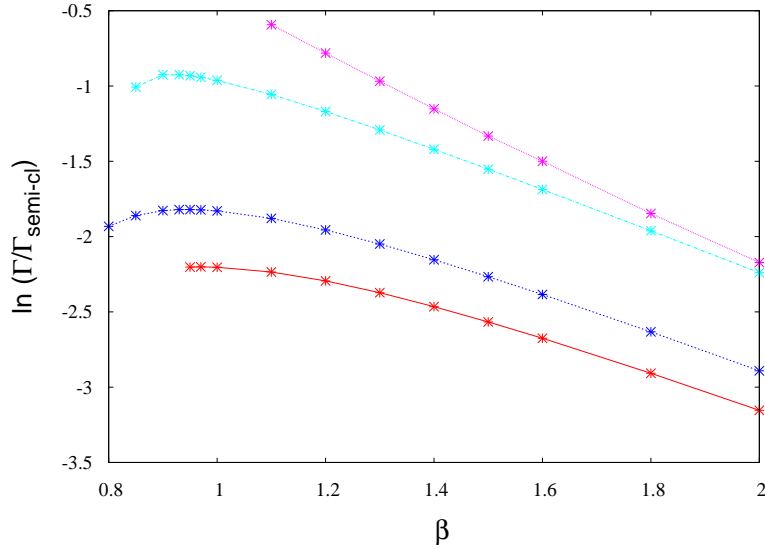Figure 4.15: Logarithm of the ratio $\Gamma/\Gamma_{semi-cl}$ as a function of β for $\alpha = 0.6$; (for notation see figure 4.8.

4.3.2 The effective actions and transition rates

To make the influence of the backreaction more transparent we plot the ratios of effective actions to the semiclassical effective action, as we have done for the 4D (see (4.11)).

In Figs. 4.12 and 4.13 are displayed results for the $\alpha = 0.3$ and $\alpha = 0.6$ parameters (for the very small values of α the critical point is found at relatively large β, this explains our choice of parameters to display).

As in the 4D model for both values of α the ratio goes to 1 for $\beta \gtrsim 6$ and they show the same behavior for the middle and large values of β: $\rho < 1$ for the one-loop approximation and is $\rho > 1$ for Hartree approximation. And as one can see in most cases the deviation from the semiclassical action is quite sizeable (goes till 30%).

The question of dominance of the different parts included in effective action here is very similar to the one for the 4D case. In the semiclassical approximation the relative contribution of the one-loop part imply $10^{-3} - 10^{-4}$ to the classical part. The situation changes when the quantum backreaction is included. For small values of β the quantum corrections become of the same order as the classical part.

Again we consider the ratio of the transition rate for the four schemes to the semiclassical one. Of course we show two plots for $\alpha = 0.3$ and $\alpha = 0.6$ in Figs. 4.14

and 4.15 respectively. To make changes more transparent we plot the logarithm of the ratio as a function of β. As one can see the ratios amount several orders of magnitude. For both values of α the ratio with backreaction is suppressed with respect to the semiclassical ratio.

4.4 Summary

We have presented results for the 4D and 2D models using the $\alpha-\beta$ parameterization for four different cases: two schemes for incorporating the quantum backreaction and two renormalization schemes. The effective action and transition rate were compared to the values obtained in the semiclassical approximation. The deviations become very sizeable for small values of β and amount several orders in magnitude to the transition rates. These deviations, of course, are approximation and renormalization scheme dependent. We find differences in the behavior of system in $3+1$ and $1+1$ dimensional models.

In 4 dimensional case we are able to make a computations for the most part of the parameter space. Here the deviation from the semiclassical approximation is found to be very sizeable. For $\alpha > 0.5$ the corrections in action amount 30% and the transition rate is suppressed for the Hartree approximation and enhanced in one-loop approximation. For the $\alpha < 0.5$ the corrections become of order 100% and the transition rate is always suppressed.

In the 2 dimensional model we were not able to cover the whole parameter space, as the iteration procedure diverges for $\beta \lesssim 0.8$. The effective action near the region of critical value in β increases rapidly and the corrections amount $20-30\%$. The correction stay suppressed with respect to the semiclassical approximation.

Part.II
Global Tunneling

"To the inventor the products of his imagination appear necessary and natural, such that he does not look at them as objects of the mind, but rather as things belonging to reality, and thus he wishes them to be seen like that."

Albert Einstein

Chapter 5
A 1+1 Dimensional Model of Global Tunneling

In this chapter we will describe the 1+1 dimensional model for the single scalar field, again with the asymmetric double-well potential. The system is assumed to be initially localized in the false vacuum and to tunnel globally into the true vacuum. This is possible only if the space is compact, here we consider a one-dimensional circle. We decompose the wave function in a discrete set of degrees of freedom. For the nonzero modes we apply the Gaussian approximation, while for the zero we solve the Schrödinger equation. The interaction of the zero mode with nonzero modes is given by fluctuation integral, which contains some divergences and should be renormalized. Another divergent quantity is energy density. We will work in the Schrödinger representation.

The first section is devoted to the general description of the model. In the second section we give some overview of the time-dependent variational principle. In the next section this principle is applied to the model we consider here. In the last section aspects of renormalization are discussed, where we use the technique discussed in the publications on the nonequilibrium dynamics (see for example, Ref. [50, 51, 52]).

5.1 The model and basic relations

We consider a scalar quantum field theory in 1+1 dimensions with a compact space, i.e. on a manifold $R \times S_1$. As one can see in the Fig. 5.1 the space is represented by a circle of radius a and an infinite time axis.

The action is given by

$$ S = \int_0^{2\pi a} dx \int dt \left[\frac{1}{2}\dot{\Phi}^2 - \frac{1}{2}\left(\frac{\partial\Phi}{\partial x}\right)^2 - U(\Phi) \right] , \qquad (5.13) $$
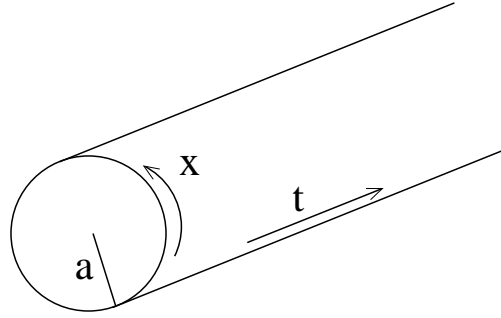
Figure 5.1: 1+1 dimensional compact space.

with asymmetric double well potential, which we choose in the following parameterization

$$U(\Phi) = \frac{1}{2}m^2\Phi^2 - \eta\Phi^3 + \frac{\lambda}{8}\Phi^4 \ . \tag{5.14}$$

It has two minima (see Fig. 5.2), one at $\Phi = \Phi_- = 0$ and the a second one at

$$\Phi_+ = \frac{3\eta}{\lambda} + \sqrt{\frac{9\eta^2}{\lambda^2} - \frac{2m^2}{\lambda}} \ . \tag{5.15}$$

As we consider the 2 dimensional theory the field Φ is dimensionless, and η and λ have the dimension $mass^2$. The upper limit of integral corresponds to the periodic boundary conditions in x.

We introduce the expansion into normal modes

$$\Phi(x,t) = \varphi_0(t) + \sum_{n=-\infty}^{\infty} \varphi_n(t)e^{ik_n x} \ , \tag{5.16}$$

with the momenta defined as

$$k_n = \frac{n}{a} \ . \tag{5.17}$$

Applying this expansion we get the action in the form

$$S = 2\pi a \int dt \left[\frac{1}{2}\dot{\varphi}_0^2 + \frac{1}{2}\sum_{n\neq 0}\dot{\varphi}_n\dot{\varphi}_{-n} - \frac{1}{2}\sum_{n}\omega_n^2\varphi_n\varphi_{-n} \right. \tag{5.18}$$

$$\left. +\eta\sum_{nn'}\varphi_n\varphi_{n'}\varphi_{-n-n'} - \frac{\lambda}{8}\sum_{nn'n''}\varphi_n\varphi_{n'}\varphi_{n''}\varphi_{-n-n'-n''} \right] \ ,$$
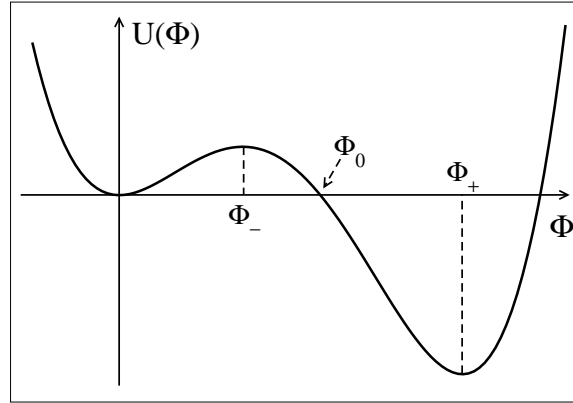
Figure 5.2: Double-well potential.

with

$$\omega_n^2 = m^2 + \frac{n^2}{a^2} \ . \tag{5.19}$$

The field Φ should be real. This requirement leads to the condition $\varphi_{-n} = \varphi_n^\dagger$. Using this condition one can introduce the real fields for $n \neq 0$ via

$$\varphi_{\pm n} = \frac{1}{\sqrt{2}}(\varphi_{n1} \pm i\varphi_{n2}), \quad n > 0 \ . \tag{5.20}$$

Going to the Schrödinger representation one can write the following Hamiltonian

$$
\begin{aligned}
H \;=\; 2\pi a \Bigg\{ & -\frac{1}{8\pi^2 a^2}\left[\frac{\partial^2}{\partial\varphi_0^2} + \sum_{n>0,j}\frac{\partial^2}{\partial\varphi_{nj}^2}\right] + \frac{1}{2}\left[m^2\varphi_0^2 + \sum_{n>0,j}\omega_n^2\varphi_{nj}^2\right] \\
& -\eta\sum_{nn'}\varphi_n\varphi_{n'}\varphi_{-n-n'} + \frac{\lambda}{8}\sum_{nn'n''}\varphi_n\varphi_{n'}\varphi_{n''}\varphi_{-n-n'-n''} \Bigg\} \ ,
\end{aligned}
\tag{5.21}
$$

where the index j stands for the real and imaginary part of the modes $j = 1, 2$. In order to get rid of overall volume factors $2\pi a$ we introduce the rescaling for the modes

$$\varphi_k = \chi_k/\sqrt{2\pi a} \ . \tag{5.22}$$

In this convention the Hamiltonian takes the form

$$
\begin{aligned}
H &= -\frac{1}{2}\left[\frac{\partial^2}{\partial\chi_0^2} + \sum_{n>0,j}\frac{\partial^2}{\partial\chi_{nj}^2}\right] + \frac{1}{2}\left[m^2\chi_0^2 + \sum_{n>0,j}\omega_n^2\chi_{nj}^2\right] \\
&\quad - \eta'\sum_{nn'}\chi_n\chi_{n'}\chi_{-n-n'} + \frac{\lambda'}{8}\sum_{nn'n''}\chi_n\chi_{n'}\chi_{n''}\chi_{-n-n'-n''} \ .
\end{aligned}
\tag{5.23}
$$

In order to get rid of the volume factors in couplings we have redefined them in following form $\eta' = \eta/\sqrt{2\pi a}$ and $\lambda' = \lambda/2\pi a$. One should notice that for the reasons which will get obvious in the future here we have still retained the complex fields in the cubic and quartic parts

$$
\chi_{\pm n} = \frac{1}{\sqrt{2}}(\chi_{n1} \pm i\chi_{n2}) \ .
\tag{5.24}
$$

5.2 Time-dependent Hartree-Fock approximation

5.2.1 Time-dependent variational principle

The quantum mechanical time-dependent theory, i.e. the time-dependent Schrödinger equation, can be derived by considering time dependent states $|\psi, t>$ and requiring that $\int dt < \psi, t|i\hbar\partial_t - H|\psi, t>$ be stationary against independent variations of $|\psi, t>$ and $< \psi, t|$. This variational principle was formulated by Dirac [53, 54] and is equivalent to Hamilton's principle. This variational principle will be applied to trial wave functions of Hartree type. The resulting scheme is nonperturbative, the solutions of the corresponding evolution equations contain arbitrary powers of the coupling constants (partial resummation of the perturbation series). They will take into account the quantum backreaction of the fluctuations onto themselves. The time evolution of the Gaussian wave function in time-dependent variational approximation was studied by Cooper and al. in Ref. [55].

In our discussion we use the time dependent Hartree-Fock approach, but we differ from the simulations in the out-of-equilibrium quantum field theory, where the Gaussian wave function is used for all modes. We will separate the zero mode from the others and consider it exactly. It is this mode, corresponding to a constant field, which describes the global tunneling.

5.2.2 Variational and Gaussian ansatzes

Now we make a variational *ansatz* for the wave function and impose a variational principle:

$$\Psi(\chi_0, \chi_n, t) = \psi_0(\chi_0, t) \prod_{n>0} \psi_n(\chi_{nj}, t) . \tag{5.25}$$

Furthermore, for the modes with $n \neq 0$ we make the *ansatz* of a Gaussian wave function

$$\psi_n(\chi_{nj}, t) = \frac{e^{-i\alpha_n(t)}}{[2\pi\sigma_n^2(t)]^{1/4}} \exp\left[-\frac{1}{2} \left(\frac{1}{2\sigma_n^2(t)} - i\frac{s_n(t)}{\sigma_n(t)} \right) \chi_{nj}^2 \right] , \tag{5.26}$$

while we do not further specify ψ_0, it remains a general Schrödinger wave function, i.e. its Schrödinger equation will be integrated exactly.

The time dependent variational principle now imposes the condition

$$\delta \int d\chi_0 \prod_{n>0,j} d\chi_{nj} \Psi^\dagger(\chi_0, \chi_{nj}, t) \left(i\partial_t - H \right) \Psi(\chi_0, \chi_{nj}, t) = 0 . \tag{5.27}$$

We have suppressed the index j in the wave function, as later on we will find that the dynamics is independent of it.

5.2.3 Separation of Hamiltonian and the Schrödinger equations

We have factorized the wave function into two different parts, the constant field mode $n = 0$ which describes the global tunneling and which we consider exactly, and the modes with $n \neq 0$ on which we apply Gaussian ansatz. So one expects to get separate Schrödinger equations for them. Therefore first of all we rewrite the Hamiltonian in a appropriate way, i.e. we split the Hamiltonian in the parts corresponding to the zero mode, nonzero modes and the interaction between the zero and nonzero modes and nonzero modes onto themselves.

The part of Hamiltonian H_{00} which exclusively contains the zero mode is given by

$$H_{00} = -\frac{1}{2}\frac{\partial^2}{\partial\chi_0^2} + \tilde{U}(\chi_0) , \tag{5.28}$$

with the part of potential containing only zero mode

$$\tilde{U}(\chi_0) = \frac{1}{2}m^2\chi_0^2 - \eta'\chi_0^3 + \frac{\lambda'}{8}\chi_0^4 . \tag{5.29}$$

The parts bilinear in the quantum modes lead to the Hamiltonian

$$H_{0n} = \sum_{n>0,j} \left[-\frac{1}{2} \frac{\partial^2}{\partial \chi_{nj}^2} + \frac{1}{2} \omega_n^2 \chi_{nj}^2 \right] . \tag{5.30}$$

which contains only nonzero modes.

Due to the Gaussian *ansatz* for the $n \neq 0$ modes the expectation values of any odd powers of $n \neq 0$ fluctuations vanish. So if we want to consider the interaction between zero and nonzero modes we need to retain only terms bilinear in the $n \neq 0$ modes. So we should consider terms of the cubic and quartic in χ_n

$$\left[\sum_{n,n'} \chi_n \chi_{n'} \chi_{-n-n'} \right]_{I0n} = 3\chi_0 \sum_{n \neq 0} \chi_n \chi_{-n} = 3\chi_0 \sum_{n>0,j} \chi_{nj}^2 \tag{5.31}$$

and

$$\left[\sum_{n,n',n''} \chi_n \chi_{n'} \chi_{n''} \chi_{-n-n'-n''} \right]_{I0n} = 6\chi_0^2 \sum_{n \neq 0} \chi_n \chi_{-n} = 6\chi_0^2 \sum_{n>0,j} \chi_{nj}^2 . \tag{5.32}$$

As result for the coupling between zero and nonzero modes we get the following Hamiltonian

$$H_{I0n} = \left(-3\eta' \chi_0 + \frac{3\lambda'}{4} \chi_0^2 \right) \sum_{n>0,j} \chi_{nj}^2 , \tag{5.33}$$

with the scaled couplings η' and λ', we have discussed in the previous section.

The part of the Hamiltonian cubic in the nonzero modes has a vanishing expectation value. The quartic term does not vanish, it has the expectation value

$$< \sum_{n,n',n''} \chi_n \chi_{n'} \chi_{n''} \chi_{-n-n'-n''} > = 3 \sum_{nj,n'j'} < \chi_{nj}^2 >< \chi_{n'j'}^2 > . \tag{5.34}$$

Here we have used the fact that the wave functions for $n \neq 0$ are Gaussian. The related part of the Hamiltonian describes the self interaction of the nonzero modes. It is given by

$$< H_{Inn} > = \frac{3}{8} \lambda' \left[\sum_{nj} < \chi_{nj}^2 > \right]^2 = \frac{3}{2} \lambda' \mathcal{F}^2 . \tag{5.35}$$

Applying the variational principle we get for the zero mode wave function the Schrödinger equation

$$i\partial_t \psi_0(\chi_0, t) = \left[-\frac{1}{2} \frac{\partial^2}{\partial \chi_0^2} + \tilde{U}(\chi_0) + \left(-6\eta' \chi_0 + \frac{3\lambda'}{2} \chi_0^2 \right) \mathcal{F} \right] \psi_0(\chi_0, t) , \tag{5.36}$$

where only the zero mode part of Hamiltonian H_{00} and the interaction part between zero and nonzero modes are presented. Here we have introduced the fluctuation integral

$$\mathcal{F} = \frac{1}{2} < \sum_{n>0,j} \chi_{nj}^2 > \ . \tag{5.37}$$

It will be specified more after introduction of the mode functions $f_n(t)$.

For the nonzero modes, $n \neq 0$ we find the Schrödinger equation to be

$$i\partial_t \psi_n(\chi_n, t) = \left[-\frac{1}{2} \frac{\partial^2}{\partial \chi_{nj}^2} + \frac{1}{2}(\omega_n^2 + W(t))\chi_{nj}^2 \right] \psi_n(\chi_n, t) \ . \tag{5.38}$$

Here we have introduced the notation

$$W(t) = < \tilde{U}''(\chi_0) - m^2 > + 3\lambda' \mathcal{F} \ , \tag{5.39}$$

where

$$< \tilde{U}''(\chi_0) - m^2 > = \int d\chi_0 \psi_0^*(\chi_0, t)[-6\eta'\chi_0 + \frac{3\lambda'}{2}\chi_0^2]\psi_0(\chi_0, t) \ . \tag{5.40}$$

In addition we introduce the quantity $\Omega_n^2(t) = \omega_n^2 + W(t)$.

As we see the Schrödinger equation for the quantum mode wave function is independent of the index j. Therefore the previous summations over j just lead to a degeneracy factor 2 and the index j by the mode functions can be really suppressed.

Using the the Gaussian *ansatz* (5.26) the Schrödinger equation for the $n \neq 0$ modes implies

$$\dot{\sigma}_n(t) = s_n(t) \ , \tag{5.41}$$

$$\dot{s}_n(t) = -\Omega_n^2(t)\sigma_n(t) + \frac{1}{4\sigma_n^3(t)} \ , \tag{5.42}$$

$$\dot{\alpha}_n(t) = \frac{1}{4\sigma_n^2(t)} \ . \tag{5.43}$$

The first two of these equations can be related to mode functions $f_n(t)$ satisfying the mode equation

$$\ddot{f}_n(t) + \Omega_n^2(t)f_n(t) = 0 \ , \tag{5.44}$$

with the effective mass squared $\Omega_n^2 = m^2 + W(t)$. Denoting $\omega_{n0} = \Omega_n(0)$, we have

$$\sigma_n(t) = \frac{|f_n(t)|}{\sqrt{2\omega_{n0}}} \ , \tag{5.45}$$

$$s_n(t) = \frac{1}{\sqrt{2\omega_{n0}}} \frac{d}{dt}|f_n(t)| \ . \tag{5.46}$$

The wave function of the nonzero modes is then given by

$$\psi_n(\chi_n, t) = e^{-i\alpha_n(t)} \left[\frac{2\omega_{n0}}{2\pi|f_n(t)|^2}\right]^{1/4} \exp\left[\frac{i}{2}\frac{\dot{f}_n^*(t)}{f_n^*(t)}\chi_n^2\right] . \tag{5.47}$$

In deriving these relation we have used repeatedly the Wronskian relation for the mode functions

$$\dot{f}_n^*(t)f_n(t) - f_n^*(t)\dot{f}_n(t) = 2i\omega_{n0} , \tag{5.48}$$

which corresponds to the initial conditions

$$f_n(0) = 1 , \qquad \dot{f}_n(0) = -i\omega_{n0} . \tag{5.49}$$

Using the Eq.(5.47) for the wave function of nonzero modes one can derive the expectation value of χ_n^2

$$\int d\chi_n \, |\psi_n(\chi_n, t)|^2 \, \chi_n^2 = \frac{|f_n(t)|^2}{2\omega_{n0}} , \tag{5.50}$$

the sum of which corresponds to the the fluctuation integral, i.e.

$$\mathcal{F}(t) = \sum_{n>0} \frac{|f_n(t)|^2}{2\omega_{n0}} . \tag{5.51}$$

The discussion of this quantity will be continued in the Sec. 5.3.

5.2.4 Initial conditions

We want to start the evolution of the system approximately in the ground state of the left well of the double-well potential. This means that we approximate the potential around $r = 0$ by an harmonic oscillator potential $m^2\phi^2/2$ and use the ground state wave function of this oscillator as the initial wave function. We then find the total energy of the system to be close to zero, as one expects for such an approximate ground state. Of course, the choice of such an initial state is quite arbitrary. However, a different choice would lead to a higher total energy. This would make the tunneling easier and indeed might convert the tunneling through the barrier into an "over the barrier" transition.

In Sec. 5.2 we have discussed the initial conditions for the nonzero modes. The system starts with the following mode functions

$$f_n(t) \simeq e^{-\omega_{n0}t} , \tag{5.52}$$

which results in the initial wave functions

$$\psi(\chi_n, 0) = \left[\frac{\omega_{n0}}{\pi}\right]^{1/4} e^{-\omega_{n0}\chi_n^2/2} . \tag{5.53}$$

Here $\omega_{n0} = \sqrt{m_0^2 + n^2/a^2}$. The effective mass m_0 is determined by the gap equation which we will introduce in the next section.

For the zero mode we likewise start with a Gaussian wave function

$$\psi(\chi_0, 0) = \left[\frac{m}{\pi}\right]^{1/4} e^{-m\chi_n^2/2} , \tag{5.54}$$

where we set the frequency $\omega = m$, that corresponds to the ground state wave function for a potential with $\eta = \lambda = 0$.

5.2.5 The energy

We have separated the Hamiltonian in the zero mode H_{00}, nonzero modes H_{0n} and two interaction parts H_{I0n} and H_{Inn}. Taking the expectation values of them we will get the corresponding energies:

classical energy

$$< H_{00} > = \int d\chi_0 \psi_0^*(\chi_0, t) \left[-\frac{1}{2}\frac{\partial^2}{\partial\chi_0^2} + \tilde{U}(\chi_0)\right] \psi_0(\chi_0, t) , \tag{5.55}$$

fluctuation energy

$$< H_{0n} > = 2\sum_{n>0} \frac{1}{2\omega_{n0}} \left[\frac{1}{2}\left|\dot{f}_n(t)\right|^2 + \frac{1}{2}\omega_n^2 |f_n(t)|^2\right] , \tag{5.56}$$

interaction energy

$$< H_{I0n} > = < \tilde{U}''(\chi_0) - m^2 > \mathcal{F} , \tag{5.57}$$

self $-$ interaction energy

$$< H_{Inn} > = \frac{3}{2}\lambda'\mathcal{F}^2 . \tag{5.58}$$

It is convenient to replace ω_n^2 by ω_{n0}^2 in $< H_{0n} >$, so that $< H_{0n} >$ becomes the free Hamiltonian for the initial fluctuation wave functions. Then the rest term $-W(0)\mathcal{F}$ should be added to the interaction energy $< H_{I0n} >$.

The sum of all parts of energy amounts the conserved energy, consistent with the Schrödinger equations presented in the previous subsection

$$E = < H_{00} + H_{0n} + H_{I0n} + H_{Inn} > . \tag{5.59}$$

The energy density we have introduced here is divergent and needs renormalization (see Sec. 5.3).

5.2.6 Particle number

In the context of our model the particle number is an artificial concept, as the "particles" never get really free. However, we use this quantity as an indicator for the excitations of the nonzero modes.

A particle number for the $n \neq 0$ modes may be defined in various ways. A Fock space is defined by the mode decomposition (5.16). To the operators χ_{nj} and their conjugate momenta $\pi_{nj} = \partial/\partial\chi_{nj}$ one can associate creation and annihilation operators. In order to do so, one has to assign to these modes a frequency. A standard choice is the the frequency ω_{n0}, then we consider particle excitation in the Fock space defined at $t = 0$, with mass $m = m_0$; this is what we will consider. Another standard choice is the adiabatic particle number, based on a Fock space with mass $m = \mathcal{M}^2(t)$ and effective frequencies $\Omega_n(t)$. In the present context such a definition has the shortcoming that the effective mass $\mathcal{M}^2(t)$ may get negative, so that the low momentum modes have imaginary frequency and the adiabatic particle number is not defined.

The creation and annihilation operators for an oscillator of frequency ω_{n0} are

$$c_{nj} = \sqrt{\frac{\omega_{n0}}{2}} \left(\chi_{nj} + \frac{1}{\omega_{n0}} \frac{\partial}{\partial\chi_{nj}} \right) , \tag{5.60}$$

$$c_{nj}^\dagger = \sqrt{\frac{\omega_{n0}}{2}} \left(\chi_{nj} - \frac{1}{\omega_{n0}} \frac{\partial}{\partial\chi_{nj}} \right) . \tag{5.61}$$

Then a particle number is the expectation value

$$\mathcal{N}_{nj} = < c_{nj}^\dagger c_{nj} > = < \frac{1}{\omega_{n0}^2} \left[-\frac{1}{2} \frac{\partial^2}{\partial\chi_{nj}^2} + \frac{1}{2} \omega_{n0}^2 \chi_{nj}^2 \right] > \tag{5.62}$$

Computing the expectation value with the wave function $\psi_n(\chi_{nj})$ given by Eq. (5.47) one finds

$$\mathcal{N}_{nj} = \frac{1}{4\omega_{n0}^2} \left[\left| \dot{f}_n(t) \right|^2 + \omega_{n0}^2 \left| f_n(t) \right|^2 \right] - \frac{1}{2} . \tag{5.63}$$

In the discussion of the excitations of the modes with $n > 0$ we will merely use the total particle number, defined as $\mathcal{N} = \sum_{nj} \mathcal{N}_{nj}$.

5.3 Renormalization

As it was already mentioned in the previous section the fluctuation integral and the energy density contain divergences and should be renormalized. In 1+1 dimensions

the renormalization is rather easy. However, we will consider it in some details, as we have take into account that we treat a nonequilibrium system with discrete momenta and that we consider the Hartree approximation, i.e. the renormalization should be done for a resumed perturbation series.

Though we treat the system in a nonperturbative approach, the divergences are related exactly to those of standard perturbation theory. The mode functions can be expanded perturbatively with respect to the potential $V(t)$ which contains the couplings η and λ; so such an expansion is at the same time an expansion with respect to these couplings.

We write the mode functions as

$$f_n(t) = e^{-i\omega_{n0}t} \left[1 + h_n(t)\right] \tag{5.64}$$

to have a possibility to convert the differential equation for the $f_n(t)$ into an integral equation for the functions $h_n(t)$:

$$h_n(t) = \frac{i}{2\omega_{n0}} \int_0^t dt' \left(e^{2i\omega_{n0}(t-t')} - 1\right) V(t') \left[1 + h_n(t')\right] , \tag{5.65}$$

where we have defined $V(t) = W(t) - W(0)$, using Eq. (5.39).

So that for the absolute value squared of the mode functions, which enters the expression for the fluctuation integral and energy density, we have

$$|f_n(t)|^2 = 1 + 2\mathrm{Re}h_n(t) + |h_n(t)|^2 \tag{5.66}$$

in terms of the functions $h_n(t)$. One can find (see Appendix D) that $\mathrm{Re}h_n(t)$ for large n behaves as

$$\mathrm{Re}h_n(t) \simeq -\frac{V(t)}{4\omega_{n0}^2} + O\left(\frac{1}{\omega_{n0}^3}\right) . \tag{5.67}$$

5.3.1 Divergent and finite parts of fluctuation integral

Using the definition of functions $h_n(t)$ and the expression (5.66) one can write the fluctuation integral as

$$\mathcal{F} = \sum_n \frac{1}{2\omega_{n0}} \left[1 - \frac{V(t)}{2\omega_{n0}^2} + O\left(\frac{1}{\omega_{n0}^3}\right)\right] , \tag{5.68}$$

where one can immediately separate a divergent and a subtracted parts

$$\mathcal{F}^{(0)} = \sum_{n=0}^{\infty} \frac{1}{2\omega_{n0}} \, , \tag{5.69}$$

$$\mathcal{F}_{sub} = \sum_{n=0}^{\infty} \frac{1}{2\omega_{n0}} \left[2\mathrm{Re}h_n(t) + |h_n(t)|^2 \right] \, . \tag{5.70}$$

The divergent part has to be regularized, this will separate it into the standard renormalization part and a finite contribution. The divergent part contains summation over the discrete momenta. In order to relate their divergent behavior to the standard divergences in field theory in an infinite volume we use the Plana formula [56].

$$\sum_{n=1}^{\infty} \frac{1}{2\omega_{n0}} = \pi a \int_{-\infty}^{\infty} \frac{dk}{(2\pi)2\omega_0} \left[1 + \frac{2}{\exp(2\pi a\omega_0) - 1} - \frac{1}{\pi a\omega_0} \right] \, , \tag{5.71}$$

with $\omega_0 = \sqrt{k^2 + m_0^2}$. The second part of the integrand resembles integrals found in quantum field theory at finite temperature. There, however, it is not space but time which satisfies periodic boundary conditions on a compact support. The details of computation for the last expression can be found in the Appendix D.

The first term in the bracket is divergent, the same term one will obtain for infinite space. It goes into the renormalization of the various couplings. The second term is specific for our model, as it arises from the periodic boundary conditions. The third part comes from the fact that $\mathcal{F}$ contains the nonzero modes only and no subtraction has been applied to the zero mode.

The first term can be regularized in a standard way [50] using the dimensional regularization

$$\left(\int \frac{dk}{(2\pi)2\omega_0} \right)_{\mathrm{reg}} = \int \frac{d^{2-\epsilon}k}{(2\pi)^{2-\epsilon}} \frac{i}{k_0^2 - k^2 - m_0^2 + io} = \frac{1}{4\pi} L_{\epsilon 0} \, , \tag{5.72}$$

with $L_{\epsilon 0} = 2/\epsilon + \ln(4\pi/m_0^2) - \gamma$. m_0^2 depends on the initial conditions, and the renormalization condition should not; therefore we redefine $L_{\epsilon 0} = L_\epsilon + \ln m^2/m_0^2$ with $L_\epsilon = 2/\epsilon + \ln(4\pi/m^2) - \gamma$ and include the $\ln m^2/m_0^2$ term into the finite part. So the remaining finite part is

$$\mathcal{F}_{fin}^{(0)} = 2\pi a \int_{-\infty}^{\infty} \frac{dk}{(2\pi)2\omega_0} \frac{1}{\exp(2\pi a\omega_0) - 1} - \frac{1}{4m_0} + \frac{a}{4} \ln \frac{m^2}{m_0^2} \tag{5.73}$$

and the finite part of the fluctuation integral becomes

$$\mathcal{F}_{fin} = \mathcal{F}_{fin}^{(0)} + \mathcal{F}_{sub} \, . \tag{5.74}$$

5.3.2 Renormalization of the energy density

As the divergence in the fluctuation integral comes from the term $\sum_{n=1}^{\infty} \frac{\omega_{n0}}{2}$ we just subtract it, so that

$$
\begin{aligned}
< H_{0n} > \;=\;& 2 \sum_{n>0} \frac{1}{2\omega_{n0}} \left[\frac{1}{2} \left| \dot{f}_n(t) \right|^2 + \frac{1}{2} \omega_n^2 \left| f_n(t) \right|^2 \right] \\
=\;& E_{fl,sub} - \frac{1}{2} m_0 + a \int_0^{\infty} dk \omega_0 - 2a \int_0^{\infty} \frac{k^2 dk}{\omega_0 \left(\exp(2\pi a \omega_0) - 1 \right)} \; ,
\end{aligned}
\tag{5.75}
$$

where the subtracted fluctuation energy is

$$
E_{fl,sub} = 2 \sum_{n>0} \frac{1}{2\omega_{n0}} \left[\frac{1}{2} \left| \dot{f}_n(t) \right|^2 + \frac{1}{2} \omega_n^2 \left| f_n(t) \right|^2 - \omega_0^2 \right] \; .
\tag{5.76}
$$

Note that here was used the Eq. (D.8) for the divergent sum.

The integral over ω_0 in Eq. (5.75) after dimensional regularization is

$$
\left[a \int_0^{\infty} dk \omega_0 \right]_{\text{reg}} = \frac{a}{4} m_0^2 \left(L_\epsilon + \ln \frac{m^2}{m_0^2} + 1 \right) \; .
\tag{5.77}
$$

The last term, the "thermal" integral in Eq. (5.75) can be recast into the form of a free energy, using an integration by parts:

$$
-2a \int_0^{\infty} \frac{k^2 dk}{\omega_0 \left(\exp(2\pi a \omega_0) - 1 \right)} = \int_0^{\infty} \frac{dk}{2\pi} \ln \left(1 - \exp(-2\pi a \omega_0) \right) \; .
\tag{5.78}
$$

So that the finite part of the fluctuation energy can be defined as

$$
E_{fl,fin} = E_{fl,sub} + \frac{a}{4} m_0^2 \left(\ln \frac{m^2}{m_0^2} + 1 \right) + \int_0^{\infty} \frac{dk}{2\pi} \ln \left(1 - \exp(-2\pi a \omega_0) \right) \; .
\tag{5.79}
$$

The renormalization is done by adding a counterterm

$$
\delta C \mathcal{M}^2 = \delta C (m^2 + < \tilde{U}''(\chi_0) - m^2 > + 3\lambda' \mathcal{F}_{fin}) \; ,
\tag{5.80}
$$

where we define the effective mass of the fluctuations by a gap equation

$$
\mathcal{M}^2 = m^2 + < \tilde{U}''(\chi_0) - m^2 > + 3\lambda' \mathcal{F}_{fin} \; .
\tag{5.81}
$$

Choosing the counterterm

$$
\delta C = -\frac{a}{4} L_\epsilon \; ,
\tag{5.82}
$$

and defining the initial mass m_0 again by the gap equation

$$m_0^2 = m^2 + <\tilde{U}''(\chi_0) - m^2> + 3\lambda' \mathcal{F}_{fin}^{(0)} , \qquad (5.83)$$

the gap equation (5.81) is satisfied for all t. It can be written as

$$\mathcal{M}^2(t) = m_0^2 + V(t) , \qquad (5.84)$$

with the potential $V(t)$ introduced in the beginning of this section

$$V(t) = <\tilde{U}''(\chi_0)> - m_0^2 + 3\lambda' \mathcal{F}_{fin}(t) , \qquad (5.85)$$

which now becomes finite.

For the energy we obtain the following finite expression

$$\begin{aligned} E_{fin} &= <H_{00}(\chi_0)> + E_{fl,fin} - \frac{1}{2}m_0 + <\tilde{U}'' - m_0^2> \mathcal{F}_{fin} + \frac{3}{2}\lambda' \mathcal{F}_{sub}^2 \\ &+ \frac{a}{4}m_0^2(\ln\frac{m^2}{m_0^2} + 1) + \int_0^\infty \frac{dk}{2\pi} \ln\left(1 - \exp(-2\pi a\omega_0)\right) . \end{aligned} \qquad (5.86)$$

The last two terms are, for a fixed radius a, independent of time; we leave them out when presenting the energy conservation. The term $-m_0/2$ marks the absence of the zero mode in the sum over fluctuations. If $m_0 = m$ this term exactly cancels, at $t = 0$, the expectation value $<H_{00}(\chi_0)>$. If one considers the initial gap equation (5.83), the term $-1/4m_0$ gets canceled, by the term $<\tilde{U}''(\chi_0) - m^2>$, for $m_0 = m$. This is equivalent to the sufficiently large a such that $am > 1$, this corresponding to a "temperature" $T_{\text{eff}}/m < 1/2\pi$, the "thermal" integrals become very small, then the solution m_0 of the gap equation is close to m and energy $E \approx 0$.

Chapter 6
The Numerical Results

In this chapter we will present the numerical results we have obtained after implementation of the expressions of previous chapter in the numerical code. In section 6.1 we discuss the problems of integration of Schrödinger equations and the solutions we have used. We point out some possibilities to check the correct implementation of equations and running of code.

For the presentation of the results we again use the $\alpha - \beta$ introduced in section 4.1.1. Here we will just briefly repeat some definitions.

To have a better possibility for interpretation of our results, which display *resonances*, we consider the case of quantum mechanical tunneling in asymmetric double-well potential and compute the approximate spectra of the left and right wells, treating them as a separate oscillators. This gives the condition for a degeneracy of a levels in the spectrum of right well with the ground state of the left well.

The results are presented for some, most interesting parts of parameter space. We were not able to cover the whole parameter space because the simulations for each parameter set require large CPU times.

6.1 General remarks

6.1.1 Details of implementation in numerical code

We have to implement in the numerical code the expressions obtained in Chap. 5. For this purpose we discretize the variable χ_0 in equidistant discrete values $\chi_{0,k}$ with a step width $\Delta\chi_0$. We used 4000 grid points, which typically extend over a region of $-10 < \chi_0 < 50$. So $\Delta\chi_0$ is of the order 10^{-2}.

Then the wave function for the zero mode $\psi_0(t)$ becomes a system of functions $\psi_0(\chi_{0k})$ and the corresponding Schrödinger equation will be spitted into a system
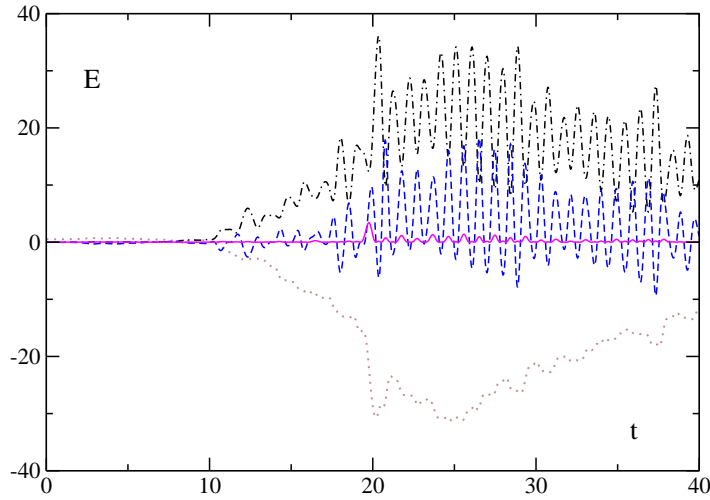
Figure 6.1: Energy conservation; parameters $m = \eta = \lambda = 1$, $a = 6$; dotted line: classical energy; dash-dotted line: fluctuation energy; dashed line: interaction energy; solid line: self-interaction of the fluctuations. The total energy (not displayed) is $E = (2.39 \pm 0.001) \times 10^{-5}$.

of the differential equations for $\psi_0(\chi_{0k})$. To discretize the second derivative of the wave function we make a replacement

$$\frac{\Delta_4}{\partial \chi_0^2} \psi_0(\chi_{0,k}) \rightarrow \frac{\psi(\chi_{0,k+1}) + \psi(\chi_{0,k-1}) - 2\psi(\chi_{0,k})}{(\Delta\chi_0)^2} \ . \tag{6.1}$$

This discretization leads to instabilities in the time evolution unless the time intervals are chosen of the order $\Delta\chi_0^2$. So the Runge-Kutta time step was chosen $\Delta t = 0.00002$. In addition to the evolution of the wave function ψ_0 we have to integrate the equations of motion for the nonzero modes, i.e. the for the functions $h_n(t)$. Furthermore for each Runge-Kutta step we have to compute sums over the nonzero modes, which typically were taken into account up to $n = 200$, and we have to compute various expectation values in the $n = 0$ wave function. All this makes the code very slow. A typical simulation takes a few hours on the standard PC for the evolution time $t \simeq 100$.

The numerical accuracy was checked in the numerical code by computing Wronskians and by verifying the energy conservation. The relative accuracy obtained was better than six significant digits. The deviation in the total energy was of order 10^{-8}

while the various parts of the energy take values of order 10^2. A typical example of energy conservation is displayed in Fig. 6.1 for $\alpha = 0.5$, $\beta = 1$ and $a = 6$.

6.1.2 $\alpha - \beta$ parameterization

The parameter space for our model consists of for parameters m, η, λ and a. So it is quite large. To make the discussion of the numerical results more transparent we introduce here, as well as in the case of the bounce, the $\alpha - \beta$ parameterization.

One introduces the rescaling $X = mx$ and $\Phi = m^2\hat{\Phi}/2\eta$. Then for infinite space the classical action takes the form

$$S_{cl} = \frac{m^4}{4\eta^2} \int d^2X \left[\frac{1}{2}\left(\nabla_X\hat{\Phi}\right)^2 + \hat{U}(\hat{\Phi})\right] = \beta\hat{S}_{cl}(\alpha) \,, \tag{6.2}$$

with $\beta = m^4/4\eta^2$, $\alpha = \lambda\beta/m^2$ and

$$\hat{U}(\hat{\Phi}) = \frac{1}{2}\hat{\Phi}^2 - \frac{1}{2}\hat{\Phi}^3 + \frac{\alpha}{8}\hat{\Phi}^4 \,. \tag{6.3}$$

The one-loop effective action is a function of α only. β multiplies the classical action, so for large β the system essentially becomes classical and the quantum effects only lead to small corrections. For small β the quantum effects become essential.

We will in the following consider parameter sets with fixed α and β, i.e., fixed λ and η, and study the dependence on a.

6.1.3 The condition for the resonances in the approximate spectra

As we will see, in some part of the parameter space the tunneling phenomena will be characterized by the occurrence of *resonances*. In quantum mechanical tunneling this phenomena was already observed (see Ref.[35]). For a better understanding of this phenomenon we approximatively consider the left and right wells as separate harmonic oscillator potentials and estimate the position of their energy levels. The resonances can then be thought of as arising from the degeneracy of levels in the left and in the right wells. The energy levels of the oscillator in the left well are $E_n^l = (n + 1/2)m$. The absolute minimum of the potential is at

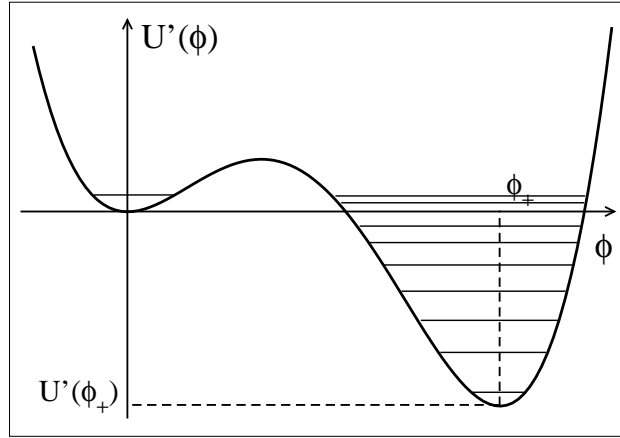$$\chi_0^+ = \sqrt{2\pi a}\Phi_+ = \sqrt{2\pi a}\frac{2\eta}{\lambda}\hat{\Phi}_+ \,, \tag{6.4}$$

Figure 6.2: Approximate levels in the both wells of potential.

where

$$\hat{\Phi}_+ = \frac{3}{2\alpha}\left(1 + \sqrt{1 - \frac{8}{9}\alpha}\right) \tag{6.5}$$

is the position of the absolute minimum in $\alpha - \beta$ parameterization. The energy levels for the oscillator in the right well are given by

$$E_n^r = \left(n + \frac{1}{2}\right)\omega_+ + \tilde{U}(\chi_0^+) , \tag{6.6}$$

with oscillator frequency

$$\omega_+^2 = \tilde{U}''(\chi_0^+) = 2m^2\left[\frac{9}{8\alpha}\left(1 + \sqrt{1 - \frac{8}{9}\alpha}\right) - 1\right] \tag{6.7}$$

and the depth of the well

$$\tilde{U}(\chi_0^+) = 2\pi a\beta\hat{U}(\hat{\Phi}_+) < 0 . \tag{6.8}$$

So the condition for a degeneracy of a level in the spectrum of the right hand well with the ground state of the left hand well (which we take as an initial state) is

$$2\pi aU(\Phi_+) + \left(n + \frac{1}{2}\right)\omega_+ = \frac{1}{2}m . \tag{6.9}$$

As we intend to study the dependence of the tunneling process on the radius of the space manifold a by fixed α and β, we present here the dependence of the tunneling phenomena on length scale. If the degeneracy holds for some value a and an integer n, it will hold again for $a' = a + \Delta a$, $n' = n - \Delta n$ with

$$\Delta a = -\frac{\omega_+}{2\pi U(\Phi_+)}\Delta n \; . \tag{6.10}$$

The constant multiplying Δn on the right hand side determines the spacing of resonance levels as a function of a at fixed α and β.

Of course one can also have resonances between *excited* states of the left well and the right well, but as we prepare our initial state to correspond roughly to the ground state of the left well, these will be less important.

A more essential feature is the excitation of field quanta of the nonzero modes, which will have a dissipative effect on the dynamics of the zero mode and broaden the resonances. The effect of the nonzero modes gets obvious if one considers the effective potential in which the zero mode is moving

$$U_0(\chi_0, t) = \tilde{U}(\chi_0) + (\tilde{U}''(\chi_0) - m^2)\mathcal{F}(t) \; . \tag{6.11}$$

The potential gets deformed by the presence of the fluctuation integral. If $\mathcal{F}(t)$ is negligible the evolution of the system proceeds like in the quantum mechanics. If $\mathcal{F}(t)$ remains small the time-dependent modifications of the potential will allow a few other approximate eigenstates of the zero mode to mix in, the resonant oscillations develop "higher harmonics" and become irregular. If $\mathcal{F}(t)$ gets large the deformations become substantial. If $\mathcal{F}(t)$ is positive the potential barrier can disappear entirely, then the zero mode may "slide" into the true minimum. If $\mathcal{F}(t)$ is negative the potential is tilted counterclockwise and the barrier is enhanced.

6.2 Results of the numerical simulations

As already mentioned we have studied the tunneling process as a function of space radius a for the fixed parameters α and β, or equivalently, for fixed η and λ. The mass determines the time and length scales, we choose it to be unity.

We present the numerical results for four parameter sets:

- set *I*: $\alpha = 0.8, \beta = 0.5$, i.e., $\lambda = 1.6, \eta = 1/\sqrt{2}$; $\Delta a = 0.529$;

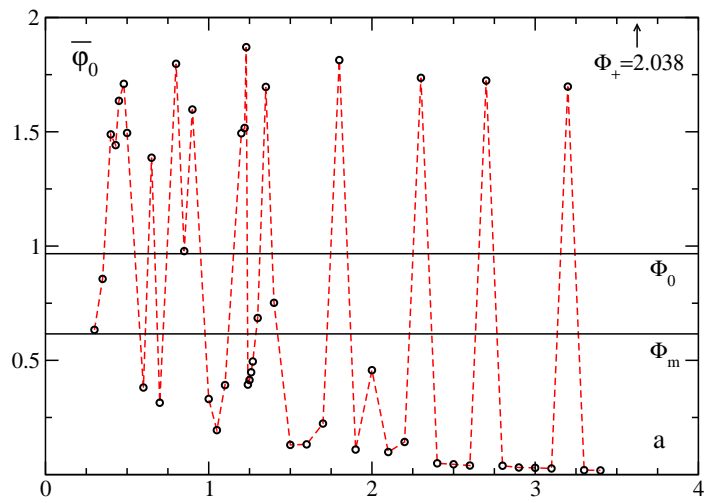- set *II*: $\alpha = 0.6, \beta = 2$, i.e., $\lambda = 0.3, \eta = 1/\sqrt{8}$; $\Delta a = 0.0338$;

Figure 6.3: The maximum $\bar{\varphi}_0$ of the expectation value $< \varphi_0(t) >$ for set I ($\alpha = 0.8, \beta = 0.5$), as a function of a.
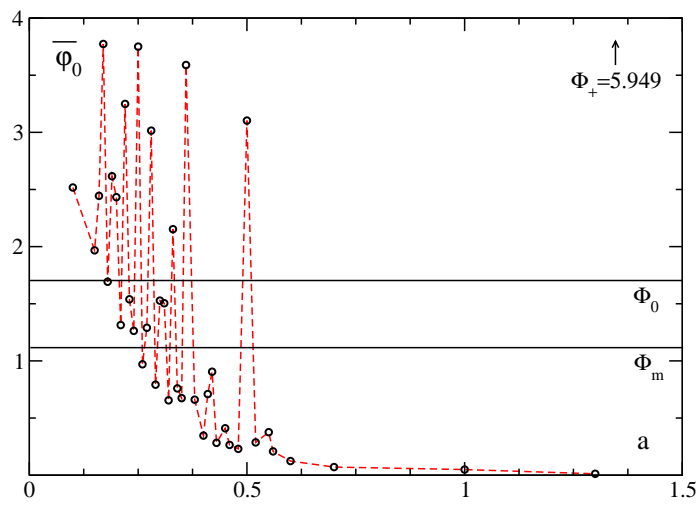

Figure 6.4: The maximum $\bar{\varphi}_0$ of the expectation value $< \varphi_0(t) >$ for set II ($\alpha = 0.6, \beta = 2$), as a function of a.

- set III: $\alpha = 0.4, \beta = 1$, i.e., $\lambda = 0.4, \eta = 1/2$; $\Delta a = 0.0167$;

- set IV: $\alpha = 0.25, \beta = 0.25$, i.e., $\lambda = \eta = 1$; $\Delta a = 0.0166$.

Corresponding to the value of β we expect large quantum corrections for the set I and IV, in case II the corrections should be small, and moderate for the set III.

We have studied the behavior of the average of the zero mode $< \chi_0(t) >$ and of its wave function $\psi_0(\chi_0)$ as a function of time. For the fluctuations we have considered the fluctuation integrals, the particle number, and the various energies. These quantities give a good detailed description of the behavior of the system as a function of time for the one single parameter set. However, in order to get an overview of the process as a function of a we have to suppress the detailed time-dependent information, we need one single quantity for each parameter set; we have chosen the *maximal value* attained by the expectation value of the zero mode during the whole time evolution. It is this quantity which we plot as a function of length scale a for fixed parameters α and β. We denote this value as $\bar{\varphi}_0$. According our observations in the cases where we have effective tunneling, this zero mode average settles at a value of φ_0 beyond the potential barrier, the late time average is typically 20% smaller than the maximal value in φ_0, reached initially.

We start with displaying results for the maximal value $\bar{\varphi}_0$ as a function of a for the four parameter sets which we have defined, in Figs. 6.3 - 6.6. They give a global picture of the tunneling in quantum field theory. The horizontal lines labeled by Φ_m and Φ_0 indicate the position of the maximum of $U(\Phi)$ and the zero of the position between the two minima. As one can see in all cases the tunneling displays a resonance phenomenon. Above by defining the parameter sets we display were given the estimates for the spacing of resonances. The observed spacings roughly correspond to these estimates. One can observe some irregular spacings which may be due to the excited states of the left oscillator or of the nonzero modes. When compared to similar figures obtained in quantum mechanical simulations [35] the resonances seen in our simulations are broader, as to be expected form the interaction with the environment of the $n \neq 0$ modes.

As another observation, the maximal value of $< \varphi_0 >$ never reaches the second minimum (the "true vacuum"), even on the resonances. In part this is due to the fact that the effective potential seen by the zero mode is modified by the quantum fluctuations. In addition some part of the wave function always remains in the false vacuum $\varphi_0 = 0$, i.e. even at late times there is a finite probability to find the system in false vacuum. The behavior of the wave function will be discussed in more detail later in this section.
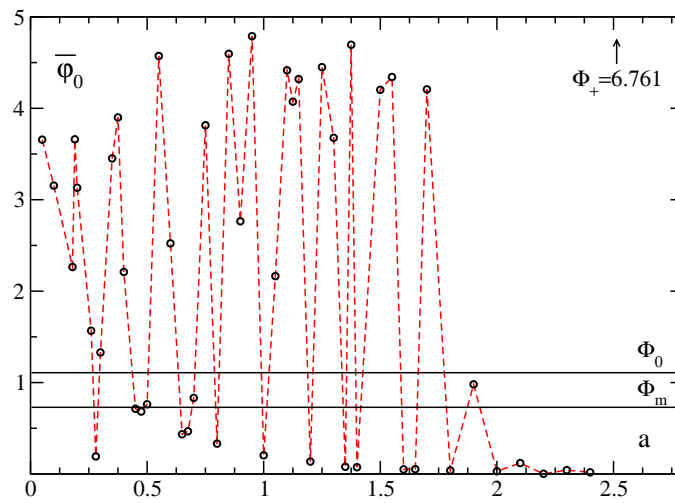
Figure 6.5: The maximum $\bar{\varphi}_0$ of the expectation value $< \varphi_0(t) >$ for set *III* ($\alpha = 0.4, \beta = 1$), as a function of a.
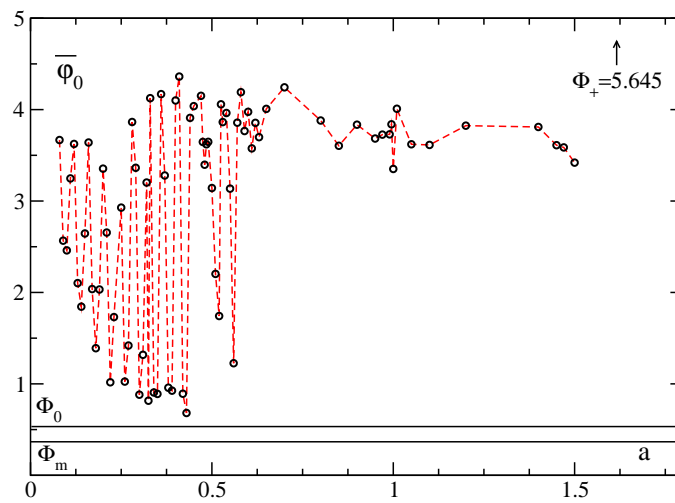

Figure 6.6: The maximum $\bar{\varphi}_0$ of the expectation value $< \varphi_0(t) >$ for set *IV* ($\alpha = 0.25, \beta = 0.25$), as a function of a.
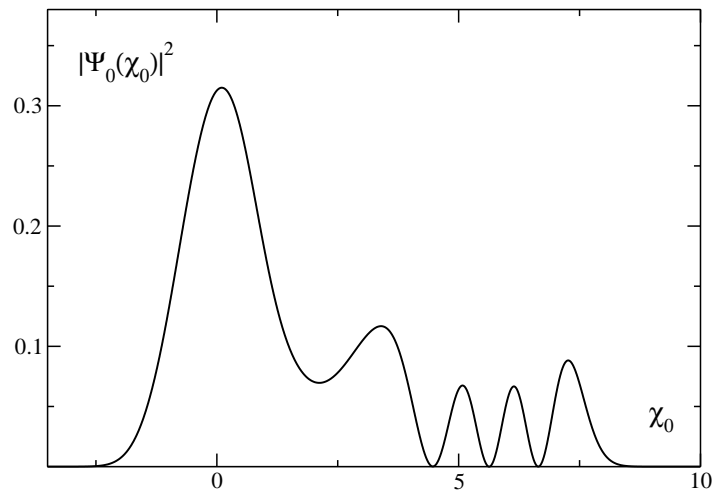
Figure 6.7: Probability density $|\psi_0(\chi_0)|^2$ at intermediate times ($t = 10$), for $\alpha = 0.8$, $\beta = 0.5$, and $a = 1.35$

For the parameter sets $I - III$ the tunneling shuts off entirely at some high values of a because the scale a multiplies the classical action. Large β implies a large classical action and, therefore, for set II this shutting-off already happens at small values, $a \simeq 0.5$. For set I one still finds resonant tunneling for $a > 3$. However, the transition time at the resonances increases substantially. For the last peak on the Fig. 6.3 it was $t \simeq 1000$. For sets II and III after some value of a the zero mode wave function displays no tunneling at all. The set IV is quite different. Here at large a the system always tunnels, due to the deformations of the effective potential caused by the large quantum fluctuations. The double well potential seen by the zero mode at early times is replaced later by a potential without barrier, and, as we will see below, the late time wave function extends over the whole range inside the potential walls from -5 to $+20$. We call this kind of transition a *sliding transition*.

After this overview over the dependence on a we now consider in detail the evolution of the zero mode wave function as a function of time.

For all parameter sets and all values of a the wave function of the zero mode initially evolves slowly; it becomes slightly asymmetric and develops a tail into the region of the potential barrier.

On the resonances the wave function, which initially is essentially the ground state wave function of the left well first connects to a particular wave function in the right
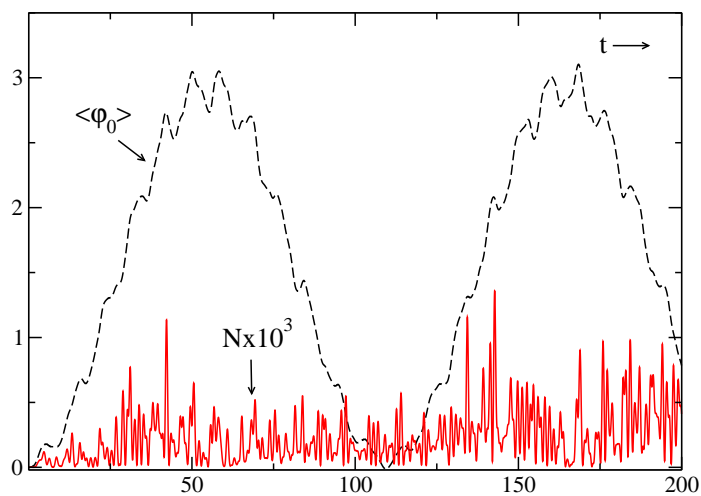
Figure 6.8: Evolution of the expectation value of the zero mode $< \varphi_0 >$ and of the particle number $\mathcal{N}$; parameters $\alpha = 0.6$, $\beta = 2$, $a = 0.5$.
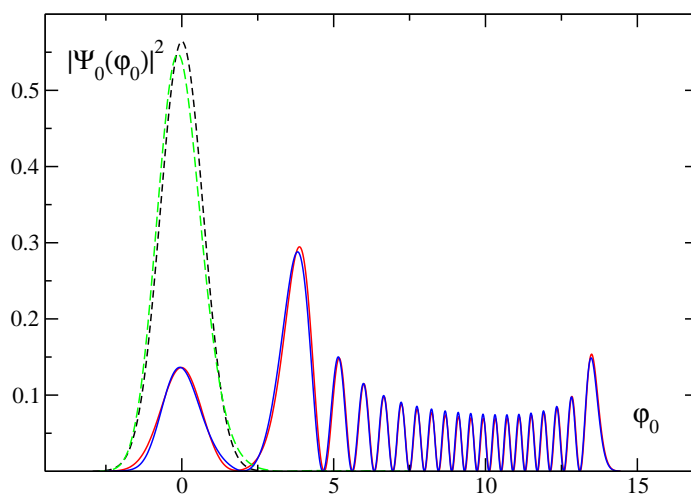

Figure 6.9: The zero mode wave function for $\alpha = 0.6$, $\beta = 2$, $a = 0.5$; dashed lines: the wave functions at $t = 0$ and 109; solid lines: the wave functions at $t = 50$ and $t = 168$.
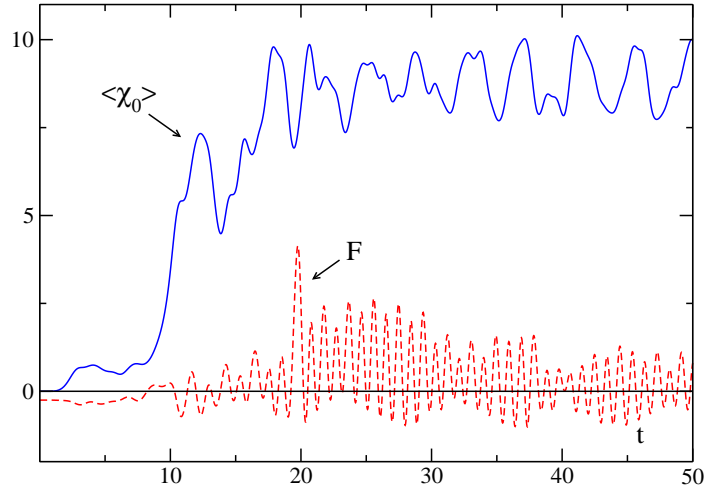
Figure 6.10: Evolution of the expectation value $< \chi_0 >$ and of the fluctuation integral $\mathcal{F}(t)$ for set IV and $a = 1.2$.

well. One can see the well-defined number of peaks in the right well on the Fig. 6.7, they indicate a specific approximate level within the right well. If the fluctuations of the quantum field remain small one observes an oscillation forth and back between these two wave functions, as usually expected in a quantum mechanical system. This case we can discuss based on the example of set II. As the parameter β is quite large the quantum fluctuations remain small and one sees the resonances expected from the qualitative picture of the degenerate levels in the separately considered wells. In Fig. 6.8 we observe the regular oscillations of the zero mode. In the same plot is shown the particle number (multiplied by 1000) as an indicator of the quantum excitations. The behavior of corresponding wave function we present at four different times in Fig. 6.9. The oscillations of the wave function appear to be very regular, it returns almost to itself after half a period $t \simeq 55$.

If the nonzero field modes get excited, then the oscillations of the zero mode are disturbed, and the other wave functions mix in. This increase the number of peaks and makes the wave function looks quite chaotic in some cases.

Off resonance the expectation value of φ_0 remains small. It still develops a tail into the right well, but this part of the wave functions does not develop further.

Parameter set III with $\beta = 1$ we expect to be intermediate in the quantum excitations, the fluctuations should get sizeable but not extremely large. As shown
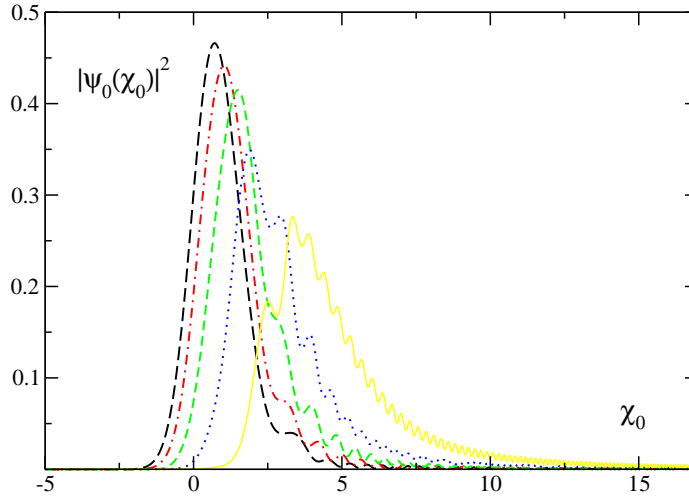
Figure 6.11: Evolution of the wave function during the barrier transition: parameters $\alpha = 0.5$, $\beta = 1$; $a = 6$; long-dashed line: $t = 7$; dash-dotted line: $t = 7.4$; short-dashed line: $t = 7.8$; dotted line: $t = 8.2$; straight line: $t = 8.6$.

in Fig. 6.5 the tunneling is still characterized by resonances which shut off after some value of a. In this case $a = 2$. For $a > 2$ the transition proceeds very slowly ($t \simeq 300$ for a last displayed resonance) and we are not able exclude further resonances anymore.

Except for the resonance region one finds efficient tunneling if the fluctuations of the nonzero momentum modes are large. In this case the penetration of the wave function into the barrier region makes the fluctuation integral positive, so that the barrier disappears and the wave function slides down, almost without changing its initial form (Gaussian wave function).

Set *IV* is close to such sliding evolution. For small a the zero mode shown still the resonant behavior, but for $a > 0.5$ the picture changes and the system ends always in the right well. However, the evolution of the system is very complex. Initially the fluctuations grow and tilt the potential. The barrier disappears and the wave function starts its movement to the right well. Then the fluctuation integral $\mathcal{F}$ gets small or negative, this causes the barrier to appears again (see Fig. 6.10). The whole evolution is a consequence of successive oscillations between these to states. Even at the late times the effective potential seen by the zero mode oscillates constantly, and
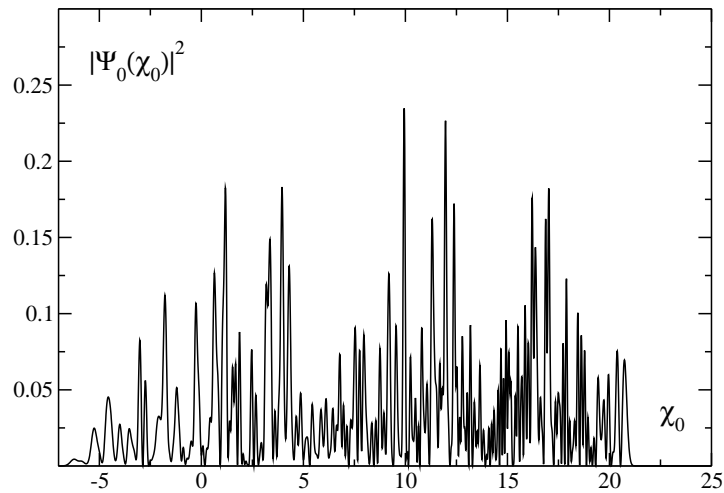
Figure 6.12: The wave function after tunneling, set IV and $a = 1.2$ and time $t = 30$.

one can not decide if it is a double or single well potential. In spite of the complexity of the process the wave function shifts towards the deeper well. This one can see at large values of a: the potential is tilted, but the fluctuation integral remains positive on the average, and the wave function *slides* down towards the modified absolute minimum. As an example we have chosen parameters $\alpha = 0.5$, $\beta = 1$ and $a = 6$ shown in the Fig. 6.11. At late times the potential shows no trace of the double-well structure, as plotted on the Fig. 6.12.

For small values of α potential is very asymmetric, therefore one could think, that the tilting of the potential is a consequence of this particular parameter choice. We therefore have done simulations for big $\alpha = 0.8$ and small $\beta = 0.2$, i.e. more symmetric potential. We again find that for $a > 1$ the transition occurs again by sliding. We display the behavior of the potential for early times (around the time when the fluctuation integral becomes negative for the first time) in the Fig. 6.13. So it seems that *sliding* occurs universally for small β and large a.

In spite of complexity of the process evolution and the drastical change of the form of the wave function the energy remains conserved better than one part in 10^8.
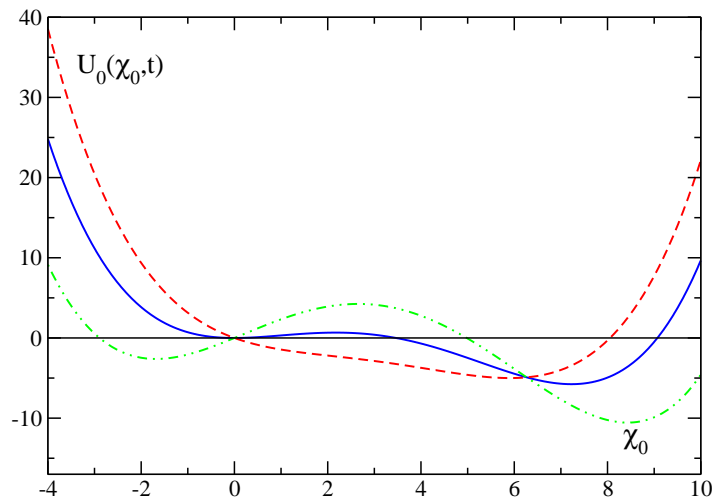
Figure 6.13: Evolution of the effective potential $U_0(\chi_0, t)$; solid line: $t = 0$; dashed line: $t = 11$; dash-double dotted line: $t = 13$.

6.3 Summary

The results we have shown display quite a different behavior of tunneling from the ones we are used to imagine by "false vacuum decay", when we just assume it to happen by bounce solution even with quantum corrections. The tunneling occurs in a variety of different ways. For large β, implying small field fluctuations, the system behaves like a quantum mechanical system with a single degree of freedom, showing resonances. The resonant tunneling happens when, as a function of the parameters, here the radius a, the levels of separate oscillators in the both wells coincide. For large spatial extension a this resonant tunneling shuts off as expected.

For smaller values of β the nonzero momentum modes are enhanced and modify the pure quantum mechanical behavior. If this enhancement is weak it can be considered as a kind of dissipation; the mean value of the zero mode shows regular periodic oscillations, on and off resonance. On resonance some more modes are involved and the wave function oscillates between the two wells. Then off resonance the wave function essentially remains in the left well, with some tail in the right hand well. For parameter sets where the excitation of the nonzero momentum modes becomes sizeable, the regular oscillations on resonance are disturbed, the behavior of

the mean value of the zero mode become irregular. At late times the wave function extends over the entire region allowed at the given energy. Off resonance at late times the system again remains concentrated in the left hand well.

If the quantum corrections become substantial appears another phenomenon: the quantum fluctuations tilt the effective potential seen by the zero mode and the barrier disappears either temporary or entirely. In such cases the wave function slides down into the new minimum.

Conclusions

We have considered the false vacuum decay as a local process, where the tunneling happens via bounces and as a global process on a compact space. In both cases the subject was the importance of the quantum backreaction.

We have presented two schemes for incorporating the quantum backreaction in the computations of the decay probability in the false vacuum decay via bounce: the one-loop backreaction and the Hartree backreaction. We have used two different sets of renormalization conditions: the $\overline{MS}$ scheme and the scheme with "physical" renormalization conditions. The numerical results were presented for the 3+1 dimensional and 1+1 dimensional models. We have considered the deviations of the effective action and transition rates in different approximations to the corresponding semiclassical values. The changes due to quantum backreaction makes several orders of magnitude in transition rates in comparison to the semiclassical approximation (the changes in the 2D model are seen to be smaller, as the iteration procedure ceases to converge for small values of β).

Besides of being possibly important for applications the magnitude of such corrections has two aspects of principle: if they are small, then this confirms the basic approach. So for most of the parameter range we can trust the semiclassical approach because it is stable with respect to higher order corrections, at least the ones we have investigated. If they are large the basic approach becomes questionable, so one learns about its possible limits. And even, as observed in the $1+1$ dimensional case, the bounce may cease to exist and one has to look for other tunneling mechanisms.

In order to do these investigations we have developed computational techniques, analytical and numerical, which allow to perform such calculations efficiently and to present data for a large number of parameter sets. Such techniques may be useful in other physical contexts.

For the analysis of global tunneling on the compact space we have used the real-time formalisms, the time-dependent Hartree-Fock approximation. The wave function of the zero mode was treated as a solution of the Schrödinger equation, while

the nonzero modes was considered in Gaussian approximation. These approximations allow to include the backreaction of the nonzero modes onto the zero mode and onto themselves.

The numerical simulations show that the tunneling in general occurs in a resonant way. If the enhancement of the nonzero modes is weak the tunneling of the zero mode occurs essentially in the same way as in quantum mechanics; the zero mode shows periodic oscillations, on and off resonance and the influence of the nonzero modes may be considered as a kind of dissipation, causing,.e.g., a broadening of the resonance peaks. If the nonzero modes are excited substantially, their backreaction causes a new phenomenon, which we have called sliding (for details see summary 6.3). If the size of space $2\pi a$ becomes large, typically $a > 1$ we find the tunneling to be suppressed, as to expected.

The variety of phenomena observed in our simulations cannot be expected to be described by WKB approximation, even if we apply the time-dependent WKB approximation to the $n = 0$ mode, as done for the quantum mechanics in Ref. [55]. The analytic estimates break down as soon as nonzero fluctuations are included.

The effects of the quantum backreaction are seen to be very sizeable. Of course in the present the cosmology of the very early universe, where such phenomena could play a rôle is not developed so far that the improvements due to one-loop corrections, with or without backreaction would be important for model building. Of course the qualitatively new features observed in global tunneling change the picture one got used to, based on the WKB approximation, and may enter into the basic conception of such models [57, 58]. We think that in any case it is important to have a very good understanding of basic mechanisms, here: the tunneling in quantum field theory, in order to build models on safe grounds. We hope to have contributed to such an understanding with the thesis presented here.

Appendix

Appendix A:
Some Definitions and Technical Tools

In this appendix we will present definitions of reducible and irreducible Feynman graphs, some details of $2PPI$ expansion, divergent integrals, their dimensional regularization and discuss Fourier transformations.

A.1: Definitions

Resummation schemes are in general based on the division of the perturbative Feynman diagrams into different classes and then the summation over all graphs within one class, in general an infinite number of them. One well-known division into classes is based on the following definition: a diagram that does not fall apart if N arbitrary propagator lines are cut is called *N-particle irreducible* (NPI). For first approximation of our interest we refer to the $1PI$ (one-particle irreducible) diagrams.

A diagram is connected if there are no isolated interaction vertices.

A diagram that does not fall apart if two propagator lines *meeting at the same point* are cut is called *two-particle-point-irreducible* ($2PPI$). The set of $2PPI$ diagrams is infinite as well. On this resummation scheme is based the second approximation we use for our computations, Hartree approximation, which is just the one-loop level of $2PPI$ expansion.

A.1: $2PPI$ Expansion

In this part of appendix we will briefly repeat the formal part of the $2PPI$ expansion following the basic work by Verschelde and his collaborators [22, 23, 59, 60, 61, 62].

As in Ref.[22], one defines the effective action of local composite operators in Euclidean space-time

$$\Gamma^{2PPI}[\phi, \Delta] = \mathcal{W}[J_1, J_2] - J_1\phi - \frac{1}{2}J_2(\phi^2 + \Delta) , \qquad (A.1)$$

where the external sources J_1 and J_2 are both local and fix the expectation value of Φ and Φ^2

$$\phi = <\Phi> = \frac{\delta\mathcal{W}}{\delta J_1} , \qquad (A.2)$$

$$\frac{1}{2}(\phi^2 + \Delta) = \frac{1}{2}<\Phi^2> = \frac{\delta\mathcal{W}}{\delta J_2} , \qquad (A.3)$$

$$\exp\left(-\mathcal{W}[J_1, J_2]\right) = \int \mathcal{D}\Phi \exp\left[-\left(S[\Phi] + J_1\Phi + J_2\Phi^2\right)\right] . \qquad (A.4)$$

Then the effective equations of motion are

$$\frac{\delta\Gamma^{2PPI}[\phi, \Delta]}{\delta\phi} = -J_1 - J_2\phi , \qquad (A.5)$$

$$\frac{\delta\Gamma^{2PPI}[\phi, \Delta]}{\delta\Delta} = -\frac{1}{2}J_2 . \qquad (A.6)$$

The combinatorial tricks how to sum all $2PR$ diagrams one can find again in Ref.[22]. The result is the complete effective action of the $2PPI$ formalism

$$\Gamma^{2PPI}[\phi, \Delta] = S[\phi] + \Gamma_q^{2PPI}[\phi, \mathcal{M}^2] - \frac{3\lambda^2}{4}\Delta^2 \qquad (A.7)$$

consisting of the classical action, the quantum part and the constant which prevents

Figure A.1: Quantum part of the 2PPI effective action including some three-loop contributions.

double counting. One should notice that the prefactor in a constant term is different by different parameterizations of potential. For the parameterization used in this thesis it should be replaced by $\frac{3\lambda^2}{8}$. The quantum part Γ_q^{2PPI} contains the one-loop

contribution ('ln det') and all $2PPI$ graphs (see Fig.A.1). These diagrams are to be computed using the propagarot

$$\mathcal{G}(k) = \frac{1}{k^2 + \mathcal{M}^2} \ , \tag{A.8}$$

with an effective mass $\mathcal{M}$. Notice that this propagator is local, however, it is different from the two-point Green's function. The effective mass depends on the local self-energy Δ which is obtained as a derivative of the quantum part of the effective action with respect to the effective mass

$$\frac{1}{2}\Delta = \frac{\delta\Gamma_q^{2PPI}[\phi, \mathcal{M}^2]}{\delta\mathcal{M}^2} \ . \tag{A.9}$$

This is equivalent to cutting a line by deriving with respect to the propagator $\mathcal{G}(k)$ and then connecting the two ends to a common third point x

$$\frac{\delta}{\delta\mathcal{M}^2} = \int [dk]\frac{\delta\mathcal{G}(k)}{\delta\mathcal{M}^2}\frac{\delta}{\delta\mathcal{G}(k)} = \int [dk]\frac{-1}{(k^2 + \mathcal{G}^2)^2}\frac{\delta}{\delta\mathcal{G}(k)} \ . \tag{A.10}$$

The mass corrections to the self-energy form one-, two- and three-loop diagrams are shown in Fig.A.2.
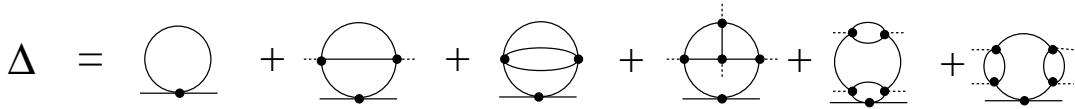

Figure A.2: 2PPI self-energy including some three-loop contributions.

A.3: Divergent Integrals

The first divergent integral which needs to be regularized appears in the leading order of the fluctuation integral

$$I_0 = \mu^\epsilon \int \frac{d^{4-\epsilon}k}{(2\pi)^{4-\epsilon}}\frac{1}{k^2 + m^2} = -\frac{m^2}{16\pi^2}\left(L_\epsilon - \ln\frac{m^2}{\mu^2} + 1\right) \ . \tag{A.11}$$

Here and everywhere else $L_\epsilon = \frac{2}{\epsilon} - \gamma + \ln 4\pi$. The factor μ^ϵ gives the integral its correct dimension in $3+1$ dimensions. The next one is the integral of the first order

$$I_1 = \mu^\epsilon \int \frac{d^{4-\epsilon}k}{(2\pi)^{4-\epsilon}} \frac{1}{(k^2 + m^2)((k+q)^2 + m^2)} \cdot$$

Using the so called Feynman trick:

$$\frac{1}{A^\alpha B^\beta} = \frac{\Gamma(\alpha+\beta)}{\Gamma(\alpha)\Gamma(\beta)} \int d\omega \frac{\omega^{\alpha-1}(1-\omega)^{\beta-1}}{(\omega A + (1-\omega)B)^{\alpha+\beta}}$$

one can write

$$
\begin{aligned}
\mu^{-\epsilon}I_1 &= \int \frac{d^{4-\epsilon}k}{(2\pi)^{4-\epsilon}} \int_0^1 \frac{d\omega}{(\omega((k+q)^2 + m^2) + (1-\omega)(k^2 + m^2))^2} \\
&= \int \frac{d^{4-\epsilon}k}{(2\pi)^{4-\epsilon}} \int_0^1 \frac{d\omega}{(k^2 + m^2 + 2\omega kq + \omega q^2)^2} \\
&= \int \frac{d^{4-\epsilon}k}{(2\pi)^{4-\epsilon}} \int_0^1 \frac{d\omega}{((k+\omega q)^2 + \mathcal{M}^2)^2} = \int_0^1 d\omega \int \frac{d^{4-\epsilon}l}{(2\pi)^{4-\epsilon}} \frac{1}{(l^2 + \mathcal{M}^2)^2},
\end{aligned}
$$

here were introduced two new variables $\mathcal{M}^2 = m^2 + \omega(1-\omega)q^2$ and $l = k + \omega q$.

$$
\begin{aligned}
I_1 &= \int_0^1 \frac{d\omega}{(4\pi)^{2-\epsilon/2}} \frac{\Gamma(2 - 2 + \epsilon/2)}{\Gamma(2)} \left(\frac{\mathcal{M}^2}{\mu^2}\right)^{-\epsilon/2} \\
&= \int_0^1 \frac{d\omega}{16\pi^2} \left(1 + \frac{\epsilon}{2}\ln 4\pi\right) \frac{2}{\epsilon} \left(1 - \frac{\epsilon}{2}\gamma\right) \left(1 - \frac{\epsilon}{2}\ln \frac{\mathcal{M}^2}{\mu^2}\right) \\
&= \frac{1}{16\pi^2} \left(\frac{2}{\epsilon} - \gamma + \ln 4\pi\right) \int_0^1 d\omega \left(1 - \frac{\epsilon}{2}\ln \frac{m^2 + \omega(1-\omega)q^2}{\mu^2}\right) \\
&= \frac{L_\epsilon}{16\pi^2} - \frac{1}{16\pi^2} \int_0^1 d\omega \ln \frac{-\omega^2 q^2 + \omega q^2 + m^2}{\mu^2} \\
&= \frac{L_\epsilon}{16\pi^2} - \frac{1}{16\pi^2} \int_0^1 d\omega \left[\ln(\omega\frac{q}{\mu} - \frac{q + \sqrt{q^2 + 4m^2}}{2\mu}) + \ln(-\omega\frac{q}{\mu} + \frac{q - \sqrt{q^2 + 4m^2}}{2\mu})\right] \\
&= \frac{L_\epsilon - \ln m^2/\mu^2}{16\pi^2} - \frac{1}{16\pi^2} \left[-2 + \frac{\sqrt{q^2 + 4m^2}}{q} \ln \frac{\sqrt{q^2 + 4m^2} + q}{\sqrt{q^2 + 4m^2} - q}\right] \cdot
\end{aligned}
$$

So the second integral of our interest is

$$
\begin{aligned}
I_1 &= \int \frac{d^{4-\epsilon}k}{(2\pi)^{4-\epsilon}} \frac{1}{(k^2+m^2)((k+q)^2+m^2)} \\
&= \frac{L_\epsilon - \ln m^2/\mu^2}{16\pi^2} - \frac{1}{16\pi^2}\left[-2 + \frac{\sqrt{q^2+4m^2}}{q}\ln\frac{\sqrt{q^2+4m^2}+q}{\sqrt{q^2+4m^2}-q}\right] .
\end{aligned}
$$
(A.12)

The computation of the next to leading order term in the fluctuation integral contains the Fourier transformation

$$
\tilde{V}(q) = \int d^4 y\, e^{-iqy} V(y) .
$$

One can show that this reduces to the Fourier-Bessel transformations

$$
\begin{aligned}
\tilde{V}(q) &= \int d^4 x\, e^{-iqx} V(x) = \int dr\, r^3 d\Omega_3 e^{-i|q|r\cos\chi} V(r) \\
&= \int_0^\infty dr\, r^3 V(r) 4\pi \int_0^\pi d\chi \sin^2\chi\, e^{-i|q|r\cos\chi} \\
&= \int_0^\infty dr\, r^3 V(r) 4\pi J_1(|q|r)\Gamma\left(\frac{3}{2}\right)\Gamma\left(\frac{1}{2}\right)\frac{2}{|q|r} \\
&= \frac{4\pi^2}{|q|}\int_0^\infty dr\, r^2 J_1(|q|r) V(r) .
\end{aligned}
$$
(A.13)

An analogous formula holds for the inverse transformation.

Appendix B.
The One-loop Effective Potential

The one-loop effective potential with renormalization conditions

In the one-loop approximation the effective mass is a second derivative of the tree level(classical) potential.In our model we have chosen potential to be

$$
U(\phi) = \frac{m^2}{2}\phi^2 - \eta\phi^3 + \frac{\lambda}{8}\phi^4 .
$$
(B.1)

So the effective mass has a form

$$
\mathcal{M}^2 = U''(\phi) = m^2 - 6\eta\phi + \frac{3}{2}\lambda\phi^2 .
$$
(B.2)

The 1-loop effective potential includes the classical potential, the part coming form the 1-loop corrections('lndet' term) and the counterterms. In our case one finds it to be

$$
\begin{aligned}
U_{eff}(\phi, \mathcal{M}^2) &= U(\phi) + \frac{1}{2} \ln \det \frac{\Box + \mathcal{M}^2}{\Box + m^2} + \delta U(\phi) \\
&= \frac{m^2}{2} \phi^2 - \eta \phi^3 + \frac{\lambda}{8} \phi^4 - \frac{\mathcal{M}^4}{64\pi^2} \left(L_\epsilon - \ln \frac{\mathcal{M}^2}{\mu^2} + \frac{3}{2} \right) \qquad \text{(B.3)} \\
&+ \frac{m^4}{64\pi^2} \left(L_\epsilon - \ln \frac{m^2}{\mu^2} + \frac{3}{2} \right) + \delta\rho\phi + \frac{1}{2}\delta m^2 \phi^2 - \delta\eta\phi^3 + \frac{1}{8}\delta\lambda\phi^4 \ .
\end{aligned}
$$

Here we have introduced the counterterms in a way most appropriate form, as a corrections to the coupling constants.We have not introduced the cosmological constant, as it is not necessary to fulfill renormalization condition $U_{eff}(0) = 0$, which will be discussed later in this appendix. As one can immediately see $\mathcal{M}^2(0) = m^2$ and two divergent terms in the effective potential cancel for $\phi = 0$.

The first and the second derivative of effective potential look like

$$
\begin{aligned}
U'_{eff} &= m^2\phi - 3\eta\phi^2 + \frac{\lambda}{2}\phi^3 + \delta\rho + \delta m^2\phi - 3\delta\eta\phi^2 + \frac{1}{2}\delta\lambda\phi^3 \\
&- \frac{\mathcal{M}^2}{32\pi^2}(3\lambda\phi - 6\eta)\left(L_\epsilon - \ln\frac{\mathcal{M}^2}{\mu^2} + 1 \right) , \qquad \text{(B.4)} \\
U''_{eff} &= m^2 - 6\eta\phi + \frac{3}{2}\lambda\phi^2 + \delta m^2 - 6\delta\eta\phi + \frac{3}{2}\delta\lambda\phi^2 \\
&- \frac{1}{32\pi^2}(3\lambda\phi - 6\eta)^2\left(L_\epsilon - \ln\frac{\mathcal{M}^2}{\mu^2} \right) - \frac{3\lambda\mathcal{M}^2}{32\pi^2}\left(L_\epsilon - \ln\frac{\mathcal{M}^2}{\mu^2} + 1 \right) . \text{(B.5)}
\end{aligned}
$$

The renormalization conditions which we can put on counterterms should serve two aims: first they should cancel the divergences and second avoid drastical changes in the form of the effective potential. As we have seen above one can have maximally five counterterms, so the maximal number of renormalization conditions is five. We

choose them to be:

1)   height of local minimum is 0
$$U_{eff}(0, \mathcal{M}^2(0)) = 0 \; , \tag{B.6}$$

2)   local minimum is not shifted
$$U'_{eff}(0, \mathcal{M}^2(0)) = 0 \; , \tag{B.7}$$

3)   curvature at local minimum is conserved
$$U''_{eff}(0, \mathcal{M}^2(0)) = m^2 \; , \tag{B.8}$$

4)   height of absolute minimum is conserved
$$U_{eff}(\phi_+, \mathcal{M}^2(\phi_+)) = U_+ \; , \tag{B.9}$$

5)   absolute minimum is not shifted
$$U'_{eff}(\phi_+, \mathcal{M}^2(\phi_+)) = 0 \; . \tag{B.10}$$

where ϕ_+ is the position of the absolute minimum

$$\phi_+ = \frac{3\eta}{\lambda} + \sqrt{\frac{9\eta^2}{\lambda^2} - \frac{2m^2}{\lambda}} \; . \tag{B.11}$$

As it was already mentioned above the first condition fixes just a cosmological constant, however, in our case the effective potential fulfills this condition automatically.

The second condition leads to the following linear counterterm:

$$\delta\rho = -\frac{12\eta m^2}{64\pi^2}(L_\epsilon - \ln\frac{m^2}{\mu^2} + 1) \; . \tag{B.12}$$

The condition on the second derivative of effective potential (third condition) fixes the quadratic counterterm

$$\delta m^2 = \frac{3}{32\pi^2}(12\eta^2 + \lambda m^2)\left(L_\epsilon - \ln\frac{m^2}{\mu^2}\right) + \frac{3\lambda m^2}{32\pi^2} \; . \tag{B.13}$$

The last two conditions lead to the system of equations:

$$\delta\rho\phi_+ + \frac{1}{2}\delta m^2\phi_+^2 - \delta\eta\phi_+^3 + \frac{1}{8}\delta\lambda\phi_+^4 = \frac{\mathcal{M}^4(\phi_+)}{64\pi^2}\left(L_\epsilon - \ln\frac{\mathcal{M}^2(\phi_+)}{\mu^2} + \frac{3}{2}\right)$$
$$-\frac{m^4}{64\pi^2}\left(L_\epsilon - \ln\frac{m^2}{\mu^2} + \frac{3}{2}\right) \; ,$$

$$\delta\rho + \delta m^2\phi_+ - 3\delta\eta\phi_+^2 + \frac{1}{2}\delta\lambda\phi_+^3$$
$$-\frac{\mathcal{M}^2(\phi_+)}{32\pi^2}(3\lambda\phi_+ - 6\eta)\left(L_\epsilon - \ln\frac{\mathcal{M}^2(\phi_+)}{\mu^2} + 1\right) = 0 \; .$$

We separate the counterterms $\delta\eta$ and $\delta\lambda$ in infinite $(\delta\eta_d, \delta\lambda_d)$ and finite $(\delta\eta_f, \delta\lambda_f)$ parts, the infinite ones one can write down immediately:

$$\delta\eta_d = \frac{9\eta\lambda}{32\pi^2}\left(L_\epsilon - \ln\frac{m^2}{\mu^2}\right) , \tag{B.14}$$

$$\delta\lambda_d = \frac{9\lambda^2}{32\pi^2}\left(L_\epsilon - \ln\frac{m^2}{\mu^2}\right) \tag{B.15}$$

to get the finite parts one should solve the following system of linear equations:

$$-\delta\eta_f\phi_+^3 + \frac{1}{8}\delta\lambda_f\phi_+^4 = \frac{1}{64\pi^2}\Big[-\mathcal{M}_+^4\left(\ln\frac{\mathcal{M}_+^2}{m^2} - \frac{3}{2}\right) - 3\lambda m^2\phi_+^2 + 12m^2\eta\phi_+$$
$$-\frac{3}{2}m^4 - \frac{9\lambda}{2}\phi_+^3(\lambda\phi_+ - 8\eta)\ln\frac{m^2}{\mu^2}\Big] , \tag{B.16}$$

$$-3\delta\eta_f\phi_+^2 + \frac{1}{2}\delta\lambda_f\phi_+^3 = \frac{6\lambda\phi_+ - 12\eta}{64\pi^2}\left[-\mathcal{M}_+^2\left(\ln\frac{\mathcal{M}_+^2}{m^2} - 1\right) - m^2\right]$$
$$+\frac{9}{64\pi^2}\lambda\phi_+^2(\lambda\phi_+ - 6\eta)\ln\frac{m^2}{\mu^2} . \tag{B.17}$$

where we have introduced a notation $\mathcal{M}_+^2 = \mathcal{M}^2(\phi_+)$. These equations were solved numerically.

The one-loop effective potential in $\overline{MS}$ renormalization scheme

In the $\overline{MS}$ renormalization scheme one does not put any renormalization conditions, i.e. one has just the divergent counterterms and no finite terms. This is equivalent to letting $L_\epsilon \to 0$ and no introduction of counterterms at all. However, to have a possibility to compare results of computation in $\overline{MS}$ scheme with ones with renormalization conditions we require the system to have the same initial conditions, i.e. at $\phi = 0$ the effective potential should coincide with classical potential. For this purpose we introduce a finite linear counterterm $\delta\rho_f\phi$, this is the only term we will need. The effective potential has a form

$$U_{eff}(\phi, \mathcal{M}^2) = \frac{m^2}{2}\phi^2 - \eta\phi^3 + \frac{\lambda}{8}\phi^4 - \frac{\mathcal{M}^4}{64\pi^2}\left(L_\epsilon - \ln\frac{\mathcal{M}^2}{\mu^2} + \frac{3}{2}\right)$$
$$+ \frac{m^4}{64\pi^2}\left(L_\epsilon - \ln\frac{m^2}{\mu^2} + \frac{3}{2}\right) \tag{B.18}$$
$$+ \delta\rho_f\phi + \delta\rho_d\phi + \frac{1}{2}\delta m_d^2\phi^2 - \delta\eta_d\phi^3 + \frac{1}{8}\delta\lambda_d\phi^4 .$$

The divergent counterterms do not differ from the ones in the previous subsection (1-loop effective potential with renormalization conditions):

$$\delta\rho_d = -\frac{12\eta m^2}{64\pi^2}L_\epsilon , \tag{B.19}$$

$$\delta m_d^2 = \frac{3}{32\pi^2}(12\eta^2 + \lambda m^2)L_\epsilon , \tag{B.20}$$

$$\delta\eta_d = \frac{9\eta\lambda}{32\pi^2}L_\epsilon , \tag{B.21}$$

$$\delta\lambda_d = \frac{9\lambda^2}{32\pi}L_\epsilon . \tag{B.22}$$

As we have discussed above the effective potential should coincide with tree level potential, so we require

$$U_{eff}(0) = 0 \tag{B.23}$$

and

$$U'_{eff}(0) = 0 . \tag{B.24}$$

The first condition is fulfilled automatically, for the second one we need the linear term we have already introduced in the effective potential. The first derivative of effective potential

$$U'_{eff} = m^2\phi - 3\eta\phi^2 + \frac{\lambda}{2}\phi^3 - \frac{\mathcal{M}^2}{32\pi^2}\left(1 - \ln\frac{\mathcal{M}^2}{m^2}\right)(-6\eta + 3\lambda\phi) + \delta\rho_f .$$

The second condition leads to

$$\delta\rho_f = -\frac{3\eta m^2}{16\pi^2}\left(1 - \ln\frac{m^2}{\mu^2}\right) . \tag{B.25}$$

So the effective potential will get

$$\begin{aligned}
U_{eff}(\phi, \mathcal{M}^2) &= \frac{m^2}{2}\phi^2 - \eta\phi^3 + \frac{\lambda}{8}\phi^4 - \frac{\mathcal{M}^4}{64\pi^2}\left(\frac{3}{2} - \ln\frac{\mathcal{M}^2}{\mu^2}\right) \\
&+ \frac{m^4}{64\pi^2}\left(\frac{3}{2} - \ln\frac{\mathcal{M}^2}{\mu^2}\right) - \frac{3\eta m^2}{16\pi^2}\phi\left(1 - \ln\frac{\mathcal{M}^2}{\mu^2}\right) ,
\end{aligned} \tag{B.26}$$

where the local minimum coincides with the one of the classical potential, but the absolute minimum at $\tilde{\phi}_+$ is shifted away from its bare value ϕ_+.

Appendix C.
The Hartree Effective Potential

The hartree effective potential with renormalization conditions

In the Hartree approximation the self-consistent effective potential is an extremum (maximum) of a variational potential

$$U_{eff} = \max_{\mathcal{M}^2} \; \mathcal{U}(\phi, \mathcal{M}^2) \; . \tag{C.1}$$

The variational potential includes the classical potential, the 1-loop corrections, the term including a local insertion in the propagator (Δ^2 term) and the counterterms

$$
\begin{aligned}
\mathcal{U}(\phi, \mathcal{M}^2) &= \frac{m^2}{2}\phi^2 - \eta\phi^3 + \frac{\lambda}{8}\phi^4 + \frac{1}{2}\ln\det\frac{\Box + \mathcal{M}^2}{\Box + m^2} - \frac{3\lambda}{8}\Delta^2(x) + \delta U(\phi) \\
&= \frac{m^2}{2}\phi^2 - \eta\phi^3 + \frac{\lambda}{8}\phi^4 - \frac{\mathcal{M}^4}{64\pi^2}\left(L_\epsilon - \ln\frac{\mathcal{M}^2}{\mu^2} + \frac{3}{2}\right) \\
&\quad + \frac{m^4}{64\pi^2}\left(L_\epsilon - \ln\frac{m^2}{\mu^2} + \frac{3}{2}\right) - \frac{3\lambda}{8}\Delta^2(x) + \delta U(\phi) \; . \tag{C.2}
\end{aligned}
$$

In this approximation exactly as in the case of the one-loop approximation we want to fulfill renormalization conditions which as far as it is possible avoid the difference in the form between the tree level potential and the effective potential. For this purpose we introduce in addition to the standard Hartree counterterms Λ_d, $A\mathcal{M}^2$, $B\mathcal{M}^4$, a finite polynomial in ϕ in the following form

$$\Lambda_f + \delta\rho_f\phi + \frac{1}{2}\delta m_f^2\phi^2 - \delta\eta_f\phi^3 + \frac{1}{8}\delta\lambda_f\phi^4 \; , \tag{C.3}$$

where we have introduced the cosmological constant, as it is necessary here in the contrary to the 1-loop case.

So the variational potential gets a form

$$
\begin{aligned}
\mathcal{U}(\phi, \mathcal{M}^2) &= \Lambda_f + \delta\rho_f\phi + \frac{m^2 + \delta m_f^2}{2}\phi^2 - (\eta + \delta\eta_f)\phi^3 + \frac{\lambda + \delta\lambda_f}{8}\phi^4 \\
&\quad - \frac{\mathcal{M}^4}{64\pi^2}\left(L_\epsilon - \ln\frac{\mathcal{M}^2}{\mu^2} + \frac{3}{2}\right) + \frac{m^4}{64\pi^2}\left(L_\epsilon - \ln\frac{m^2}{\mu^2} + \frac{3}{2}\right) \\
&\quad - \frac{3\lambda}{8}\Delta^2(x) + \Lambda_d + B\mathcal{M}^4 \; , \tag{C.4}
\end{aligned}
$$

with

$$\Delta(\phi, \mathcal{M}^2) = \frac{2}{3\lambda} \left(\mathcal{M}^2 - (m^2 + \delta m_f^2) + 6(\eta + \delta\eta_f)\phi - \frac{3}{2}(\lambda + \delta\lambda_f)\phi^2 \right) \qquad \text{(C.5)}$$

and do not write the quadratic term in the effective mass, as it is obvious that we will not need this counterterm to cancel the divergences.

According definition (1.28) Δ is a variation of the potential (C.4) with respect to the effective mass:

$$\frac{\partial \mathcal{U}(\phi, \mathcal{M}^2)}{\partial \mathcal{M}^2} = 0 \qquad \text{(C.6)}$$

one has

$$\Delta(\phi, \mathcal{M}^2) = -\frac{\mathcal{M}^2}{16\pi^2} \left(L_\epsilon - \ln \frac{\mathcal{M}^2}{\mu^2} + 1 \right) + 4B\mathcal{M}^2 \ . \qquad \text{(C.7)}$$

Putting together everything we just have discussed, we derive the gap equation

$$\begin{aligned} \mathcal{M}^2 &= (m^2 + \delta m^2) - 6(\eta + \delta\eta_f)\phi + \frac{3}{2}(\lambda + \delta\lambda_f)\phi^2 \\ &\quad + \frac{3}{2}\lambda \left[-\frac{\mathcal{M}^2}{16\pi^2} \left(L_\epsilon - \ln \frac{\mathcal{M}^2}{\mu^2} + 1 \right) + 4B\mathcal{M}^2 \right] \ . \end{aligned} \qquad \text{(C.8)}$$

To make the gap equation finite we should put $B = L_\epsilon/64\pi^2$. However, we take '$1 - \ln \frac{m^2}{\mu^2}$' with

$$B = \frac{1}{64\pi^2} \left(L_\epsilon - \ln \frac{m^2}{\mu^2} + 1 \right) \ . \qquad \text{(C.9)}$$

This entails

$$\Delta(\phi, \mathcal{M}^2) = \frac{\mathcal{M}^2}{16\pi^2} \ln \frac{\mathcal{M}^2}{m^2} \qquad \text{(C.10)}$$

and

$$\mathcal{M}^2 = (m^2 + \delta m_f^2) - 6(\eta + \delta\eta_f)\phi + \frac{3}{2}(\lambda + \delta\lambda_f)\phi^2 + \frac{3}{2}\lambda \frac{\mathcal{M}^2}{16\pi^2} \ln \frac{\mathcal{M}^2}{m^2} \ . \text{(C.11)}$$

For the further discussion we will need the first derivative of the effective potential

$$U'_{eff}(\phi) = \frac{dU_{eff}(\phi)}{d\phi} = \frac{\partial \mathcal{U}(\phi, \mathcal{M}^2)}{\partial \phi} + \frac{\partial \mathcal{U}(\phi, \mathcal{M}^2)}{\partial \mathcal{M}^2} \frac{d\mathcal{M}^2}{d\phi} \ ,$$

where $\mathcal{M}^2$ is a solution of the gap equation, that means the second term in the last expression vanishes. Therefore, for the first derivative of the effective potential one

has

$$
\begin{aligned}
U'_{eff}(\phi) &= \delta\rho_f + (m^2 + \delta m_f^2)\phi - 3(\eta + \delta\eta_f)\phi^2 + \frac{\lambda + \delta\lambda_f}{2}\phi^3 \\
&\quad + \frac{3\mathcal{M}^2}{32\pi^2}\ln\frac{\mathcal{M}^2}{m^2}\left[-2(\eta + \delta\eta_f) + (\lambda + \delta\lambda_f)\phi\right] .
\end{aligned}
$$

Now we are ready to impose the renormalization conditions. There will be again five conditions, but as a first condition we will require no change of effective mass (bare vacuum condition) at $\phi = 0$, $\mathcal{M}^2(0) = m^2$. One can easily check that this condition is equivalent to the one on the curvature of the effective potential at false minimum:

1)   effective mass at local minimum is conserved
$$
\mathcal{M}^2(0) = m^2 , \tag{C.12}
$$
2)   height of local minimum is 0
$$
U_{eff}(0, \mathcal{M}^2(0)) = 0 , \tag{C.13}
$$
3)   local minimum is not shifted
$$
U'_{eff}(0, \mathcal{M}^2(0)) = 0 , \tag{C.14}
$$
4)   height of absolute minimum is conserved
$$
U_{eff}(\phi_+, \mathcal{M}^2(\phi_+)) = U_+ , \tag{C.15}
$$
5)   absolute minimum is not shifted
$$
U'_{eff}(\phi_+, \mathcal{M}^2(\phi_+)) = 0 , \tag{C.16}
$$

where ϕ_+ is again the position of the absolute minimum

$$
\phi_+ = \frac{3\eta}{\lambda} + \sqrt{\frac{9\eta^2}{\lambda^2} - \frac{2m^2}{\lambda}} . \tag{C.17}
$$

From the first condition is obvious that

$$
\delta m_f^2 = 0 . \tag{C.18}
$$

The second condition fixes the cosmological constant. The divergent part of the cosmological constant cancels $m^4 L_\epsilon/64\pi^2$ term in the effective potential, so that $\Lambda_d = -m^4 L_\epsilon/64\pi^2$, so we define it analogously to the B counterterm

$$
\Lambda = -\frac{m^4}{64\pi^2}\left(L_\epsilon - \ln\frac{m^2}{\mu^2} + 1\right) . \tag{C.19}
$$

The requirement the local minimum to be not shifted (third condition) leads to determination of the linear counterterm:

$$\delta\rho_f = 0 \ . \tag{C.20}$$

The last two conditions on the effective potential at absolute minimum lead to the nonlinear system for equations for $\delta\eta_f$ and $\delta\lambda_f$ counterterms:

$$\delta\eta_f\phi_+^3 - \frac{\delta\lambda_f}{8}\phi_+^4 = \frac{\mathcal{M}_+^4}{64\pi^2}\left(\ln\frac{\mathcal{M}_+^2}{m^2} - \frac{1}{2}\right) + \frac{m^4}{128\pi^2} - \frac{3\lambda}{8}\Delta_+^2 \ , \tag{C.21}$$

$$3\delta\eta_f(\phi_+^2 + \Delta_+) - \frac{\delta\lambda_f}{2}\phi_+(\phi_+^2 + 3\Delta_+) = -\frac{1}{2}\left[6\eta - 3\lambda\phi_+\right]\Delta_+ \ , \tag{C.22}$$

here we again use the notation $\mathcal{M}_+^2 = \mathcal{M}^2(\phi_+)$ and have introduced the new one, $\Delta_+ = \Delta(\phi_+, \mathcal{M}_+^2)$. One should notes that the equations are independent of μ. This is a consequence of Hartree resummation scheme. The above system of equations was solved numerically using an iterative procedure:

$$\begin{array}{cccc}
& \mathcal{M}_+^2 = \tilde{\mathcal{M}}_+^2 & & \\
& \Downarrow & & \\
\uparrow \ (C.10) & \Rightarrow & \Delta_+ & \\
& \Downarrow & & \\
| \ (C.21, C.22) & \Rightarrow & \delta\eta_f, \delta\lambda_f & \\
& \Downarrow & & \\
| \ (C.11) & \Rightarrow & \mathcal{M}_+^2 \ . &
\end{array} \tag{C.23}$$

In the first step one puts the effective mass to be equal its tree level value at an absolute minimum $\tilde{\mathcal{M}}_+^2 = m^2 - 6\eta\phi_+ + \frac{3}{2}\lambda\phi_+^2$, as a second step one computes Δ_+ for this value on effective mass. Then one determines corresponding $\delta\eta_f$ and $\delta\eta_f$ and computes the new value of an effective mass according (C.11) with just computed values of counterterm coefficients and Δ_+. Now this value of effective mass is a new input for the whole procedure (one should start with second step).

The hartree effective potential in $\overline{MS}$ renormalization scheme

In $\overline{MS}$ scheme for the Hartree approximation in contrary to the one-loop case one should ensure that the effective mass obeys the bare vacuum condition at local

minimum $\mathcal{M}^2(0) = m^2$. In this case has a gap-equation the following form:

$$
\begin{aligned}
\mathcal{M}^2 \ = \ & m^2 - 6\eta\phi + \frac{3}{2}\lambda\phi^2 \\
& + \frac{3}{2}\lambda\left[-\frac{\mathcal{M}^2}{16\pi^2}\left(L_\epsilon - \ln\frac{\mathcal{M}^2}{\mu^2} + 1 \right) + 4B\mathcal{M}^2 \right] \ . \qquad \text{(C.24)}
\end{aligned}
$$

To fulfill the bare vacuum condition we choose the coefficient of the counterterm B as in the previous subsection (C.9)

$$
B = \frac{1}{64\pi^2}\left(L_\epsilon - \ln\frac{m^2}{\mu^2} + 1 \right) \ . \qquad \text{(C.25)}
$$

We are forced to put the 'ln' term in counter term. This will remove the μ dependence from the whole of calculations, but as the most of results we present is computed for $\mu^2 = m^2$, it will not be important. The only thing we can not do is to investigate the dependence of our results in Hartree $\overline{\text{MS}}$ scheme on the renormalization scale.

In addition as in the one-loop $\overline{MS}$ we want to fix effective potential at $\phi = 0$, therefore we define a cosmological constant in a similar to (C.19). So the effective potential is given by:

$$
\begin{aligned}
U_{eff}(\phi, \mathcal{M}^2) \ = \ & \frac{m^2}{2}\phi^2 - \eta\phi^3 + \frac{\lambda}{8}\phi^4 - \frac{\mathcal{M}^4}{64\pi^2}\left(\frac{1}{2} - \ln\frac{\mathcal{M}^2}{m^2} \right) \\
& + \frac{m^4}{128\pi^2} - \frac{3}{8}\lambda\Delta^2 \ . \qquad \text{(C.26)}
\end{aligned}
$$

The condition $U_{eff}(0) = 0$ and $U'_{eff}(0) = 0$ are fulfilled automatically.

The last comment, as in the one-loop case of $\overline{MS}$ scheme, the absolute minimum is shifted from its bare value ϕ_+.

Appendix D.
Some details of renormalization for tunneling process

Here we present how the expression (5.67) is obtained. The functions $h_n(t)$ satisfy the following integral equation

$$
h_n(t) = \frac{i}{2\omega_{n0}}\int_0^t dt' \left(e^{2i\omega_{n0}(t-t')} - 1 \right) V(t')\left[1 + h_n(t') \right] \qquad \text{(D.1)}
$$

and we should separate the real part of it. It is obvious that the term

$$-\frac{i}{2\omega_{n0}} \int_0^t dt' V(t') \left[1 + h_n(t')\right]$$

is always imaginary, so we can neglect it for our aims. So that

$$\mathrm{Re}h_n(t) = \mathrm{Re}\frac{i}{2\omega_{n0}} \int_0^t dt' e^{2i\omega_{n0}(t-t')} V(t') \left[1 + h_n(t')\right] \ .$$

This integral can be integrated partially, as a result be get

$$
\begin{aligned}
\mathrm{Re}h_n(t) &= \mathrm{Re}\left\{-\frac{1}{4\omega_{n0}^2} V(t)[1 + h_n(t)]\right.\\
&\left.-\frac{i}{2\omega_{n0}} \int_0^t dt' e^{2i\omega_{n0}(t-t')} \left[\frac{\partial V(t')}{\partial t'}(1 + h_n) + V(t')\dot{h}_n(t)\right]\right\} \ . \quad (\text{D.2})
\end{aligned}
$$

The integral term is of the order ω_{n0}^{-3} at least, and we do not want to expand till this order. The function $h_n(t)$ is also of the order ω_{n0}^{-1} at least, so the only term of our interest is

$$\mathrm{Re}h_n(t) = -\frac{1}{4\omega_{n0}^2} V(t) + \mathcal{O}\left(\frac{1}{\omega_{n0}^3}\right) \ . \quad (\text{D.3})$$

The next point we want to address here is a computation of the divergent sums appearing in the fluctuation integral and the energy density.

The sum in the divergent part of the fluctuation integral can be rewritten

$$\sum_{n=1}^{\infty} \frac{1}{2\omega_{n0}} = \sum_{n=1}^{\infty} \int_{-\infty}^{\infty} \frac{dk}{2\pi} \frac{1}{k^2 + k_n^2 + m_0^2} \ , \quad (\text{D.4})$$

with $k_n = n/a$. The sum can be done as

$$
\begin{aligned}
\sum_{n=1}^{\infty} \frac{1}{k^2 + n^2/a^2 + m_0^2} &= \frac{\pi a}{2\omega_0} \coth(\pi a\omega_0) - \frac{1}{2\omega_0^2}\\
&= \frac{\pi a}{2\omega_0}\left(1 + \frac{1}{\exp(2\pi a\omega_0) - 1}\right) - \frac{1}{2\omega_0^2} \ ,
\end{aligned}
$$

with $\omega_0 = \sqrt{k^2 + m_0^2}$. So one can write

$$\sum_{n=1}^{\infty} \frac{1}{2\omega_{n0}} = \pi a \int_{-\infty}^{\infty} \frac{dk}{(2\pi)2\omega_0}\left[1 + \frac{2}{\exp(2\pi a\omega_0) - 1} - \frac{1}{\pi a\omega_0}\right] \ . \quad (\text{D.5})$$

Alternatively this expression can be derived using the Abel-Plana formula [56]:

$$\sum_{n=0}^{\infty} f(n) = \frac{1}{2} f(0) + \int_0^{\infty} dx f(x) + i \int_0^{\infty} dt \frac{f(it + \epsilon) - f(-it + \epsilon)}{e^{2\pi t} - 1} . \qquad (D.6)$$

The small real ϵ is imposed by the fact that the formula is derived using the residue theorem, opening up a contour originally enveloping the positive real axis. As our function $f(x) = 1/2 \sqrt{m_0^2 + x^2/a^2}$ has cuts along the imaginary axis, starting at $x = \pm i a m_0$ the contour has to run along the side with a small positive real part.

For $f(it \pm \epsilon)$ we find

$$\sqrt{m_0^2 + \frac{(it \pm \epsilon)^2}{a^2}} = \sqrt{-\frac{t^2}{a^2} + m_0^2 \pm i\epsilon'} = \pm \sqrt{\frac{t^2}{a^2} - m_0^2} ,$$

with $\epsilon' = 2t\epsilon/a^2 > 0$. Therefore

$$i(f(it + \epsilon) - f(-it + \epsilon)) = \frac{2}{\sqrt{\frac{t^2}{a^2} - m_0^2}} \Theta(t - am_0) .$$

So the second integral in the Plana formula becomes

$$i \int_{am_0}^{\infty} \frac{dt}{\sqrt{\frac{t^2}{a^2} - m_0^2}} \frac{f(it + \epsilon) - f(it - \epsilon)}{e^{2\pi t} - 1}$$

$$= 2a \int_{m_0}^{\infty} \frac{d\omega_0}{\sqrt{\omega_0^2 - m_0^2}} \frac{1}{e^{2\pi a \omega_0} - 1} = 2a \int_0^{\infty} \frac{dk}{\omega_0} \frac{1}{e^{2\pi a \omega_0} - 1} .$$

Here we have substituted $t = a\omega_0$ and $k = \sqrt{\omega_0^2 - m_0^2}$.
In the first integral we substitute $x = ak$ and finally get

$$\sum_{n=0}^{\infty} \frac{1}{2\omega_{n0}} = \frac{1}{4m_0} + a \int_0^{\infty} \frac{dk}{2\omega_0} + a \int_0^{\infty} \frac{dk}{\omega_0} \frac{1}{e^{2\pi a \omega_0} - 1} \qquad (D.7)$$

for the divergent sum in the fluctuation integral.

Another sum which will appear as a leading contribution to the energy density is

$$\sum \frac{1}{2} \omega_{n0}$$

It can be computed easily using the same strategy, one obtains

$$\sum \frac{1}{2} \omega_{n0} = \frac{1}{4} m_0 + a \int_0^{\infty} dk \frac{1}{2} \omega_0 - a \int \frac{dk k^2}{\omega_0} \frac{1}{e^{2\pi a \omega_0} - 1} . \qquad (D.8)$$

Bibliography

[1] D. Cormier and R. Holman, Phys. Rev. **D62**, 023520 (2000), [hep-ph/9912483].

[2] D. Cormier and R. Holman, Phys. Rev. **D60**, 041301 (1999), [hep-ph/9812476].

[3] D. Boyanovsky, H. J. de Vega and R. Holman, hep-ph/9903534.

[4] J. Garcia-Bellido, M. Garcia Perez and A. Gonzalez-Arroyo, Phys. Rev. **D67**, 103501 (2003), [hep-ph/0208228].

[5] I. Y. Kobzarev, L. B. Okun and M. B. Voloshin, Sov. J. Nucl. Phys. **20**, 644 (1975).

[6] S. R. Coleman, Phys. Rev. **D15**, 2929 (1977).

[7] J. Callan, Curtis G. and S. R. Coleman, Phys. Rev. **D16**, 1762 (1977).

[8] A. D. Linde, Nucl. Phys. **B216**, 421 (1983).

[9] S. R. Coleman and F. De Luccia, Phys. Rev. **D21**, 3305 (1980).

[10] J. C. Hackworth and E. J. Weinberg, Phys. Rev. **D71**, 044014 (2005), [hep-th/0410142].

[11] V. Vanchurin and A. Vilenkin, Phys. Rev. **D74**, 043520 (2006), [hep-th/0605015].

[12] J. Baacke and V. G. Kiselev, Phys. Rev. **D48**, 5648 (1993), [hep-ph/9308273].

[13] J. Baacke and T. Daiber, Phys. Rev. **D51**, 795 (1995), [hep-th/9408010].

[14] J. Baacke, Phys. Rev. **D52**, 6760 (1995), [hep-ph/9503350].

[15] A. Strumia, N. Tetradis and C. Wetterich, Phys. Lett. **B467**, 279 (1999), [hep-ph/9808263].

[16] G. Munster and S. Rotsch, Eur. Phys. J. **C12**, 161 (2000), [cond-mat/9908246].

[17] G. Munster, A. Strumia and N. Tetradis, Phys. Lett. **A271**, 80 (2000), [cond-mat/0002278].

[18] J. Baacke and G. Lavrelashvili, Phys. Rev. **D69**, 025009 (2004), [hep-th/0307202].

[19] G. V. Dunne and H. Min, Phys. Rev. **D72**, 125004 (2005), [hep-th/0511156].

[20] A. Surig, Phys. Rev. **D57**, 5049 (1998), [hep-ph/9706259].

[21] J. M. Cornwall, R. Jackiw and E. Tomboulis, Phys. Rev. **D10**, 2428 (1974).

[22] H. Verschelde and M. Coppens, Phys. Lett. **B287**, 133 (1992).

[23] M. Coppens and H. Verschelde, Z. Phys. **C58**, 319 (1993).

[24] S. W. Hawking and I. G. Moss, Phys. Lett. **B110**, 35 (1982).

[25] N. Turok and S. W. Hawking, Phys. Lett. **B432**, 271 (1998), [hep-th/9803156].

[26] J. B. Hartle and S. W. Hawking, Phys. Rev. **D28**, 2960 (1983).

[27] T. Vachaspati and A. Vilenkin, Phys. Rev. **D37**, 898 (1988).

[28] K. Hirota, Phys. Rev. **D61**, 123502 (2000).

[29] A. Vilenkin, Phys. Rev. **D50**, 2581 (1994), [gr-qc/9403010].

[30] A. Vilenkin, Nucl. Phys. Proc. Suppl. **88**, 67 (2000), [gr-qc/9911087].

[31] J.-y. Hong, A. Vilenkin and S. Winitzki, Phys. Rev. **D68**, 023520 (2003), [gr-qc/0210034].

[32] D. H. Coule and J. Martin, Phys. Rev. **D61**, 063501 (2000), [gr-qc/9905056].

[33] J. Hong, A. Vilenkin and S. Winitzki, Phys. Rev. **D68**, 023521 (2003).

[34] D. Levkov, C. Rebbi and V. A. Rubakov, Phys. Rev. **D66**, 083516 (2002), [gr-qc/0206028].

[35] M. M. Nieto, V. P. Gutschick, F. Cooper, D. Strottman and C. M. Bender, Phys. Lett. **B163**, 336 (1985).

[36] S. Michalski, *Chiral symmetry restoration in quantum field theories at finite temperatrure* (Dissertation, Dortmund University, Oktober, 2006).

[37] J. Kripfganz, A. Laser and M. G. Schmidt, Nucl. Phys. **B433**, 467 (1995), [hep-ph/9405225].

[38] E. Mottola, Phys. Rev. **D31**, 754 (1985).

[39] A. Erdelyi, editor, *Higher Transcendental Functions* (McGraw-Hill Book Company, Inc., New York, 1953).

[40] J. Baacke, Z. Phys. **C53**, 402 (1992).

[41] J. Baacke, Acta Phys. Polon. **B22**, 127 (1991).

[42] S. Coleman, *Aspects of Symmetry* (Cambridge University Press, 1985).

[43] I. M. Gelfand and A. M. Yaglom, J. Math. Phys. **1**, 48 (1960).

[44] J. Baacke and R. Koch, Nucl. Phys. **B135**, 304 (1978).

[45] Y. Bergner and L. M. A. Bettencourt, Phys. Rev. **D69**, 045012 (2004), [hep-ph/0308107].

[46] J. Baacke and N. Kevlishvili, Phys. Rev. **D71**, 025008 (2005), [hep-th/0411162].

[47] M. Dine, R. G. Leigh, P. Y. Huet, A. D. Linde and D. A. Linde, Phys. Rev. **D46**, 550 (1992), [hep-ph/9203203].

[48] M. Dine, R. G. Leigh, P. Huet, A. D. Linde and D. A. Linde, Phys. Lett. **B283**, 319 (1992), [hep-ph/9203201].

[49] R. Zurmühl, *Praktische Mathematik für Ingenieure und Physiker* (Springer, Berlin, 1984).

[50] J. Baacke, K. Heitmann and C. Patzold, Phys. Rev. **D55**, 2320 (1997), [hep-th/9608006].

[51] J. Baacke and S. Michalski, Phys. Rev. **D65**, 065019 (2002), [hep-ph/0109137].

[52] Y. Nemoto, K. Naito and M. Oka, Eur. Phys. J. **A9**, 245 (2000), [hep-ph/9911431].

[53] P. Dirac, *The principles of quantum mechanics* (Proc. Camb. Phil. Soc.26, 1930).

[54] R. Jackiw and A. Kerman, Phys. Lett. **A71**, 158 (1979).

[55] F. Cooper, S.-Y. Pi and P. N. Stancioff, Phys. Rev. **D34**, 3831 (1986).

[56] G. H. Hardy, *Divergent series* (Oxford University Press, Oxford, 1949), section 13.14.

[57] A. Aguirre, S. Gratton and M. C. Johnson, hep-th/0612195.

[58] S. H. Henry Tye, hep-th/0611148.

[59] H. Verschelde and J. De Pessemier, Eur. Phys. J. **C22**, 771 (2002), [hep-th/0009241].

[60] H. Verschelde, Phys. Lett. **B497**, 165 (2001), [hep-th/0009123].

[61] G. Smet, T. Vanzielighem, K. Van Acoleyen and H. Verschelde, Phys. Rev. **D65**, 045015 (2002), [hep-th/0108163].

[62] D. Dudal and H. Verschelde, Phys. Rev. **D67**, 025011 (2003), [hep-th/0210098].

Acknowledgements